

4

NAVAL POSTGRADUATE SCHOOL

Monterey, California

AD-A230 135



DTIC
ELECTE
DEC 20 1990
S B D
Lo

LOMPOC VALLEY DIFFUSION EXPERIMENT DATA REPORT

C.E. Skupniewicz, R.F. Kamada, S.A. Drake, and L. McKay
Naval Postgraduate School
R.N. Abernathy, K.C. Herr, and G.J. Scherer
Aerospace Corporation, Los Angeles, Ca.
A. Guenther, *CIRES, Boulder, Co.*

1 Nov 1990

Approved for public release
Distribution unlimited
Prepared for USAF Space Division (SSD/CLGR),
Los Angeles California 90009

NAVAL POSTGRADUATE SCHOOL
Monterey, California

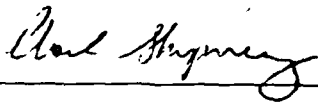
RADM R.W. West, Jr.
Superintendent

H. Shull
Provost

The work reported herein was supported in part by the U.S. Air Force Space Division (SSD/CLGR)

Reproduction of all or part of this report is authorized.

Principal authors for this report were

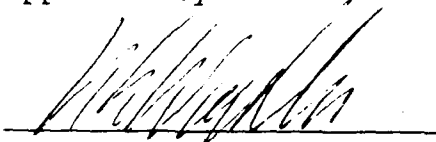


C.E. Skupniewicz,
Meteorologist



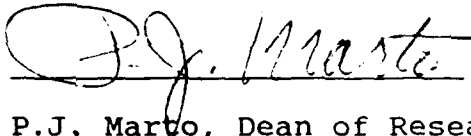
R.F. Kamada, Adjunct
Research Professor of Physics

Approved by:



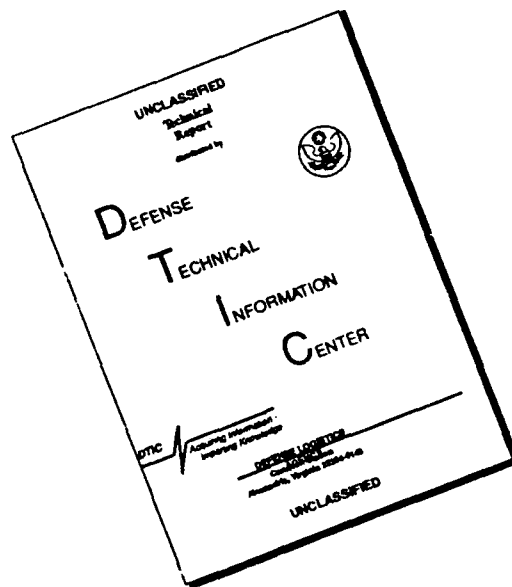
K.E. Woehler, Chairman
Dept. of Physics

Released by:



P.J. Marvo, Dean of Research

DISCLAIMER NOTICE



THIS DOCUMENT IS BEST
QUALITY AVAILABLE. THE COPY
FURNISHED TO DTIC CONTAINED
A SIGNIFICANT NUMBER OF
PAGES WHICH DO NOT
REPRODUCE LEGIBLY.

REPORT DOCUMENTATION PAGE				Form Approved OMB No 0704-0188	
1a REPORT SECURITY CLASSIFICATION unclassified			1b RESTRICTIVE MARKINGS		
2a SECURITY CLASSIFICATION AUTHORITY			3 DISTRIBUTION AVAILABILITY OF REPORT approved for public release; distribution unlimited		
2b DECLASSIFICATION/DOWNGRADING SCHEDULE					
4 PERFORMING ORGANIZATION REPORT NUMBER(S) NPS-PH-91-001			5 MONITORING ORGANIZATION REPORT NUMBER(S)		
6a NAME OF PERFORMING ORGANIZATION Naval Postgraduate School		6b OFFICE SYMBOL (If applicable) PH	7a NAME OF MONITORING ORGANIZATION Aerospace Corp., Chemical Systems		
6c ADDRESS (City, State, and ZIP Code) Monterey, California 93943-5000			7b ADDRESS (City, State, and ZIP Code) Los Angeles, California 90009		
8a NAME OF FUNDING SPONSORING ORGANIZATION USAF Space Division		8b OFFICE SYMBOL (If applicable) SSD/CLGR	9 PROCUREMENT INSTRUMENT IDENTIFICATION NUMBER MPIR FY76169000643		
8c ADDRESS (City, State, and ZIP Code) Los Angeles, California 90009			10 SOURCE OF FUNDING NUMBERS		
			PROGRAM ELEMENT NO	PROJECT NO	TASK NO
					WORK UNIT ACCESSION NO
11 TITLE (Include Security Classification) Lompoc Valley Diffusion Experiment Data Report (unclassified)					
12 PERSONAL AUTHOR(S) S.A. Drake, L. McKay, R.N. Abernathy, C.E. Skupniewicz, R.F. Kamada, K.C. Herr, G.J. Scherer, and A. Guenther					
13a TYPE OF REPORT technical		13b TIME COVERED FROM 9-88 TO 9-90		14 DATE OF REPORT (Year, Month, Day) 1 Nov 1990	
15 PAGE COUNT 150					
16 SUPPLEMENTARY NOTES Lompoc Valley Diffusion Experiment Data Report, Lompoc Valley, California, 1988-1990.					
17 COSAT CODES			18 SUBJECT TERMS (Continue on reverse if necessary and identify, by block number)		
FIELD	GROUP	SUB-GROUP			
			Atmospheric Diffusion, plume dispersion, Vandenberg AFB, Lompoc, tracer, SF6		
19 ABSTRACT (Continue on reverse if necessary and identify by block number)					
<p>A data base representing the results of the Lompoc Valley Diffusion Experiment is described in detail, outlining formats and defining the contents of the data set. Preliminary analyses are performed, showing concentrations, trajectories and plume widths of a tracer gas plume released from the Hypergolic Stockpile and Storage Facility at Vandenberg Air Force Base, California, and estimating the effects of a potential release of fuel or oxidizer. Future analysis plans are outlined.</p>					
20 DISTRIBUTION AVAILABILITY OF ABSTRACT <input checked="" type="checkbox"/> UNCLASSIFIED/DISTRIBUTED <input type="checkbox"/> SAME AS REPORT <input type="checkbox"/> DTIC USERS			21 ABSTRACT SECURITY CLASSIFICATION unclassified		
22a NAME OF RESPONSIBLE INDIVIDUAL C.E. Skupniewicz			22b TELEPHONE (include Area Code) 4086462451		22c OFFICE SYMBOL PH

LOMPOC VALLEY DIFFUSION EXPERIMENT DATA REPORT

C.E. Skupniewicz, R.F. Kamada, S.A. Drake, and L. McKay
Naval Postgraduate School, Monterey, California

R.N. Abernathy, K.C. Herr, and G.J. Scherer
Aerospace Corporation, Los Angeles California

A. Guenther
Cooperative Institute for Research in
Environmental Sciences, Boulder, Colorado

1 Nov 1990



Accession For	
NTIS GRA&I	<input checked="checked" type="checkbox"/>
DTIC TAB	<input type="checkbox"/>
Unannounced	<input type="checkbox"/>
Justification	
By	
Distribution/	
Availability Codes	
Dist	Avail and/or Special
A-1	

TABLE OF CONTENTS

<u>Title</u>	<u>Pages</u>
1. Introduction	3
2. Releases	5
3. Tracer Gas Sampling	58
4. Infrared Molecular Plume Imagery	18
5. DASS Data	10
6. WINDS System Data	11
7. Regional Tower Network	2
8. Rawinsonde Data	2
9. Surface-layer Profile Mast	8
10. Release Site Surface-layer Data and Radiation	8
11. Cloud Coverage Analysis	15
12. Synoptic Meteorology	14
13. Analysis Plan	3
14. Acknowledgements	1
15. References	2
16. Data Base Reference Catalog	2
17. Distribution List	3
	<hr/>
	165

1. INTRODUCTION

The Hypergolic Stockpile and Storage Facility (HSSF) on Vandenberg Air Force Base (VBG) is a potential source of hypergolic air emissions. Both wind measurements and flow models show that trajectories from the HSSF may pass through Lompoc during the early phases of the normal summertime sea breeze day (900 -1500 LDT) or during southwesterly anomalous wind events (Mikkelsen et al., 1988, Thiekier-Nielsen et al., 1988, Skupniewicz et al. 1988, Kamada et al. 1989, Yamada and Bunker, 1990). Under such conditions diffusion models, i.e. Ocean Breeze / Dry Gulch (OB/DG) used for VBG simulations suggest that some very large releases from the HSSF may result in unacceptable concentration levels of propellant vapors downwind ranges reaching beyond VBG boundaries. The likelihood of a large vapor release from the HSSF is considered remote, since it has been designed and equipped to prevent spills and the resulting vaporization. The actual release rates required to exceed acceptable exposure levels varies greatly, depending on the accepted time-weighted-average standard (TWA), anticipated clean-up time, and other regulatory, mitigational, and physical factors. However, we can say that the plume growth algorithms used in these diffusion models are based on the Mt. Iron tracer release tests conducted during the mid-nineteen sixties from SLC4 and SLC6; and that these algorithms have also

been extrapolated beyond the downwind range of the measurements upon which they are based.

To meet the need for actual long range tracer tests from the HSSF, the Environmental Physics Group at the Naval Postgraduate School, Monterey, California (EPG/NPS) conceived and conducted the Lompoc Valley Diffusion Experiment (LVDE). Funding and approval came from USAF Space Division, Los Angeles (POC: Cpt. F. Smith, MPIR# FY76169000643). EPG/NPS directed the experiment with significant participation from the Laser Chemistry and Spectroscopy Laboratory at the Aerospace Corporation, Los Angeles, California (LCSP/AC), the Laboratory for Atmospheric Research at Washington State University (WSU), USAF Space Systems Division, Los Angeles (SSD), and the 30th Weather Squadron at Vandenberg Air Force Base.

The LVDE consisted of a series of diffusion tests in the California Lompoc Valley during the period 10-17 Aug 1989. The mid-summer date was chosen because the daily sea breeze pattern is very regular at that time of year and is most typical of flow observed at other times. The main objective was to measure plume parameters to be used in dispersion modeling of surface releases from the HSSF at VBG during up-valley sea breeze dominated flow conditions.

This report summarizes all the data collected during LVDE, and

supplies a protocol for accessing a 20 Mb data archive available to the Vandenberg wind flow and diffusion modeling community. Due to reproduction costs, the data archive has only been distributed to key selected individuals (see Distribution List, section 17). Additional copies can be made available upon request. This report will be followed by a second report describing results of RAMS modeling and quantities derived from the raw data such as plume parameterizations. See Analysis Plan, section 13, for more detail.

2. RELEASES

SF6 was used as the tracer gas. SF6 has the advantages of relatively low cost and short analysis time. Global background levels of near 1 ppt are not a problem for the relatively short LVDE ranges. It is also the gas of choice for near source infrared imaging (discussed below).

From 10-14 Aug, EPG/NPS released gas from the 12 ft level of Tower 057, directly adjacent to the HSSF. From 15-17 Aug, the tracer gas release stand was transferred to the EPG/NPS mobile laboratory, and the release site was moved to the floor of the Lompoc valley about 2 km north of the HSSF. This was done to compare results between a flat domain and the HSSF domain, which includes some moderately complex terrain along the plume trajectory. On 15 Aug tracer was released from the parking lot at Ocean Park at the mouth of the Lompoc Valley which divides North and South Base. 16 Aug releases originated from the junction of Hwy 246 and Arguello Rd, just south of the North Base gate, and 17 Aug releases were from the north side of the Lompoc Valley about 1.6 miles north of Hwy 246 on Union Sugar Rd. Table 2.1 shows the dates, times, release rates, sites, and latitude/longitude coordinates.

Table 2.1 LVDE SF6 Tracer Release Data

Date	Time* Hrs	Release Rate kg/hr	Site	Latitude 34°+ min	Longitude 120°+ min
8/10/89	12.42	35.	Tower 57 by HSSF	40.044'	35.342'
"	13.09	25.	"	"	"
"	13.15	0.	"	"	"
"	13.77	250.	"	"	"
"	13.81	20.	"	"	"
"	16.00	0.	"	"	"
8/11/89	10.12	20.	"	"	"
"	12.37	0.	"	"	"
"	12.67	250.	"	"	"
"	12.72	0.	"	"	"
"	12.92	250.	"	"	"
"	12.97	0.	"	"	"
"	13.17	250.	"	"	"
"	13.22	0.	"	"	"
"	13.75	20.	"	"	"
"	14.74	0.	"	"	"
"	14.92	250.	"	"	"
"	14.97	0.	"	"	"
"	15.17	250.	"	"	"
"	15.22	0.	"	"	"
"	15.47	250.	"	"	"
"	15.52	0.	"	"	"
8/12/89	9.33	20.	"	"	"
"	10.32	0.	"	"	"
"	10.65	20.	"	"	"
"	12.69	0.	"	"	"
"	14.17	20.	"	"	"
"	14.99	250.	"	"	"
"	15.08	20.	"	"	"
"	16.00	250.	"	"	"
"	16.08	0.	"	"	"
8/13/90	8.75	20.	"	"	"
"	15.50	0.	"	"	"
8/14/89	9.89	20.	"	"	"
"	14.84	250.	"	"	"
"	14.89	20.	"	"	"
"	15.17	250.	"	"	"
"	15.22	20.	"	"	"
"	15.50	0.	"	"	"
8/15/89	10.18	20.	Ocean Park	41.384'	35.952'
"	12.00	250.	"	"	"

** Time of change in the release rate

Table 2.1 continued

Date	Time Hrs	Release Rate kg/hr	Site	Latitude 34°+ min	Longitude 120°+ min
"	12.08	20.	"		"
"	13.00	250.	"		"
"	13.08	20.	"		"
"	14.00	250.	"		"
"	14.08	20.	"		"
"	15.00	100.	"		"
"	15.14	20.	"		"
"	15.50	0.	"		"
8/16/89	9.27	20.	Arguello & 246	40.267'	33.531'
"	10.05	10.	"		"
"	13.00	0.	"		"
"	13.77	10.	"		"
"	15.00	0.	"		"
8/17/89	9.10	20.	246 + 1.6mi on Union	40.664'	32.137'
"	9.69	0.	"		"
"	10.21	20.	"		"
"	11.13	20.	"		"
"	11.22 **	0.	"		"
"	11.22	20.	"		"
"	11.75	250.	"		"
"	11.78	20.	"		"
"	12.60	250.	"		"
"	12.63	20.	"		"
"	13.00	10.	"		"
"	13.48	0.	"		"
"	13.50	250.	"		"
"	13.53	0.	"		"
"	13.72	250.	"		"
"	13.75	0.	"		"

** release linearly decreased between 11.13 and 11.22

SF6 was released for four to six hours per day at a standard rate of 20 kg/hr. The gas issued from a moveable test stand with four flow regulators mounted in parallel. This avoided release interruptions while depleted cylinders were exchanged for fresh standard compressed gas cylinders. Since SF6 is liquid at high pressure, an unused cylinder holds ~ 130 lbs of SF6, good for about three hours at the standard release rate. The calibration was checked by weighing a cylinder before and after release.

For most days, the sea breeze front signalled the start of the tracer release, since westerly winds associated with it pose the greatest risk to Lompoc in the event of a spill. When clouds are present, the sea breeze front is usually seen at VBG as a strong backing to the west closely followed by stratus burn-off (Kamada et al., 1989). The sea breeze and stratus conditions during LVDE were typical for August. Clouds moved inland nightly, the sea breeze front passed around 1000 PDT and the clouds burned back to within a few kilometers of the coast by 1200 PDT. Due to this weather pattern, the HSSF was almost always under clouds during LVDE. The tracer plume exited the clouds after a few kilometers of travel and most sampling took place under clear skies.

At times we detached the regulator and vented unthrottled SF6

at ~ 250 Kg/hr in order to see the plume with infrared imaging, examine puff travel time through the domain, and study longitudinal puff growth. We released up to six such 3 - 5 minute duration puffs per day in this fashion. All six puffs on August 11 and the final puff on August 17 were temporally isolated from the background flow. All other puffs were released in tandem with the standard flow rate by simultaneously venting one regulated and one unregulated cylinder.

3. TRACER GAS SAMPLING

The taggant gas was sampled with 3 gas analyzers; two gas chromatographs with electron capture detectors (GC) operated by LCSP/AC and a specialized electron capture based fast response instrument (FGA) operated by WSU. All devices used very small sampling volumes, so the samples could be regarded as point measurements. The sampling frequency was .017 hz (1 minute) for the GCs, and 1 hz for the FGA. The FGA speed is achieved by burning away the otherwise masking oxygen signal by combustion with excess hydrogen. This bypasses the older method of gradual SF₆/O₂ separation through a chromatographic column. However, the combustion process increases baseline drift. Thus, the FGA requires frequent re-calibration, and was calibrated once per sampling transect (about every 30 min) against three standards (0.1, 1, and 10 ppb). The GCs were calibrated against a series of standards, including the FGA standards. The GC calibration was verified on a daily basis using a dynamic dilution system and a 1 ppb standard. The FGA's useful dynamic range is ~ 20 ppt - 10 ppb, somewhat less than the GC's 10 ppt - 35 ppb (or more).

Emphasis was placed on accurately measuring surface horizontal concentration profiles along the trajectory of the plume between the release site and Lompoc. Each gas sampler was

mounted in a separate vehicle and sampling was performed along preselected routes of opportunity. Most of these roads were marked at 0.1-0.2 mile intervals, and locations were logged by the operator in concert with the data recording. When road markers were not available, odometer readings were recorded at major intersections and along the sampling routes. Two of the vehicles also recorded position as estimated from a LORAN receiver, but these data were often contaminated by ground wave distortion due to terrain features, and the primary positioning was accomplished with the road marker log and vehicle odometers.

Pibol releases from the release site identified the most likely points at which to detect the plume centroid. The sparsity of roads perpendicular to the anticipated plume trajectory prohibited measurements of the plume at a wide variety of ranges. Figure 3.1 shows all sampling routes used during LVDE. Measurements were concentrated along route 2, the nearest transect to the source, and route 13, an area of significant population density. The FGA mainly sampled the routes nearest the release site, while the 2 GC's concentrated on the more distant routes, where sampling frequency was less important and instrument sensitivity was more critical. SSD coordinated a radio network from Building 900 (near the release site), to relay information between vehicles and the release site.

Figures 3.2-13 show each day's release rates and SF6

concentrations vs time from the three instruments. In these figures, the GCs are referred to as the "truck" and "trailer", while the FGA operated from the "van". Though not directly revealed in the figures, the recorded sampling times and distances suggest that one or more instruments "witnessed" the majority of the puff events. The raw data also show some peaks prior to the release. During the experiment these peaks were traced to Building 900 where we found and sealed a slow leak in one of the SF6 cylinders housed there. The slow leak rate affected apparent concentrations only within the immediate vicinity of Building 900. In addition the truck data display a few calibration peaks.

For the standard 20 kg/hr release rate, the FGA typically measured peak centerline concentrations of $\sim 5 - 15$ ppb along route 2, roughly 3 km from the source. The truck usually displayed similar peaks, but at times the GC recorded higher concentrations (up to 35 ppb), which are above the saturation level of the FGA. Along the more distant, off-base routes, the trailer showed peak concentrations of ~ 1 ppb with typical values of $\sim 0.1 - 0.5$ ppb at 20 kg/hr.

How do these measurements relate to exposure limits? Let us assume a 1000 kg spill of UDMH which evaporates over the course of 1 hour. If we use the SPEGL public exposure limit of .24 ppm for 1 hour, the limit will be exceeded when $1.9 \times$ ppb SF6 is

greater than 1, for a 20 kg/hr release rate. Therefore, a typical measurement near Lompoc of 0.5 ppb is roughly equivalent to the TWA, and a 1000 kg/hr plume would not be considered a hazard during the conditions prevalent during LVDE. Increases in the release rate are multiplicative, therefore keeping the release size small and clean up time short becomes essential. If we use the SPEGL limit of 1 ppm for nitrogen dioxide, the equation becomes $0.10 \times \text{ppb SF}_6$, similar to the UDMH case.

The primary caveats to these estimates are that we are assuming these values are average for 1 hour, and no losses or transformations occur along the trajectory. We also ignore spill mitigation actions at the HSSF which, in the case of hydrazine fuels, would include dilution with water to drastically lower the vaporization rate. Oxidizer spills would flow to sumps and waste tanks to reduce vaporization.

Figures 3.14-21 show daily locations of peak concentrations recorded during each crosswind transect. Figure 3.22 shows transect peak concentrations locations for all releases from the HSSF. We note here that these figures do not indicate the intensity of the measurement, just the approximate position of the plume centroid. The figures suggest a remarkable regularity of pattern in daily plume widths and directions, save for 17 Aug, when synoptic conditions forced more northerly winds. Otherwise, seabreeze westerlies (flow type 2, see Kamada et al., 1989)

chronically followed the early morning stagnation (flow type 5). Plume paths from the HSSF regularly impinged upon Miguelito Canyon and the southern half of Lompoc.

For more detail, figs. 3.23-30 and 3.31-38 show daily temporal changes in plume width and centerline direction, as measured by the FGA. Low mean winds during the early morning stagnation period allow for significant, turbulence induced, lateral dispersion which should result in broader, shorter toxic hazard corridors (THCs). By afternoon, however, plumes tend to narrow as the seabreeze picks up speed.

For the tracer data a record identifier is supplied at the beginning of each record. "V" refers to data collected by the FGA (WSU) sampler, while "A" is data collected by the GCs (LCSP/AD). Trailing numbers identify the chronological order of the traverse with the first number referring to one of the eight sampling days. Thus, V112 refers to the twelfth traverse (or stationary sampling period) of day 1 (8/10/90). The LCSP/AD data is not identified by days, and the number simply refers to the chronological order of the traverse.

Since the FGA was typically much closer the release point and operated at a higher frequency. over 90% of the records are from the FGA. The FGA's 285 data collection periods include three categories: 213 horizontal ground-level transects, 62 periods of

stationary measurements and 10 vertical profiles.

A sample of the mobile traverse data is shown in table 3.1. Each file contains a header, with summary statistics and information associated with that file, followed by the tracer measurements.

Transect results are interpreted in terms of "crosswind" standard deviation and "downwind" distance. These definitions are interpreted with reference to a vector between the release site and the maximum measured concentration; the transport direction. The "local" wind direction (wind at the sampling location) may have been quite different from that vector. Moreover, the transect path sometimes departed by as much as 45 degrees from being normal to the plume transport direction, due to the limited number of available routes mentioned earlier. Hence, the downwind distance is actually a mean along the path. A line normal to the transport direction and bisecting the average downwind distance represents the crosswind coordinate system, and transect data were projected onto this idealized sampling route. All tranverse statistics, e.g. crosswind standard deviation, were calculated from these transformed coordinates.

TABLE 3.1 Example of Traverse Data Statistics

TRAVERSE STATISTICS (V402)
 File scans: data (366 to 520), moment (385 to 490)
 Date : 08-13-1989 Time : 9:14: 6 to 9:16:40
 Source location: (lat: 34 40.044 , long: 120 35.342)
 Power Law Cal. : Time = 9.25 , ppt = 792.7 *(voltage)^ 1.04
 At time = 16.12 , ppt = 821.9 *(voltage)^ 1

Method	Sigma Y (m)	Mean Abs. Res. (%) (ppt)	Max conc. (ppt)	Plume center (m)
Moment :	125.8	60.72 1308.47	3392	-92.6
Hanna :	121.4	41.96 835.83	3715	-18.0
Maximum :	71.1	59.63 828.35	6346	0.0

CIC (ppt m): 1130597, % in moment : 94.62
 Skewness : -1.122 Kurtosis : 3.56
 Maximum conc. location : (lat: 38.925 , long: 34.13)
 Transport from 317.8564 deg
 Downwind distance : 2782.329 m

Transects lacking background measurements on either side of the plume cross section were omitted. Since anomalously high values in the "wings" of the crosswind distribution can dramatically affect the statistics, we applied to each transect a window or "moment interval" which included only the main portion of the plume and excluded outliers. Figure 3.39 gives an example of this procedure. The crosswind integrated concentration (CIC) is given in parts per trillion*meters. The percent mass within one standard deviation of the plume center and the moment coefficients of skewness (third moment/standard deviation³) and kurtosis (fourth moment/standard deviation⁴) are calculated to evaluate the similarity of the observed data distributions to the normal distribution. A plume that resembles a Gaussian (normal) curve will generally have more than 80% of the CIC within the moment segment, while the skewness and kurtosis values will be near 0.0 and 3.0, respectively. The location of the maximum measured concentration, the transport direction, and mean downwind distance of the traverse are also given.

Three measures of the crosswind standard deviation, the maximum concentration, and its location are supplied. The "moment" method is simply the second moment of the mass distribution, i.e.

$$\sigma_y = \left(\frac{\sum C_i (y_i - \bar{y})^2}{\sum C_i} \right)^{1/2} \quad (3.1)$$

The "Hanna 2SY" assumes the standard deviation is half the distance between the locations of the 16th and 84th percentiles of the crosswind integrated concentration (CIC), based on an assumed Gaussian shape to the mass distribution. The "concentration maxima" method assumes also assumes a Gaussian profile, but bases the standard deviation on the theoretical relationship between the and the CIC and the peak value;

$$\sigma_y = \frac{\int C dy}{\sqrt{2\pi} C_{\max}} \quad (3.2)$$

Traverse Record Specifics

Suggested Input Format: {fixed} field, ASCII

*** For all data, ASCII text identifies the variables.
Therefore, line by line format is not supplied.

Stationary Record Summary

Statistics were compiled for periods when the samplers were stationary and roughly downwind of the release site. Procedurally, the plume centroid was determined during a traverse, then the sampling vehicle stopped and remained at that location for periods of 5 to 10 minutes.

An example of a stationary data record is shown in table 3.2. We include the raw FGA data along with the following information: 1) 1-second maximum concentration, 2) mean concentration, 3) conditional mean (based only on non-zero concentrations). 4) 99th percentile to mean concentration ratio (indicates the maximum concentrations to be expected for a given time averaged concentration), 5) plume intermittency (fraction of time with concentrations above baseline), 6. concentration fluctuation intensity (standard deviation of the concentration normalized by the mean concentration, a measure of concentration variability), 7) conditional concentration fluctuation intensities (based only on non-zero concentration periods), and finally, 8) the concentration frequency percentiles (fraction of time that concentrations were below the level indicated). Near-source sites usually show less intermittency and larger concentration fluctuation intensity, giving higher peak-to-mean ratios. These statistics also depend on crosswind distance to plume centerline, terrain, meteorological conditions and other factors.

TABLE 3.2 Example of Stationary Data Statistics

Stationary Statistics (V411A)

Scans : 221 to 1480

Date : 08-13-1989 Start Time : 10:32:01

Source location : (lat: 34 40.044 , long: 120 35.342)

Receptor location : (lat: 34 39.3 , long: 120 34.19)

Transport from 307.749 deg. DW dis= 2242.669 m; Z= 1.5 m AGL

Power Law Cal. : Time = 9.25 , ppt = 792.7 *(voltage)^ 1.04

At time = 16.12 , ppt = 821.9 *(voltage)^ 1

Period # 1

Time : 10 : 32 : 0 to 10 : 52 : 59 (1260 s)

Maximum Concentration (ppt) : 6515

Mean Concentration (ppt) : 1938

Conditional Mean Concentration (ppt) : 2020

Peak (99 perc) to mean ratio : 3.19

Plume intermittency : .96

Concentration fluc. intensity (%) : 76.5

Conditional conc. fluc. intensity (%): 72.2

Percentile: 50 99 (Interpolated)

Conc. (ppt) : 1687 6186

Percentile: 4.05 4.13 5.08 14.68 37.06 73.49 93.17 95.40 98.33

Conc. (ppt): 2 14 81 467 1125 2707 4200 5006 5967

During continuous releases, these data are of marginal value for estimating concentration fluctuations at the plume centroid because the center quickly meanders away from its original location at the beginning of the time segment. However, the statistics do supply a rough measure of the range of instantaneous concentrations that can be expected for a given downwind distance. The primary value of these data segments is in determining transport time and longitudinal dispersion during the puff releases.

Stationary Record Specifics

Suggested Input Format: {fixed} field, ASCII

*** For all data, ASCII text identifies the variables.
Therefore, line by line format is not supplied.

Vertical Record Summary

Vertical plume samples were drawn from a tube suspended from a 7 X 22 ft tetroom operated by LCSP/AC. Typically, the FGA located the plume centroid and directed a box truck housing the pre-inflated tetroom to that site. The tube would be connected to the truck GC or van FGA to sample at various altitudes as the tetroom was power winched up or down. Altitudes were calculated from the cable's elevation angle and tether cable length. In this way, vertical profiles up to 150 m were gathered in winds up

to 8 m/s in about 10 min. In stronger winds, the tetron became unstable and operations were halted. The major problem with these measurements was that the plume would meander away from the tetron position during the vertical profile. This seriously aliased the data. Thus, we cannot separate concentration changes due to lateral plume meander from those in the vertical profile and calculation of reliable vertical plume parameters was not possible. An example of a vertical profile is shown in fig. 3.40 for review. These data have not been processed further, but the data from about 15 profiles is available upon request.

Raw Data Summary

Raw data from each of the FGA traverses and stationary time periods is appended to the statistics files. Raw data from the GC's are included in separate data sets. Samples of each are shown in table 3.3. Each file contains a header with information associated with that file, followed by the tracer measurements. For each format, the first column gives time of day (hr:min:s) and the second column shows the observed concentration in parts per trillion. The stationary format has a location code (if any) listed in the third column, instead of the height in meters above ground level listed in the vertical format. The third column in the traverse format shows predicted concentration determined by using the moment method (discussed below) to fit a Gaussian curve to the

data. The next three columns contain the crosswind distance (meters from the maximum concentration), latitude (min) and longitude (min) for the instant sampling site. The seventh column contains a location code (if any). The raw GC data from the truck and trailer sampling units is not differentiated by traverses or stationary locations. The columns contain the following: 1) ppb SF6, 2) time in hours and minutes, 3) sampling location in latitude and longitude in minutes minus 34 and 120 degrees, respectively, 4) landmark position (normally road markers), and 5) remarks. Calibration data is flagged with a "NA" symbol in the position (4) column.

Raw Tracer Data Record Specifics

Suggested Input Format: {fixed} field, ASCII

*** For all data, ASCII text identifies the variables.
Therefore, line by line format is not supplied.

TABLE 3.3 Example of Raw Tracer Data

FGA TRAVERSE DATA

Time	Obs Conc	Pred Conc	CW	Dis.	Location		(code)
HR:MN:SC	(ppt)	(ppt)	(m)		lat	lon	
9:14: 7	284	34	289.0		38.7200	34.1600	2
9:14: 8	249	50	273.0		38.7288	34.1563	.
9:14: 9	247	70	258.0		38.7375	34.1525	6
9:14:10	220	97	243.0		38.7463	34.1488	
9:14:11	203	132	228.0		38.7550	34.1450	
9:14:12	189	177	213.0		38.7638	34.1413	
9:14:13	172	235	198.0		38.7725	34.1375	
9:14:14	143	308	183.0		38.7813	34.1338	
9:14:15	104	397	168.0		38.7900	34.1300	2
9:14:16	107	445	161.0		38.7953	34.1300	.
9:14:17	113	489	155.0		38.8006	34.1300	7
9:14:18	96	545	148.0		38.8059	34.1300	
9:14:19	83	605	141.0		38.8112	34.1300	
9:14:20	75	660	135.0		38.8165	34.1300	
9:14:21	60	729	128.0		38.8218	34.1300	
9:14:22	106	792	122.0		38.8271	34.1300	
9:14:23	91	869	115.0		38.8324	34.1300	
9:14:24	82	939	109.0		38.8377	34.1300	
9:14:25	84	1025	102.0		38.8430	34.1300	
9:14:26	89	1103	96.0		38.8483	34.1300	
9:14:27	117	1197	89.0		38.8535	34.1300	
9:14:28	339	1295	82.0		38.8588	34.1300	
9:14:29	627	1382	76.0		38.8641	34.1300	
9:14:30	839	1487	69.0		38.8694	34.1300	
9:14:31	1552	1579	63.0		38.8747	34.1300	
9:14:32	2790	1689	56.0		38.8800	34.1300	b
9:14:33	3911	1833	47.0		38.8875	34.1300	8
9:14:34	4800	1979	38.0		38.8950	34.1300	
9:14:35	5405	2143	28.0		38.9025	34.1300	
9:14:36	5867	2289	19.0		38.9100	34.1300	

TABLE 3.3 Example of Raw Tracer Data (continued)

FGA STATIONARY DATA

Time HR:MN:S	Conc (ppt)	Code	Time HR:MN:S	Conc (ppt)	Code	Time HR:MN:S	Conc (ppt)	Code
10:32: 1	5299	c	10:32:27	3546		10:32:53	3397	
10:32: 2	5264	3	10:32:28	3318		10:32:54	3304	
10:32: 3	5152		10:32:29	3078		10:32:55	3153	
10:32: 4	5046		10:32:30	2923		10:32:56	3119	
10:32: 5	4968		10:32:31	2936		10:32:57	3125	
10:32: 6	4878		10:32:32	3084		10:32:58	3132	
10:32: 7	4862		10:32:33	3409		10:32:59	3142	
10:32: 8	4563		10:32:34	3565		10:33: 0	3130	
10:32: 9	4322		10:32:35	3584		10:33: 1	3138	
10:32:10	4002		10:32:36	3563		10:33: 2	3064	
10:32:11	3709		10:32:37	3537		10:33: 3	3019	
10:32:12	3556		10:32:38	3510		10:33: 4	2986	
10:32:13	3513		10:32:39	3499		10:33: 5	2939	
10:32:14	3522		10:32:40	3561		10:33: 6	2899	
10:32:15	3616		10:32:41	3629		10:33: 7	2869	
10:32:16	3795		10:32:42	3663		10:33: 8	2859	
10:32:17	3840		10:32:43	3665		10:33: 9	2791	
10:32:18	3752		10:32:44	3648		10:33:10	2816	
10:32:19	3671		10:32:45	3625		10:33:11	2806	
10:32:20	3688		10:32:46	3576		10:33:12	2810	
10:32:21	3729		10:32:47	3516		10:33:13	2787	
10:32:22	3688		10:32:48	3465		10:33:14	2766	
10:32:23	3684		10:32:49	3455		10:33:15	2774	
10:32:24	3718		10:32:50	3512		10:33:16	2755	
10:32:25	3804		10:32:51	3484		10:33:17	2736	
10:32:26	3684		10:32:52	3435		10:33:18	2707	

TABLE 3.3 Example of Raw Tracer Data (continued)

ALL GC DATA

08/10/89 GC TRAILER:

ppb	Hr	min	LAT. 34deg+	LONG. 120deg+	DIR.	POSITION	REMARKS
0.01	12:	54.9	38.82	27.95	0	"O"/COLLEGE	NEAR MISSILE VILLE
0.00	12:	55.9	38.82	27.95	0		
0.01	12:	56.9	38.82	27.95	0		
0.01	12:	57.8	38.82	27.95	0		
0.05	12:	58.9	38.82	27.95	0		
0.07	12:	59.8	38.82	27.95	0		NOTED HIT
0.29	13:	1.7	38.82	27.95	0		
0.61	13:	2.8	38.82	27.95	0		GREAT HITS
0.50	13:	3.8	38.82	27.95	0		
0.45	13:	4.9	38.82	27.95	0		
0.40	13:	5.8	38.82	27.95	0		RELEASE ENDED 13:09
0.66	13:	6.9	38.82	27.95	0		
0.57	13:	7.8	38.82	27.95	0		
0.43	13:	9.7	38.82	27.95	0		
0.59	13:	10.8	38.82	27.95	0		
0.55	13:	11.8	38.82	27.95	0		
0.44	13:	12.9	38.82	27.95	0		
0.35	13:	13.8	38.82	27.95	0		
0.40	13:	14.9	38.82	27.95	0		
0.40	13:	15.8	38.82	27.95	0		
0.53	13:	17.7	38.82	27.95	0		
0.44	13:	18.8	38.82	27.95	0		
0.49	13:	19.8	38.82	27.95	0		
0.52	13:	20.9	38.82	27.95	0		GETTING GOOD HITS
0.45	13:	21.8	38.82	27.95	0		
0.57	13:	22.9	38.82	27.95	0		
0.47	13:	23.8	38.82	27.95	0		
0.42	13:	25.7	38.82	27.95	0		
0.49	13:	26.8	38.82	27.95	0		
0.55	13:	27.8	38.82	27.95	0		
0.53	13:	28.9	38.82	27.95	0		
0.39	13:	29.8	38.82	27.95	0		
0.40	13:	30.9	38.82	27.95	0		
0.37	13:	31.8	38.82	27.95	0		
0.39	13:	33.7	38.82	27.95	0		END RELEASE @13:09
0.52	13:	34.8	38.82	27.95	0		
0.45	13:	35.8	38.82	27.95	0		
0.47	13:	36.9	38.82	27.95	0		
0.34	13:	37.8	38.82	27.95	0		
0.19	13:	38.9	38.82	27.95	0		
0.04	13:	39.8	38.82	27.95	0		
0.01	13:	41.8	38.82	27.95	0		
0.01	13:	42.9	38.82	27.95	0		

SECTION 3 FIGURE CAPTIONS

F3.1 LVDE tracer gas sampling routes, with primary roads of travel indicated in the key. Star symbols identify the routes. VBG base boundary is outlined.

F3.2-13 Near-surface release rates and sampled concentrations as a function of time (LDT) during LVDE. No distinction is made between mobile, stationary, or vertical sampling. Some data may represent calibration procedures; e.g. near 1700 on 8/10/89. For clarity, some days have been separated by sampling device.

F3.14-21 Locations of peak measured concentrations from mobile traverses during LVDE. Release sites are indicated with a star symbol.

F3.22 Locations of peak measured concentrations from mobile traverses for all LVDE releases from the HSSF.

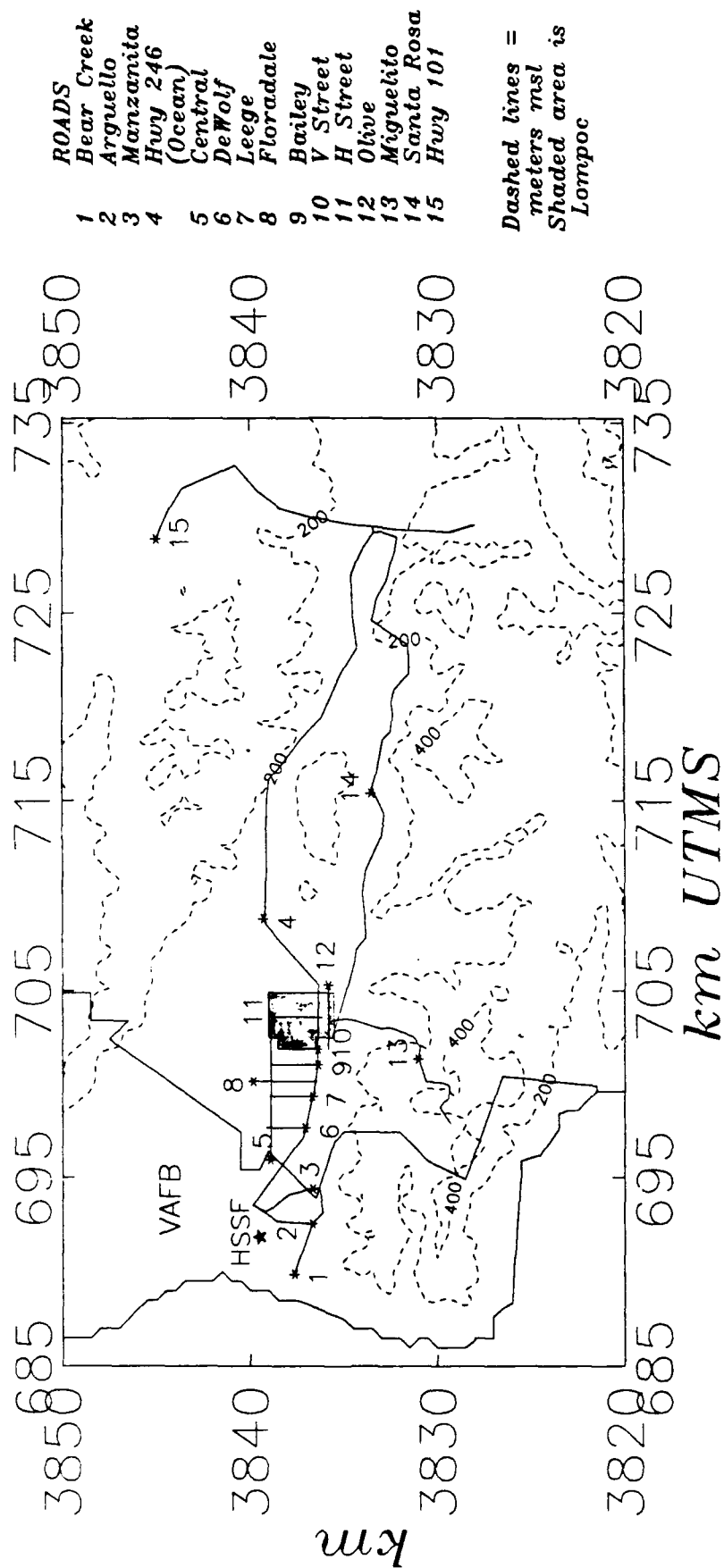
F3.23-30 Plume widths for mobile traverses during LVDE measured by the FGA only. The width is calculated as $4.6 \times \sigma_y$ (moment method), which approximates the plume boundaries as defined by 10% of maximum concentration.

F3.31-38 Direction of the maximum measured concentration from the release site for mobile traverses during LVDE measured by the FGA only.

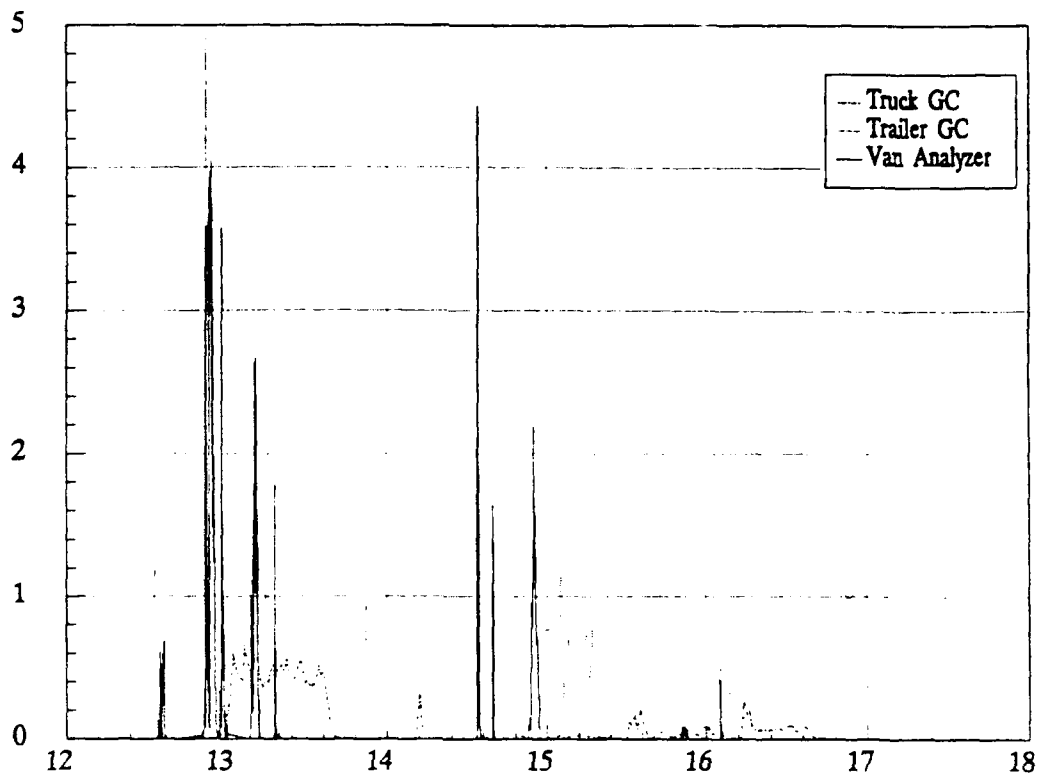
F3.39 Example of technique for estimating mobile traverse statistics.

F3.40 Example of vertical sampling results from the FGA during LVDE.

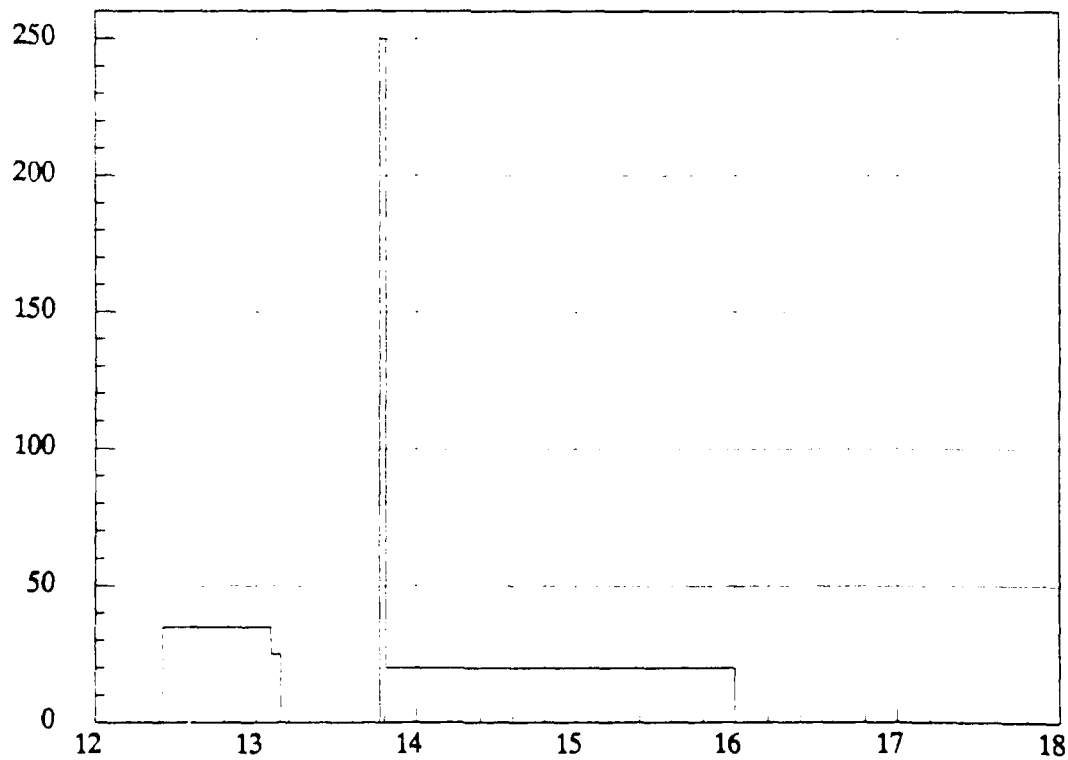
SAMPLING ROUTES



PPB SF6

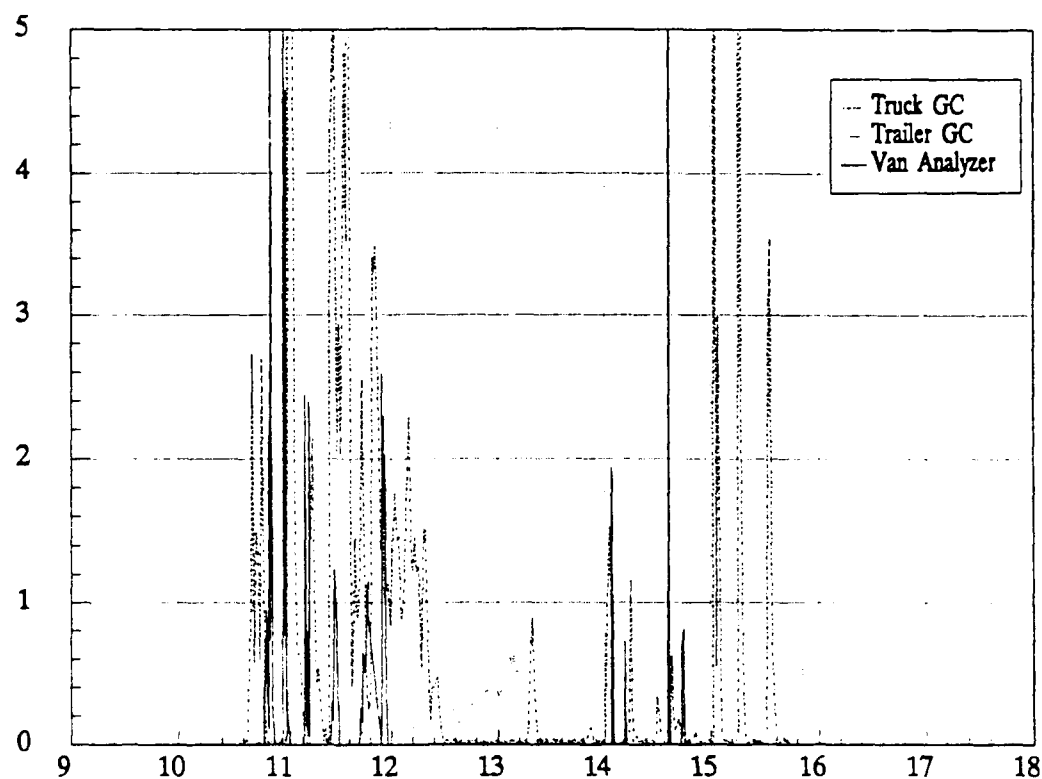


SF6 Release Rate, Kg/hr

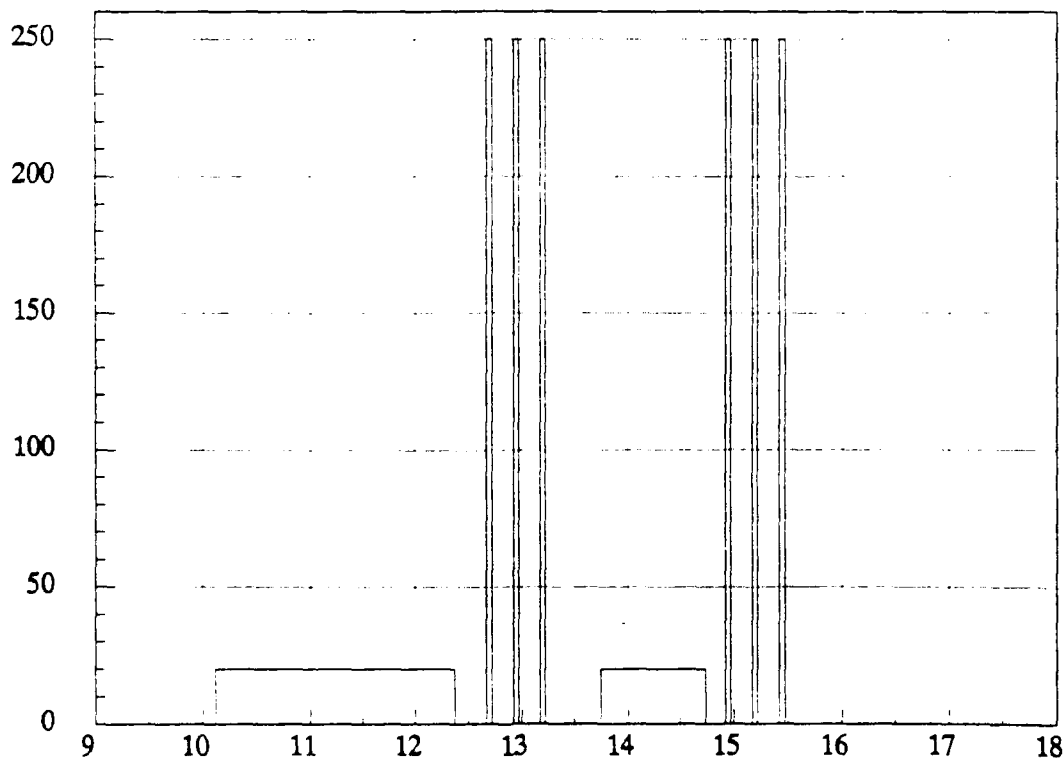


Hour on 8/10/89

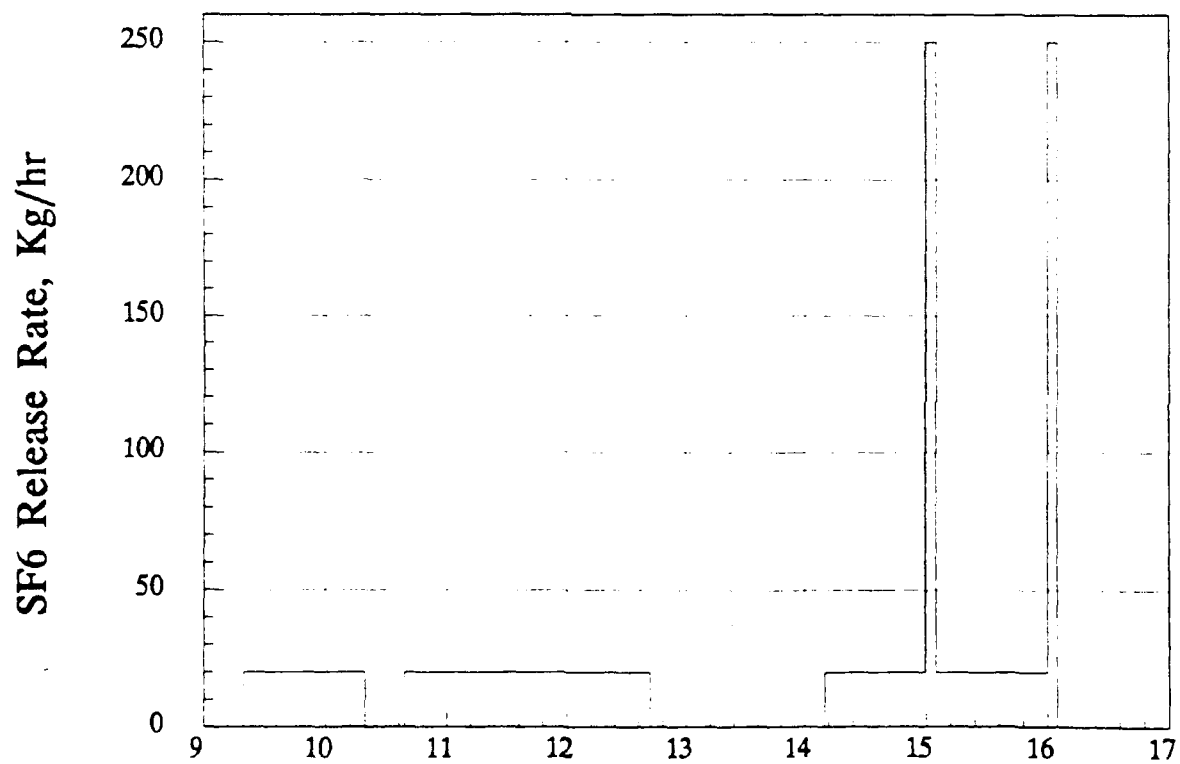
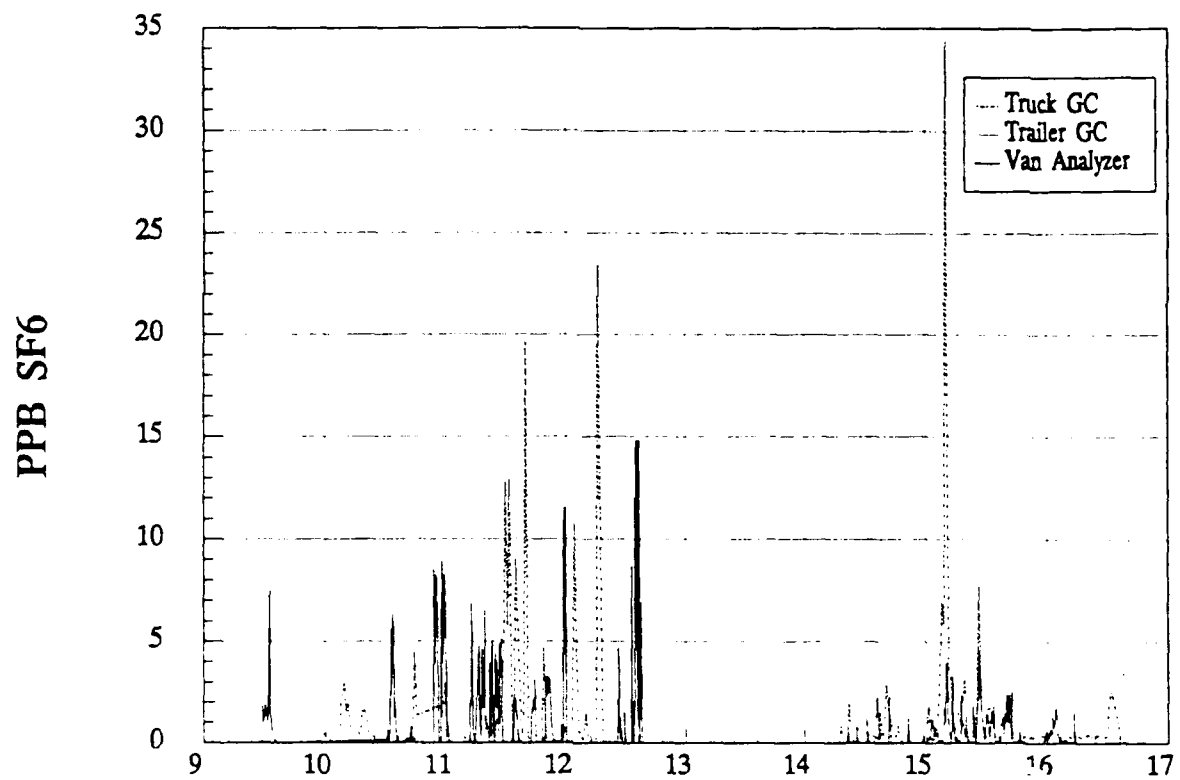
PPB SF6



SF6 Release Rate, Kg/hr

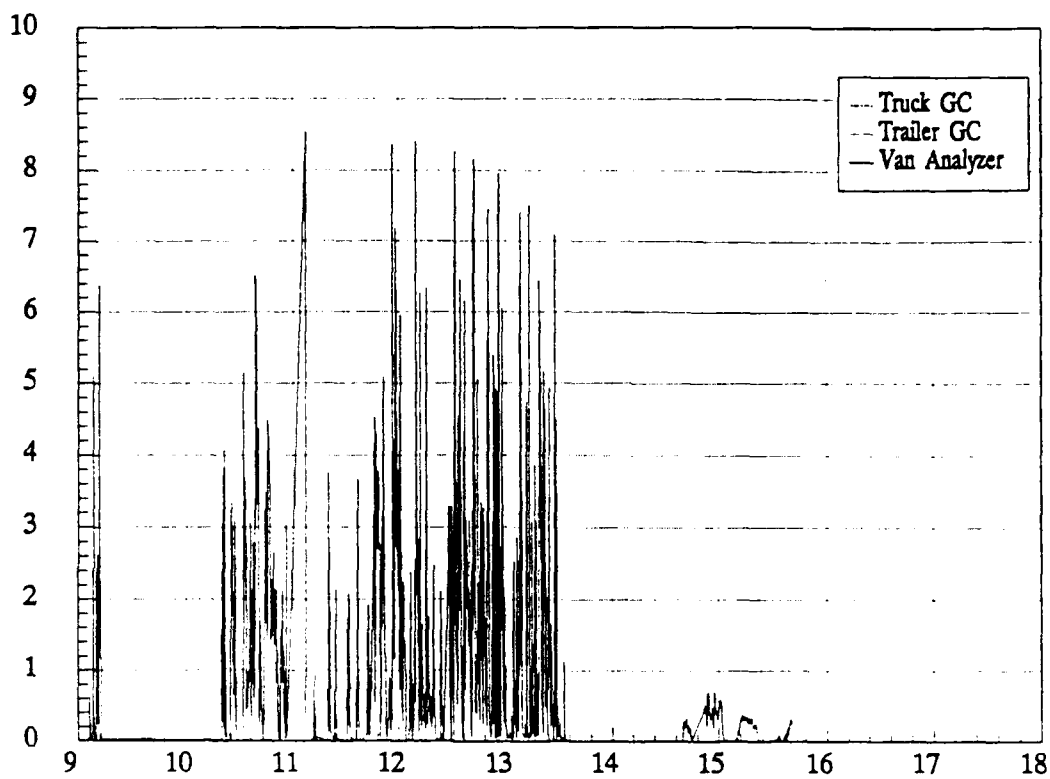


Hour on 8/11/89

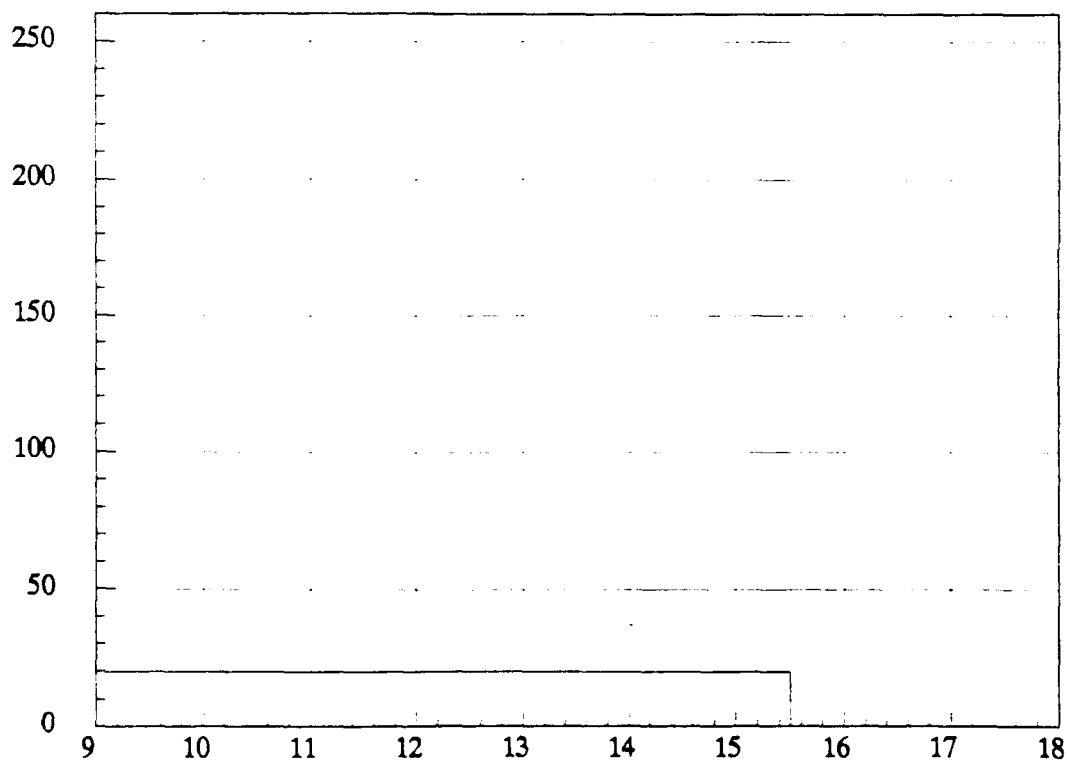


Hour on 8/12/89

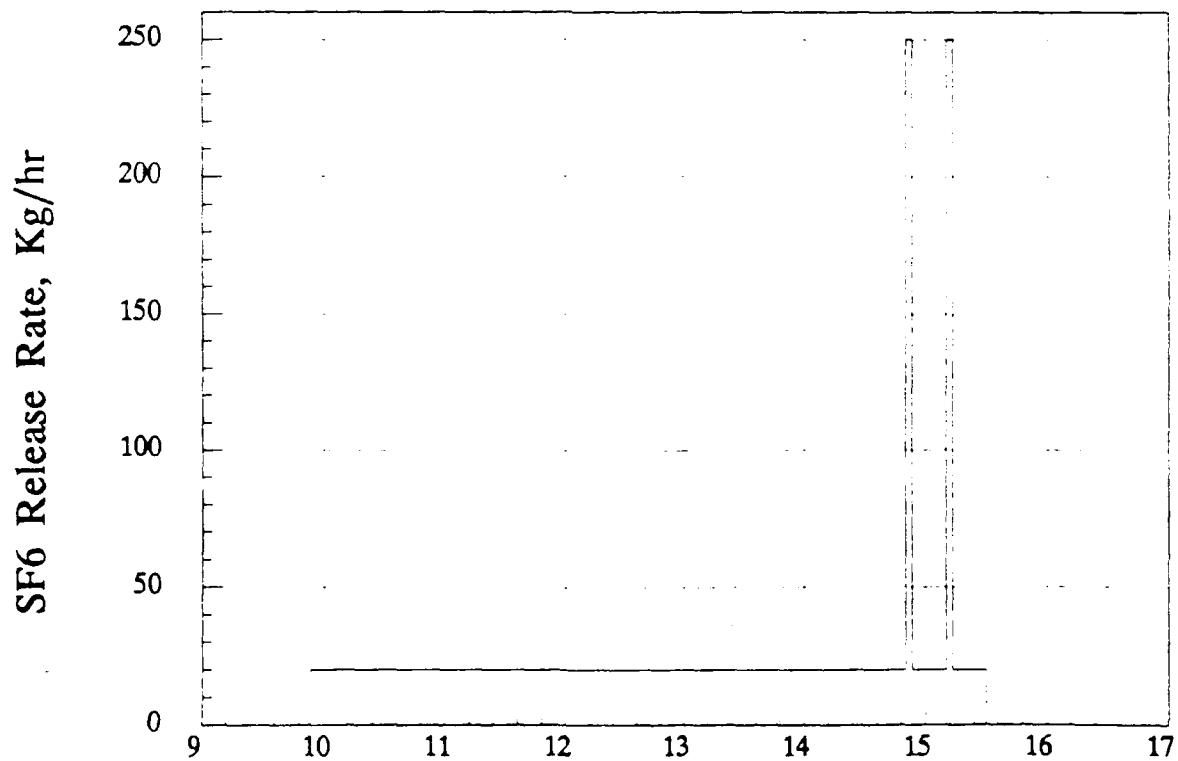
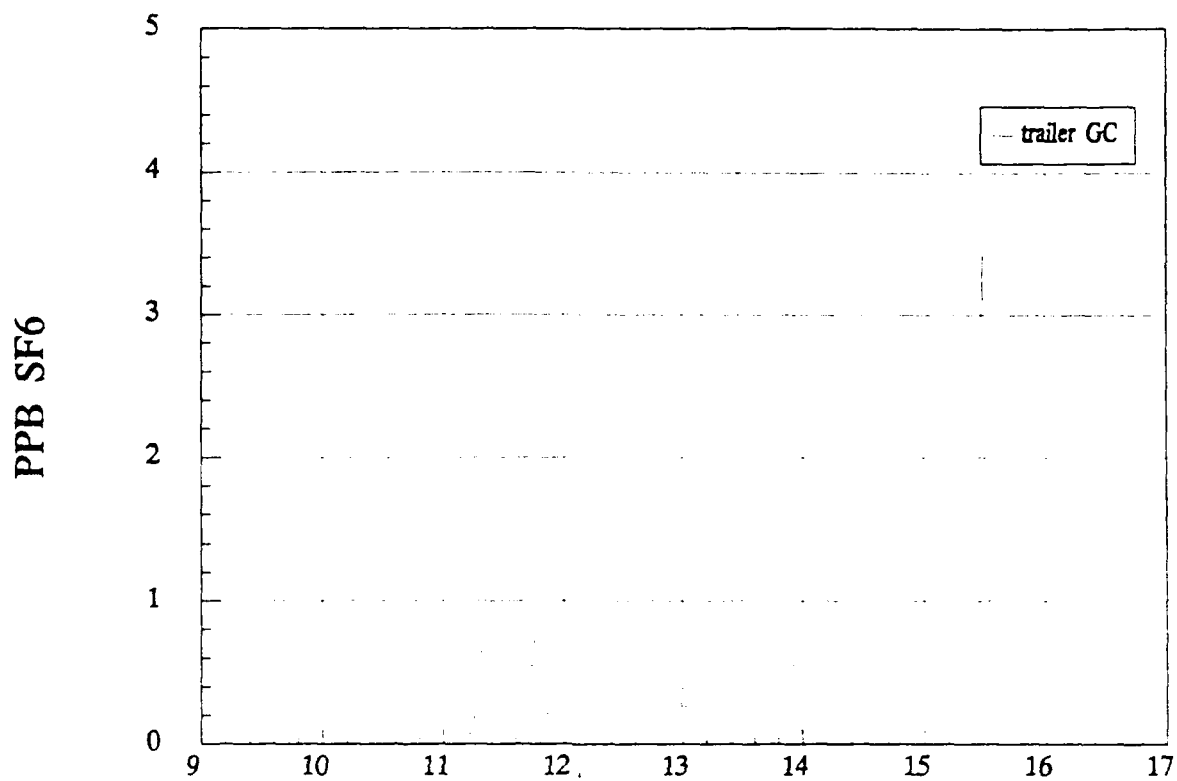
PPB SF6



SF6 Release Rate, Kg/hr

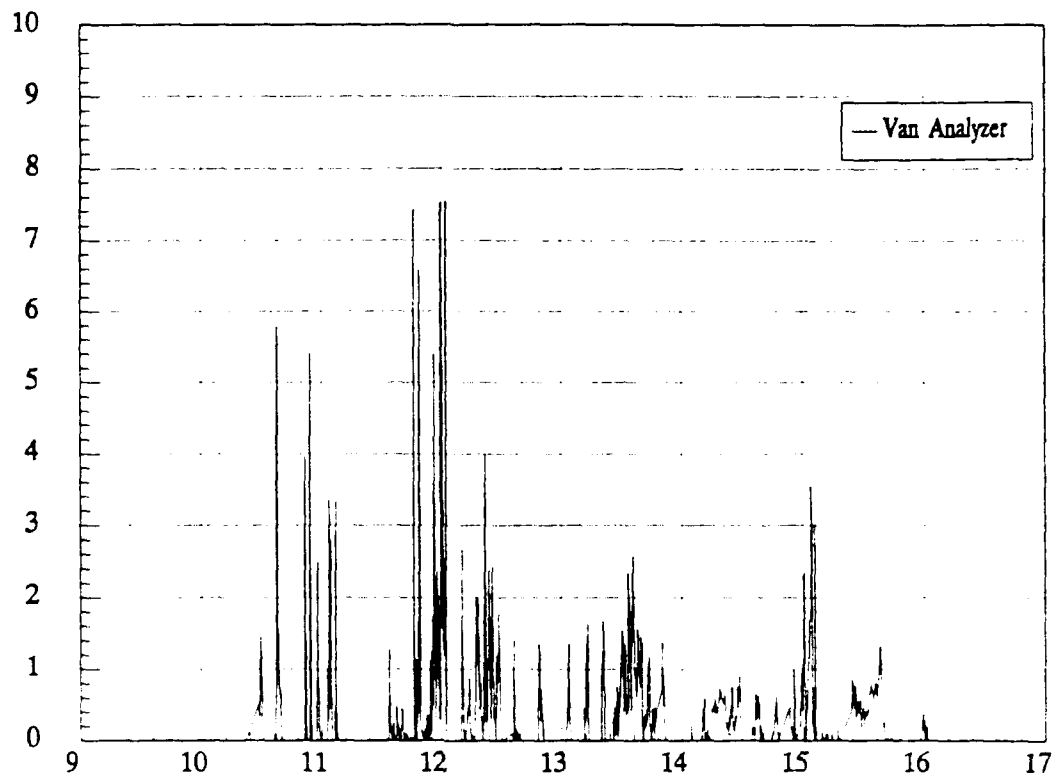


Hour on 8/13/89

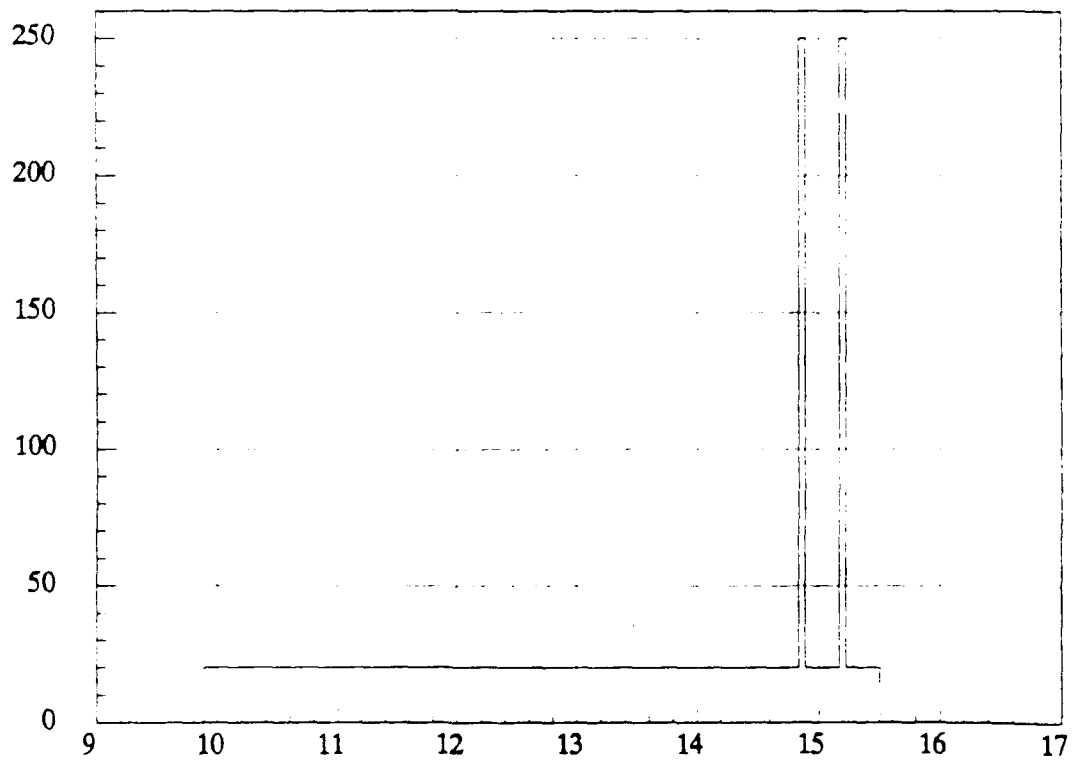


Hour on 8/14/89

PPB SF6

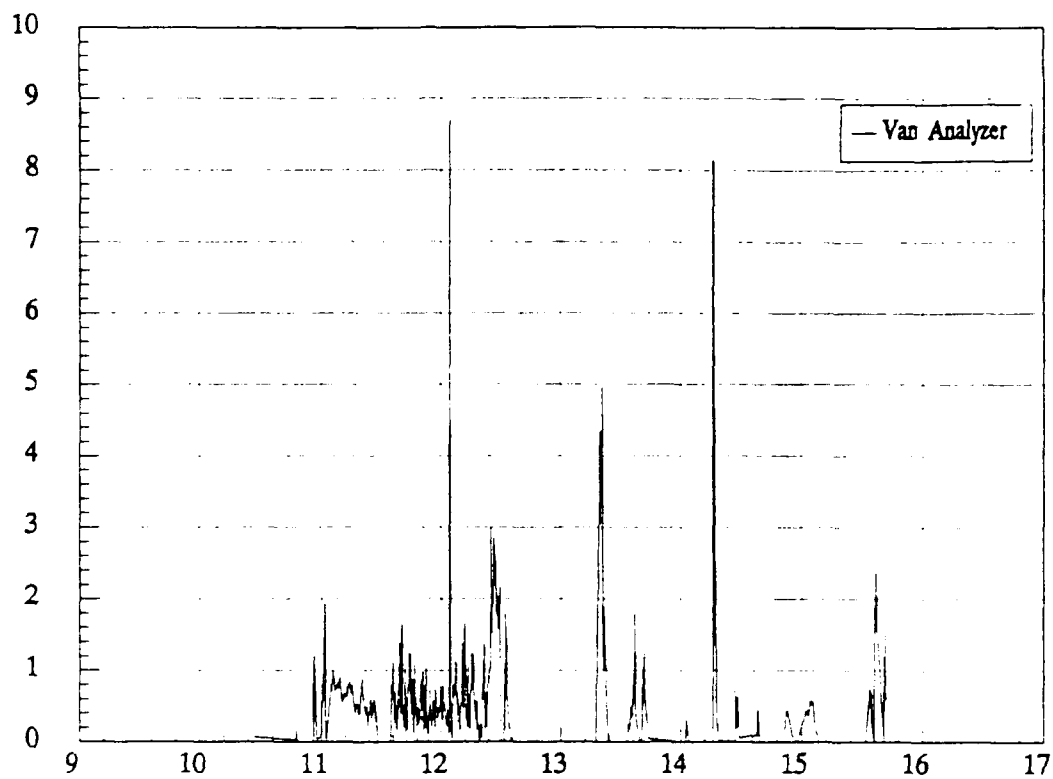


SF6 Release Rate, Kg/hr

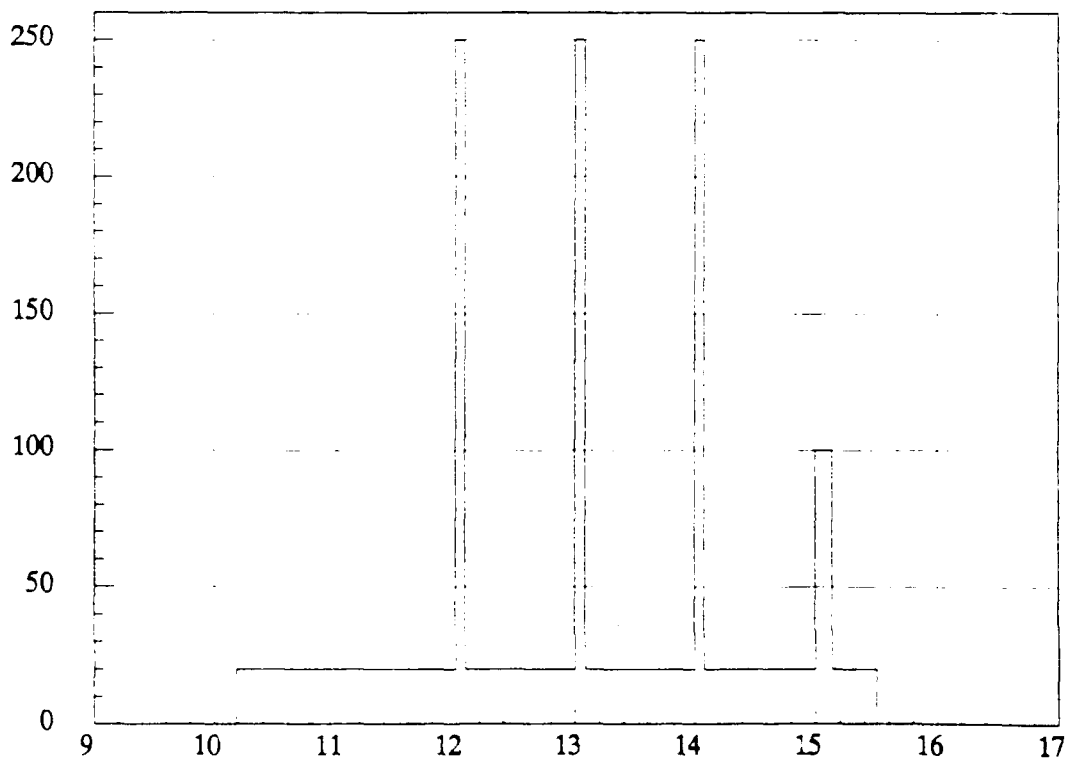


Hour on 8/14/89

PPB SF6

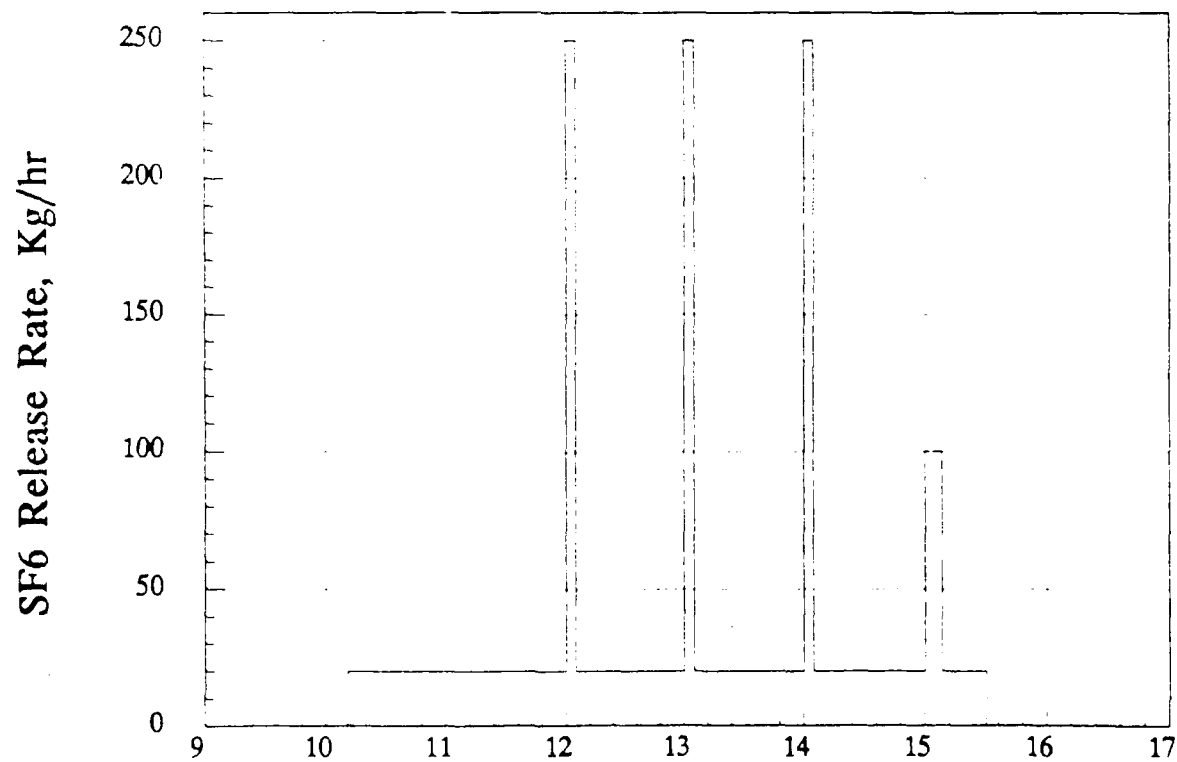
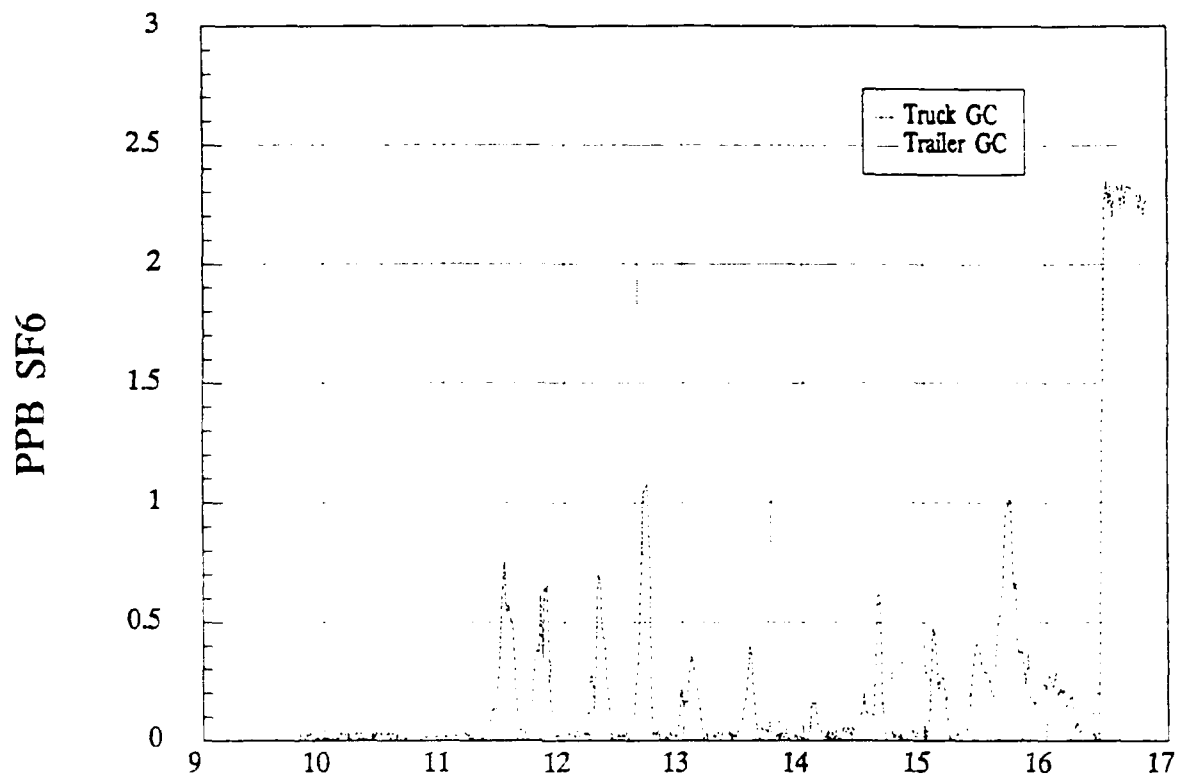


SF6 Release Rate, Kg/hr

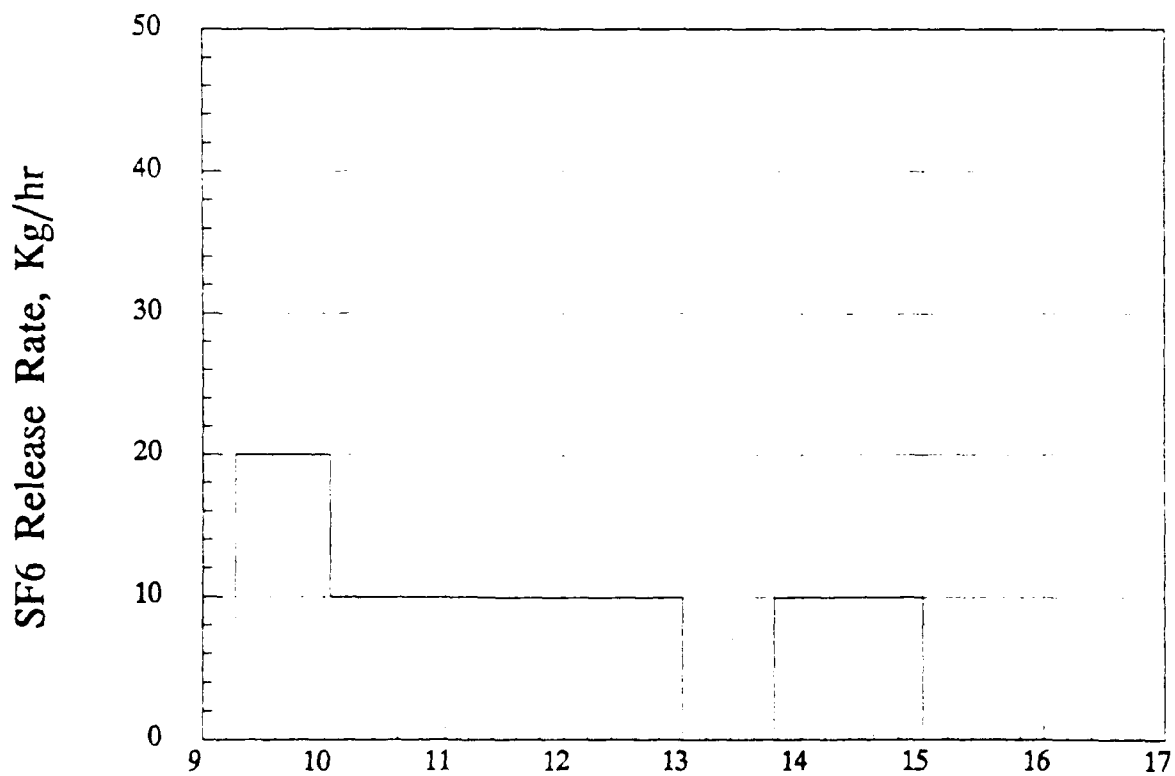
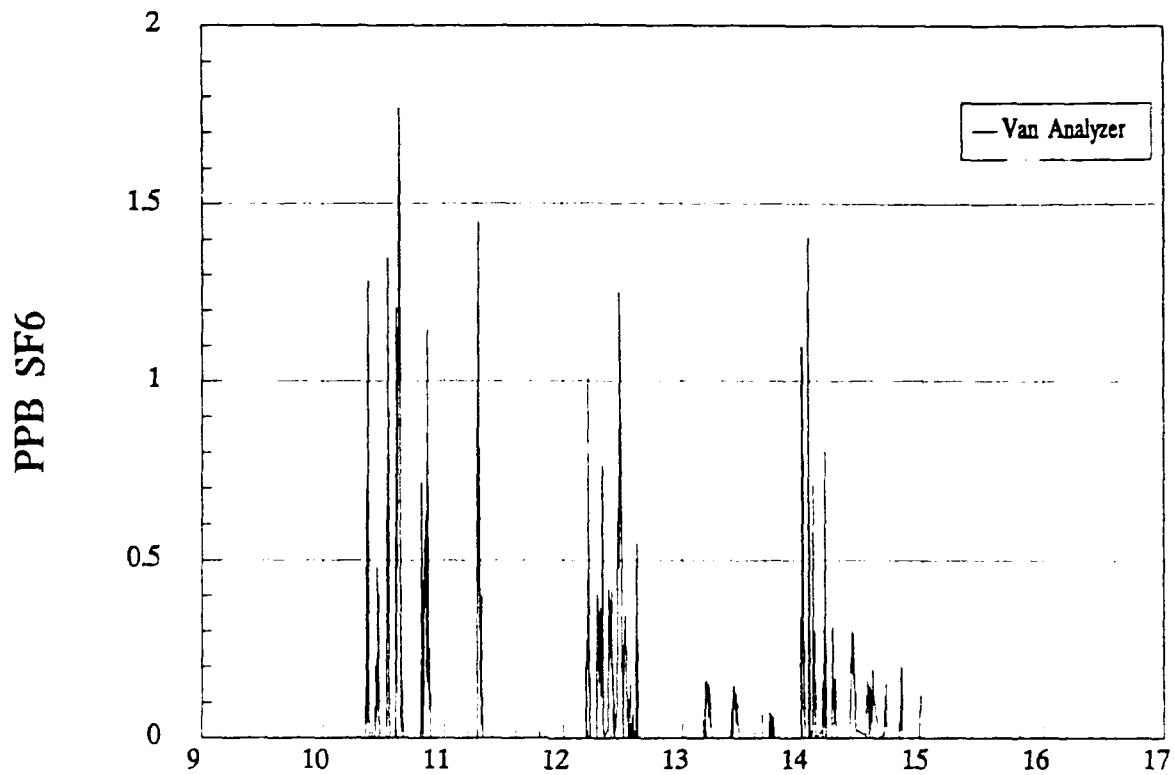


Hour on 8/15/89

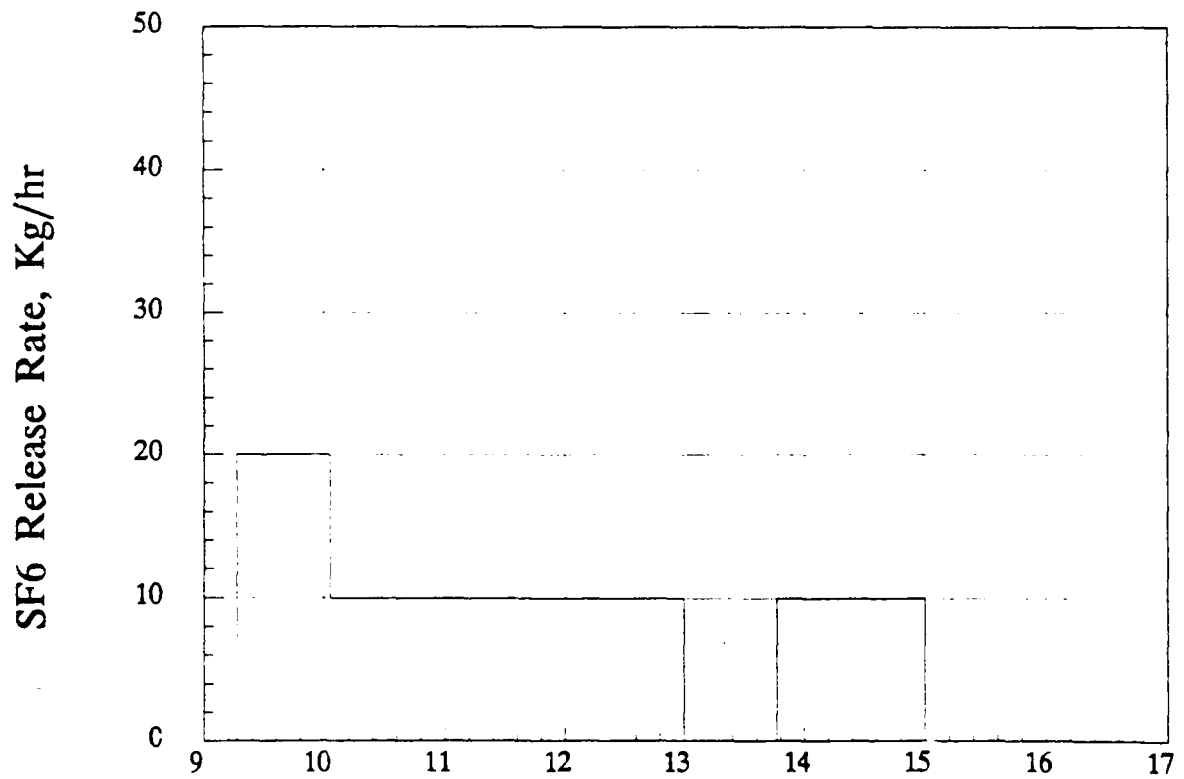
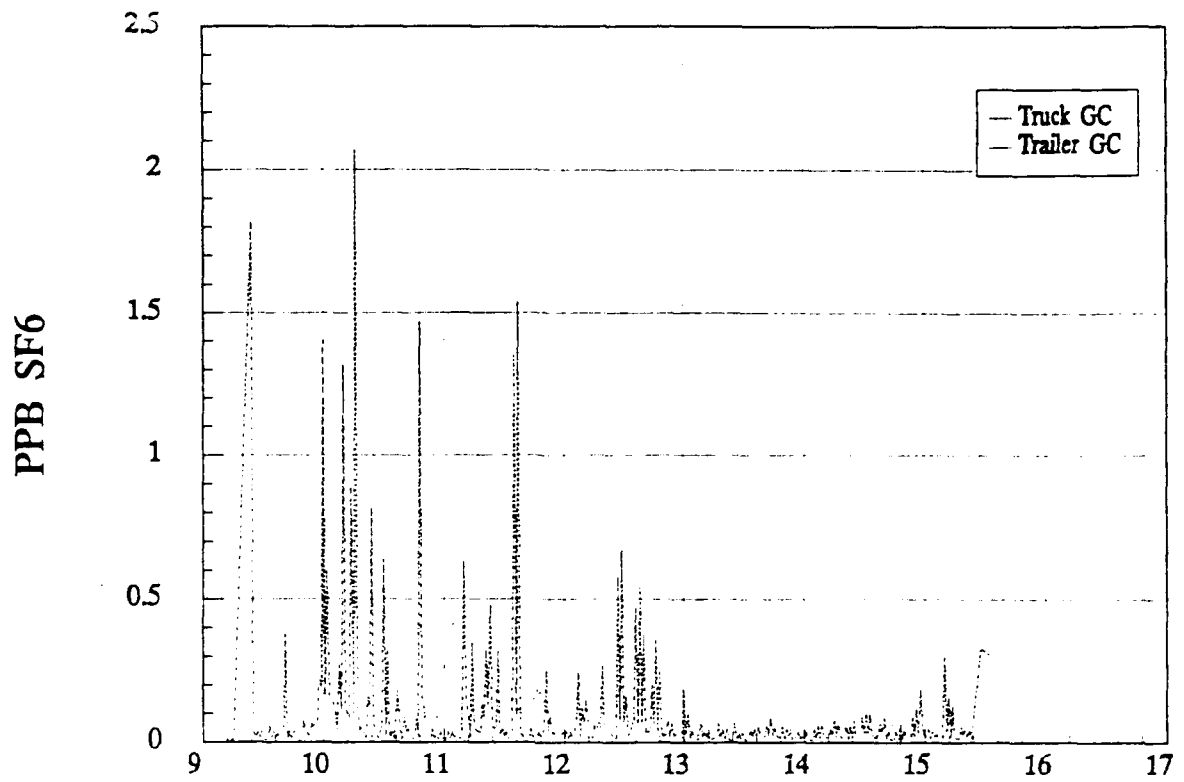
F3.8



Hour on 8/15/89

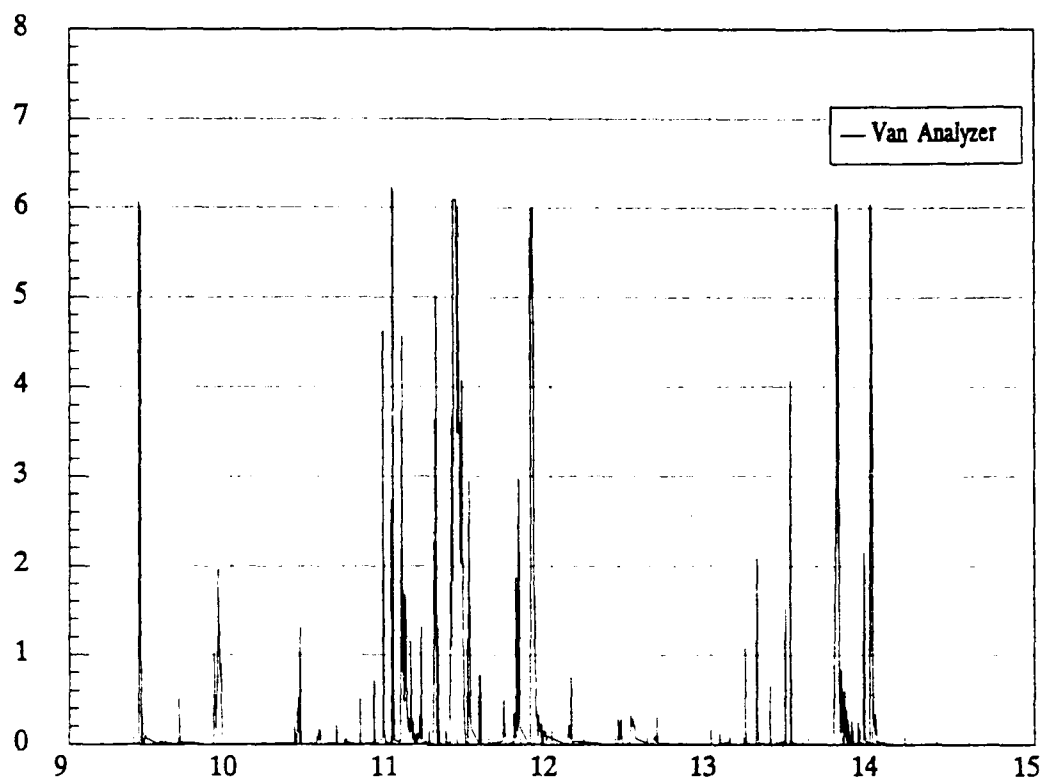


Hour on 8/16/89

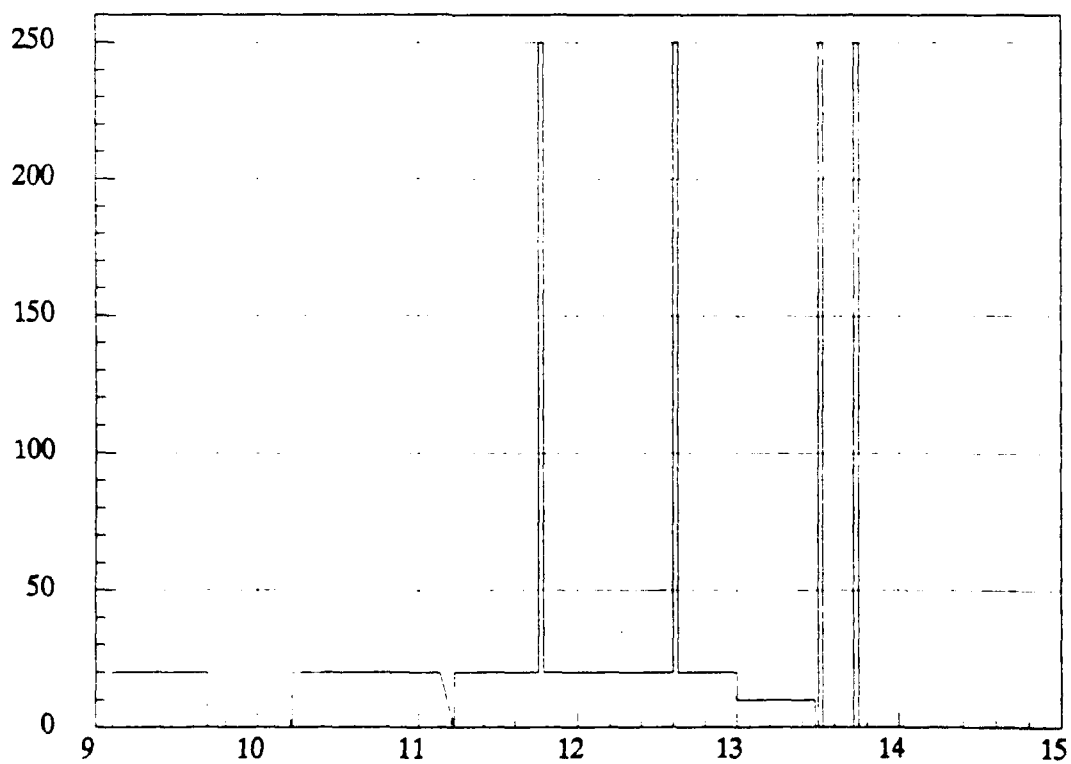


Hour on 8/16/89

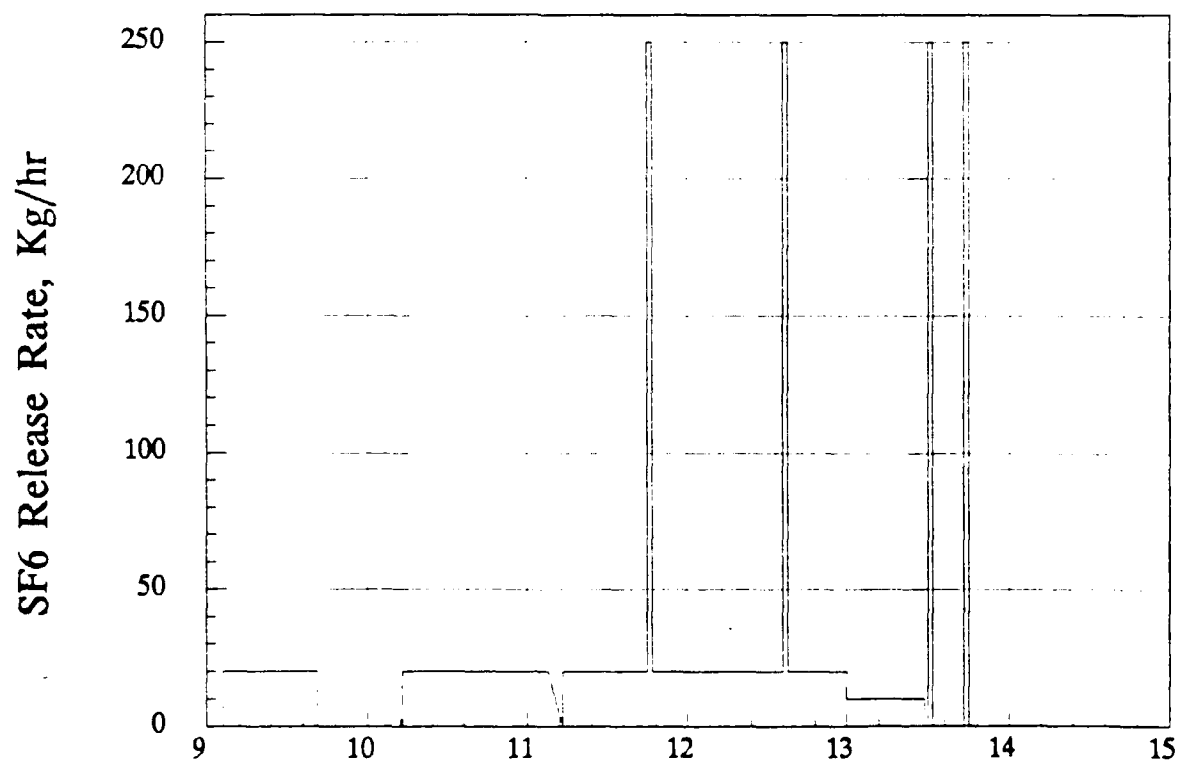
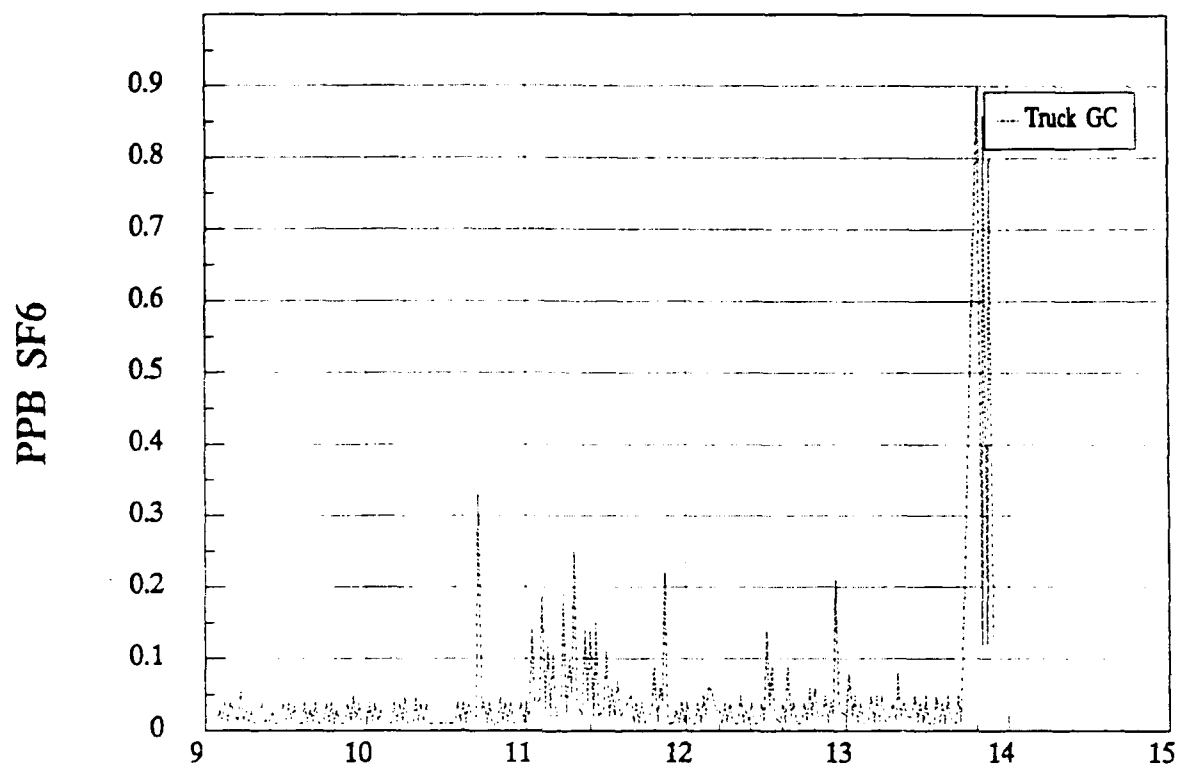
PPB SF6



SF6 Release Rate, Kg/hr



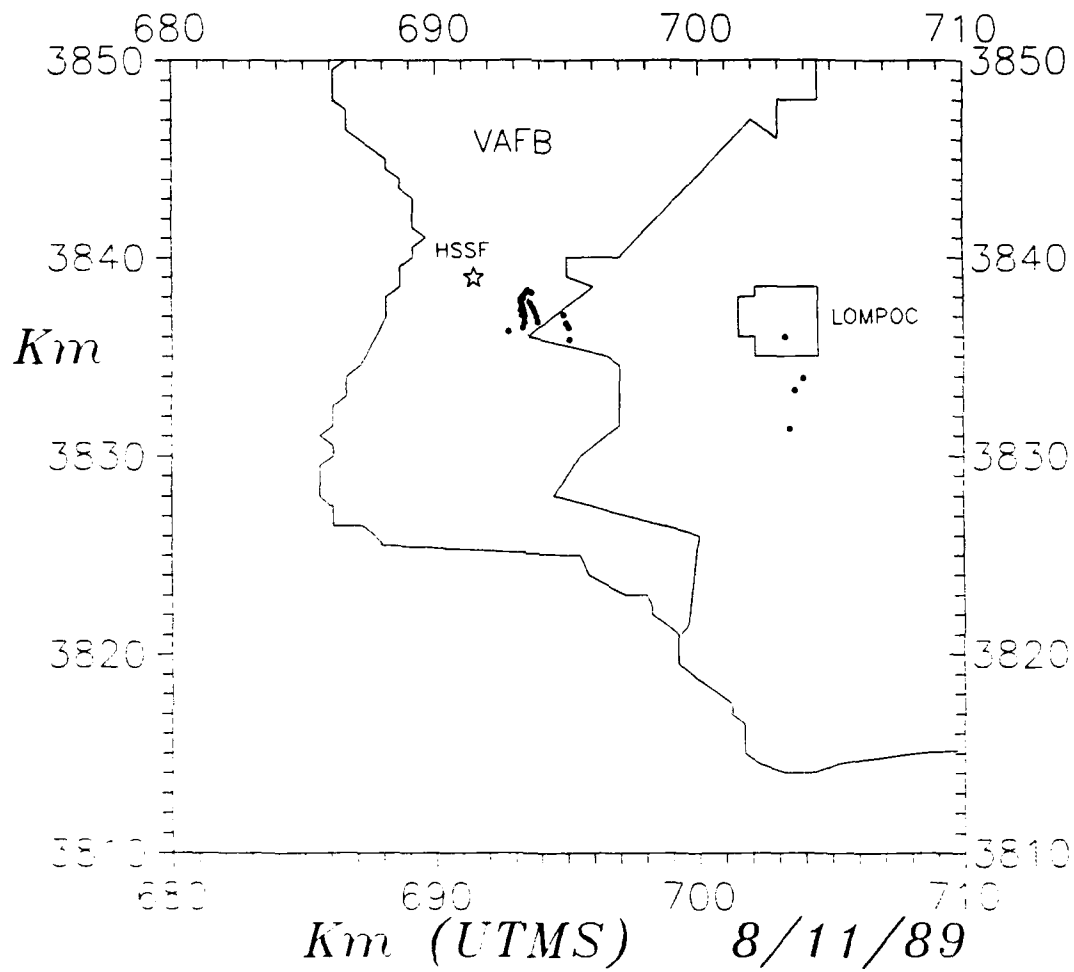
Hour on 8/17/89



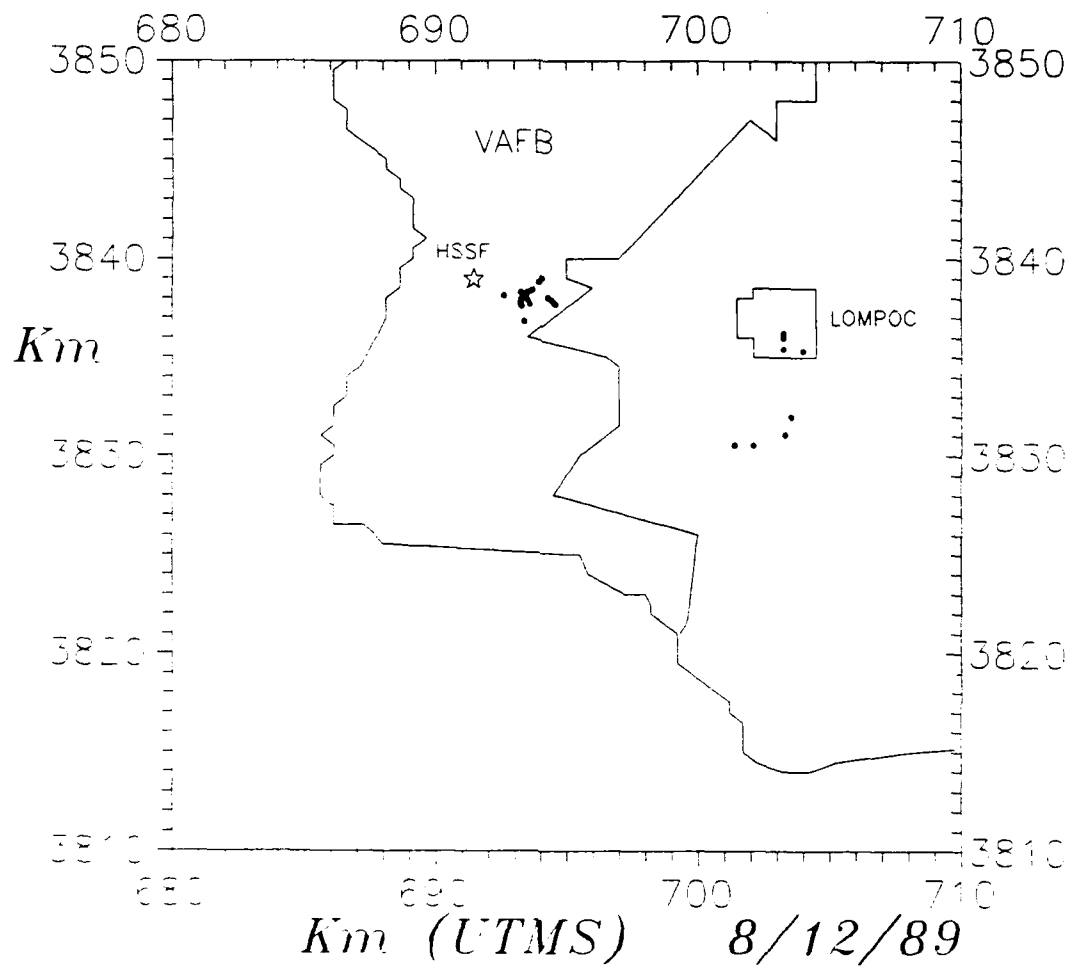
Hour on 8/17/89

Map of the Los Mochis area showing the VAFB, HSSF, and LOMPOC. The map includes a coordinate grid with latitude (Km) and longitude (Km (UTMS)) axes. The VAFB is a large area on the left, HSSF is a small area in the center, and LOMPOC is a small area on the right. The map is dated 8/10/89.

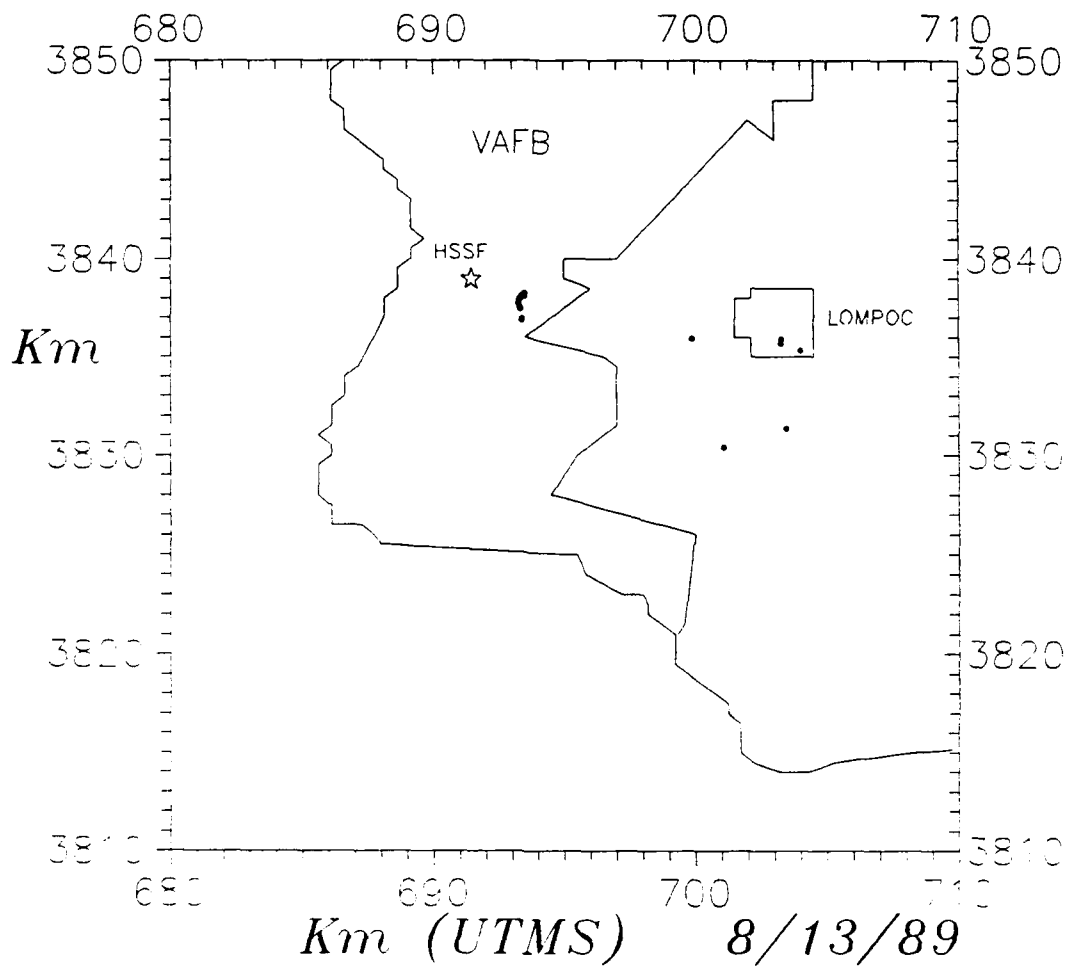
TRANSECT CENTERLINE LOCATIONS



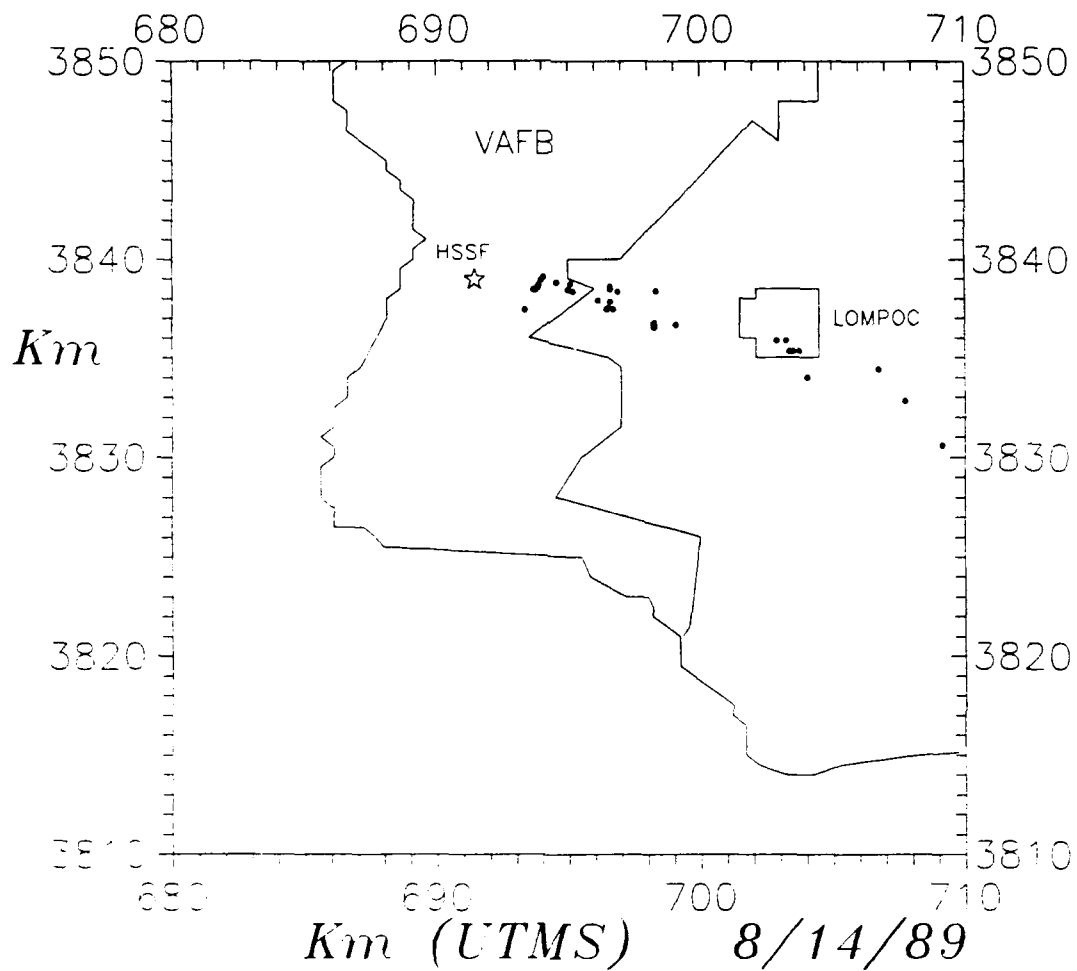
TRANSECT CENTERLINE LOCATIONS



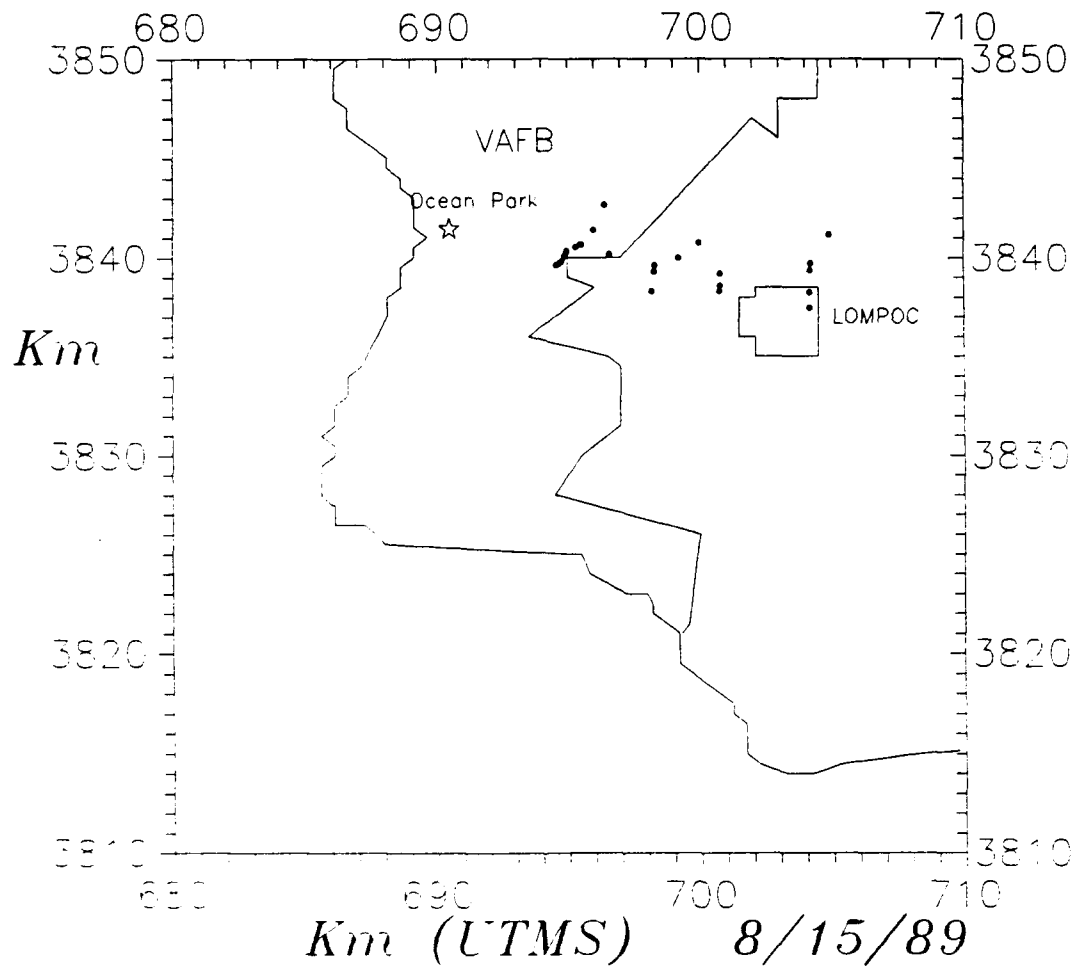
TRANSECT CENTERLINE LOCATIONS



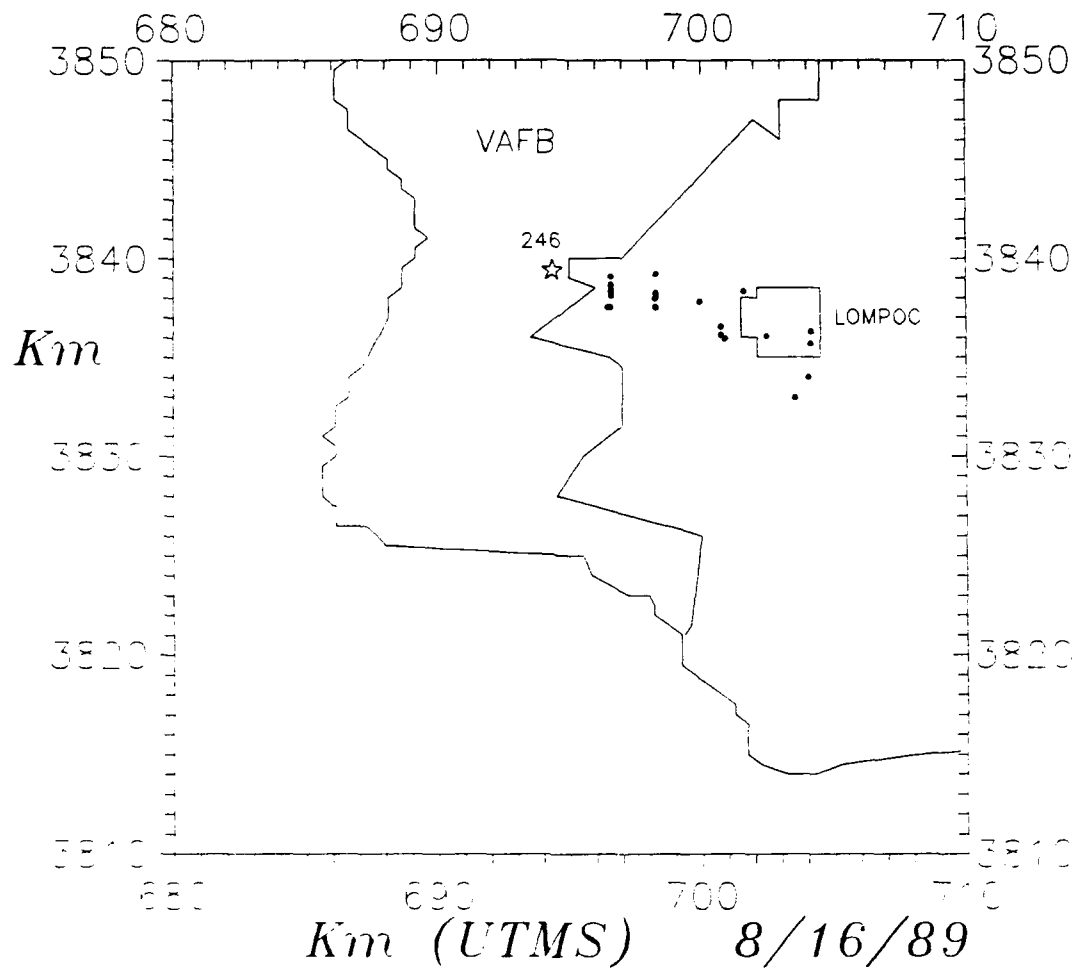
TRANSECT CENTERLINE LOCATIONS

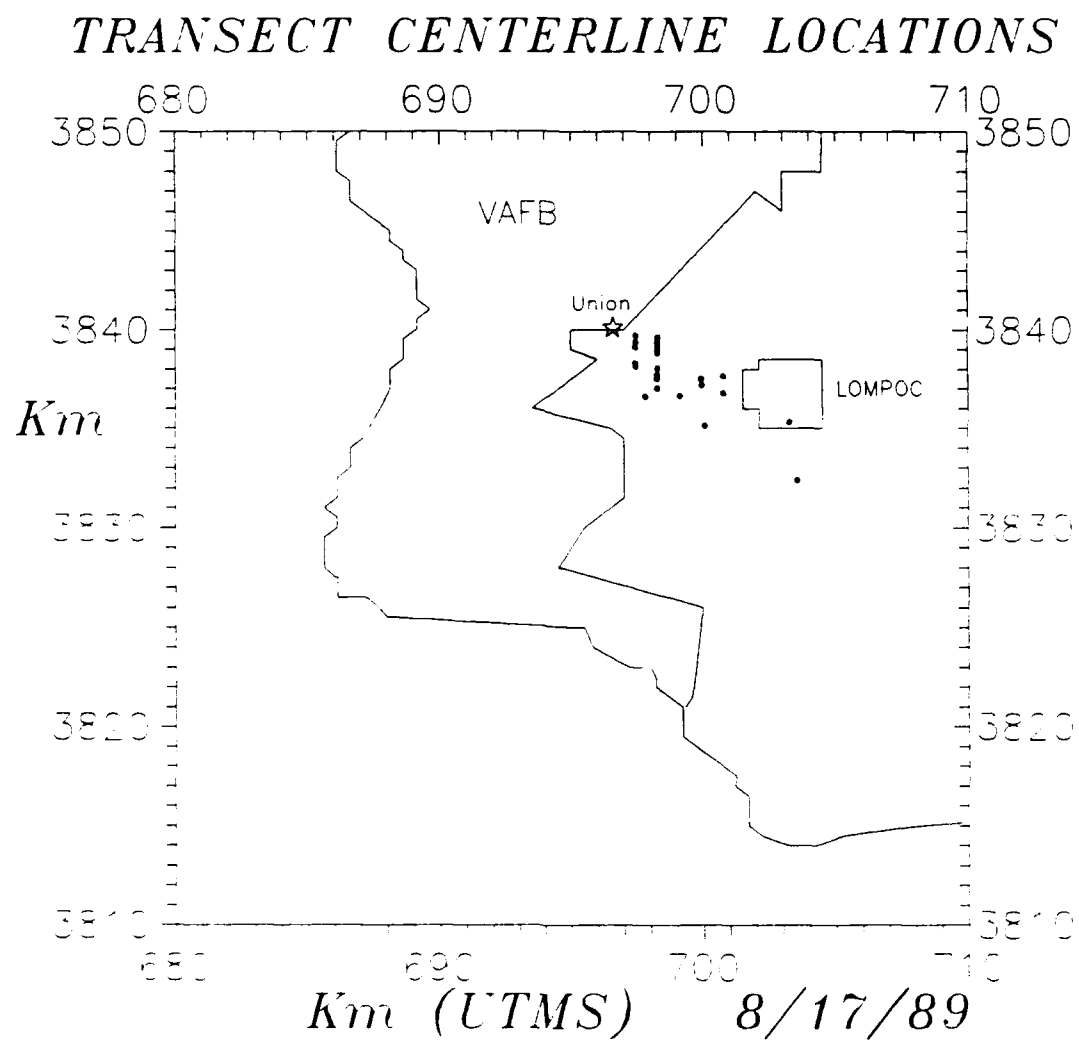


TRANSECT CENTERLINE LOCATIONS

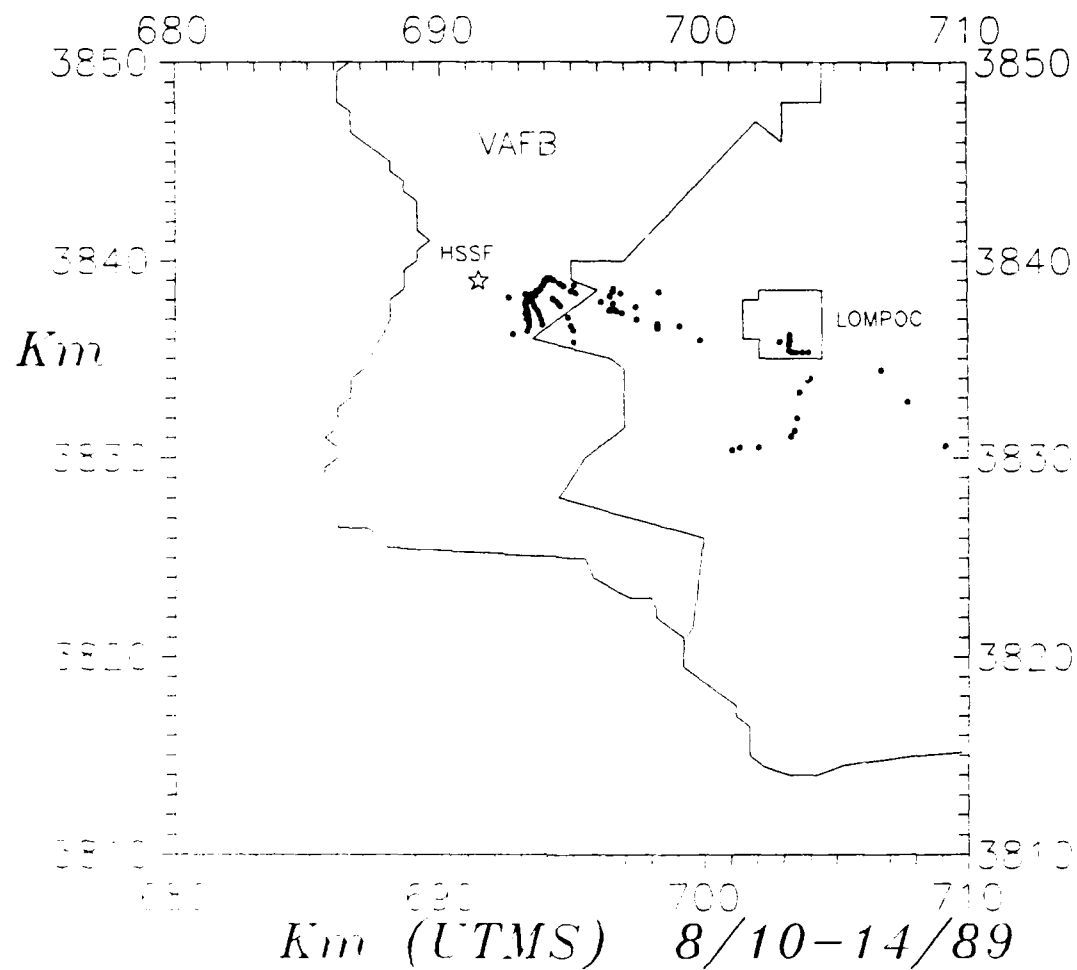


TRANSECT CENTERLINE LOCATIONS



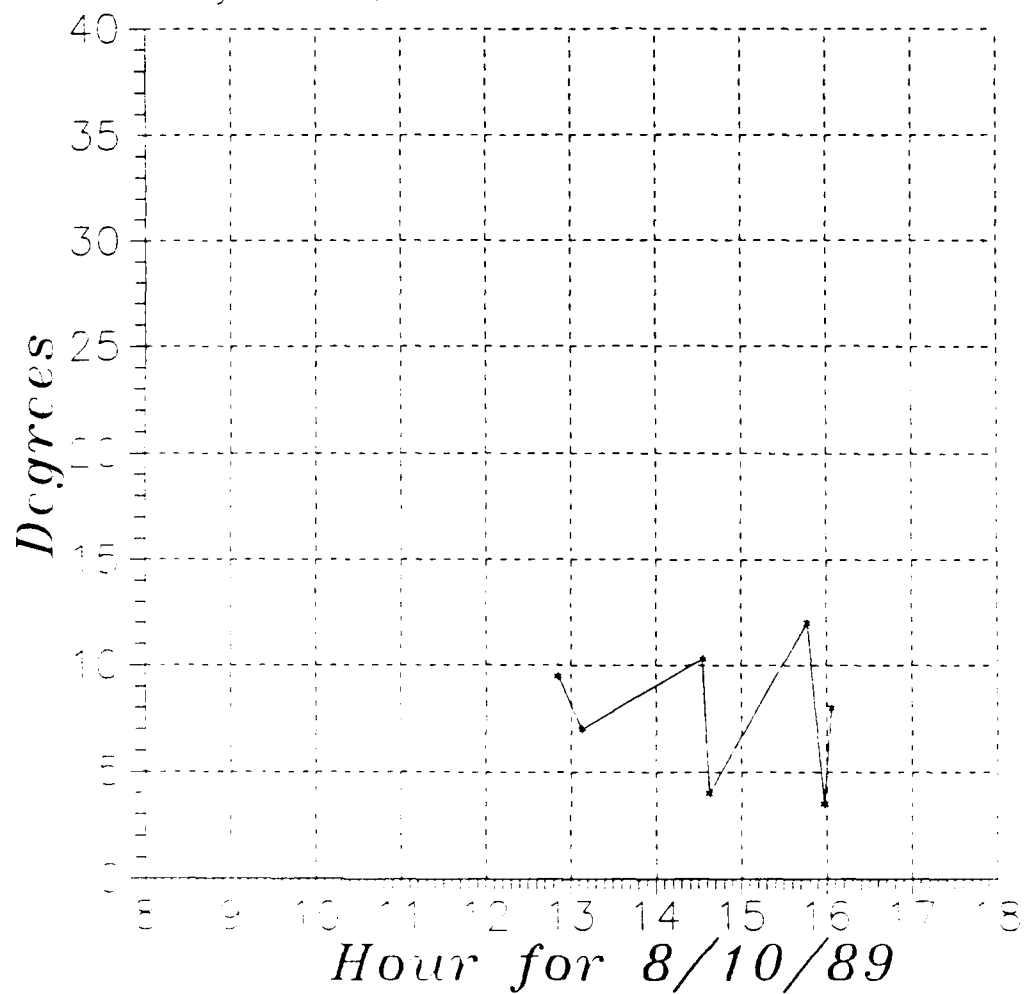


TRANSECT CENTERLINE LOCATIONS



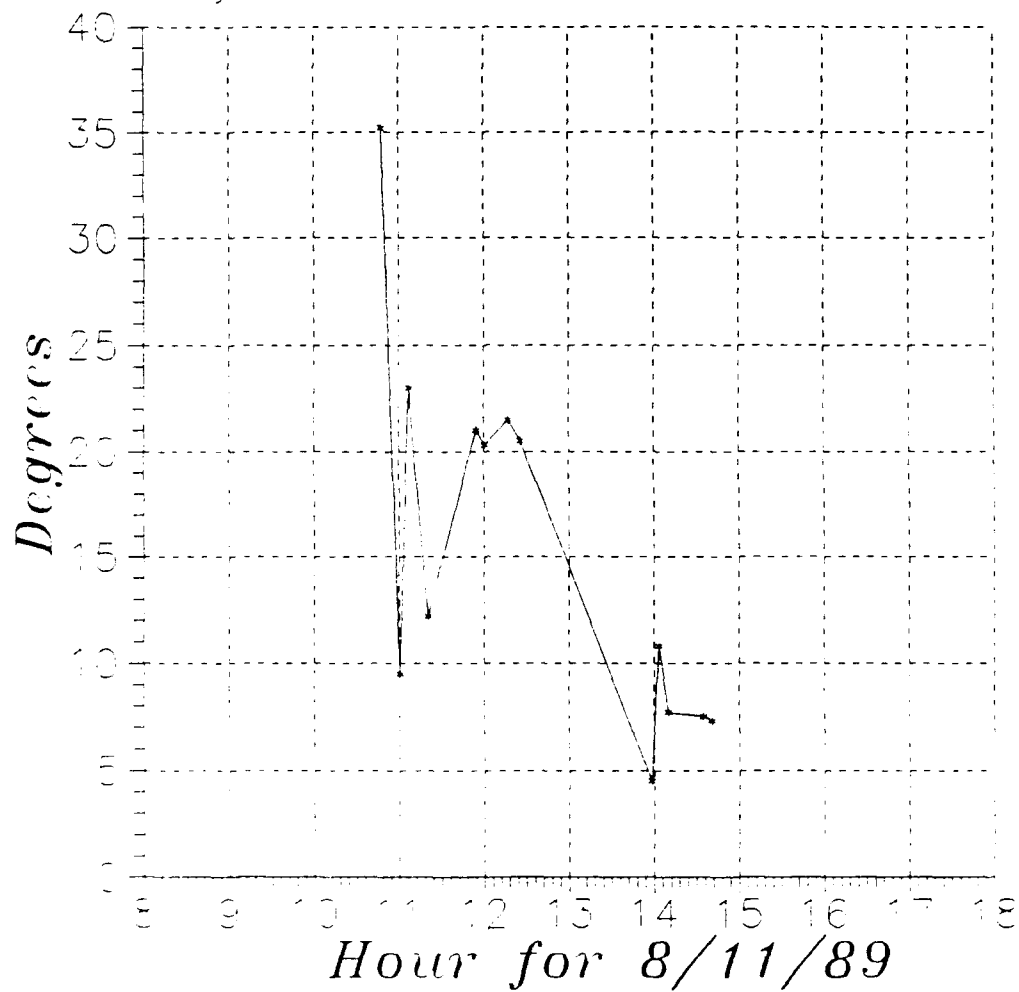
PLUME WIDTH (to 0.1 max conc.)

Van Analyzer data, SF6 Release from HSSF



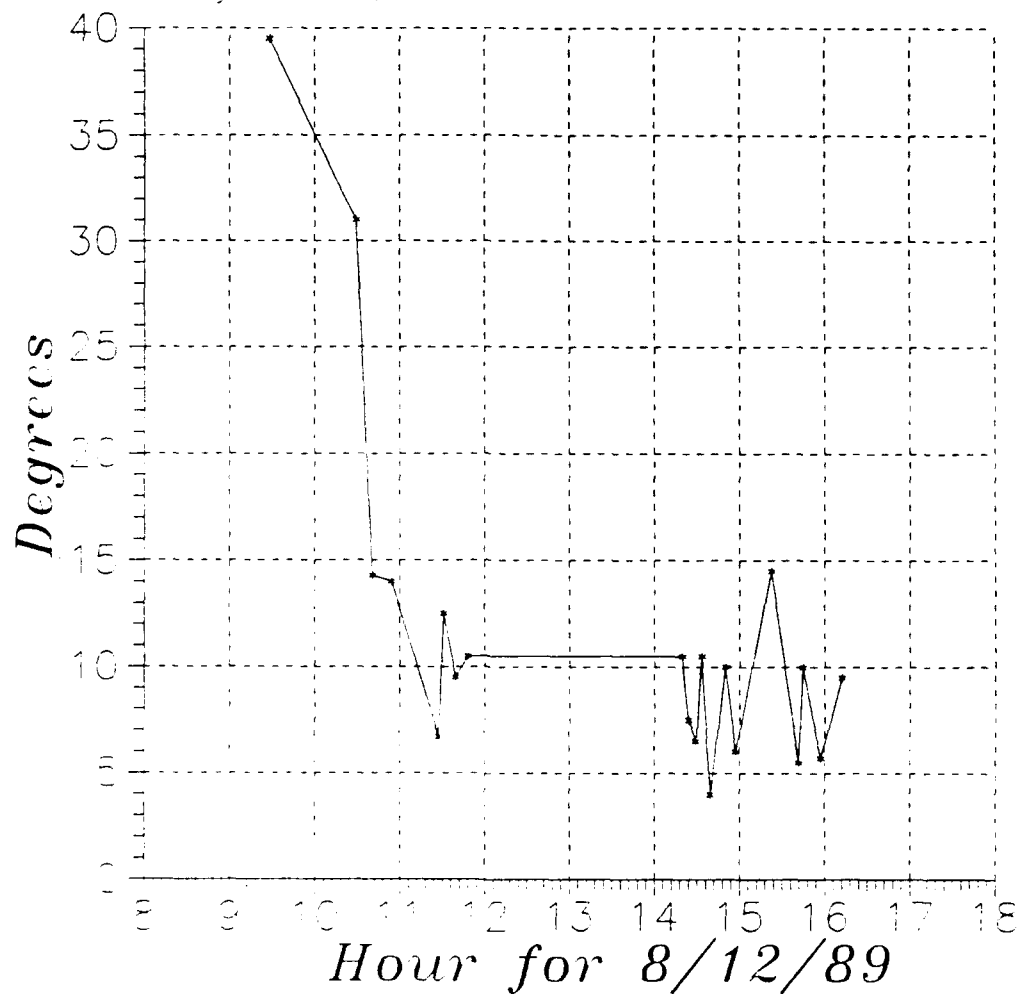
PLUME WIDTH (to 0.1 max conc.)

Van Analyzer data, SF6 Release from HSSF



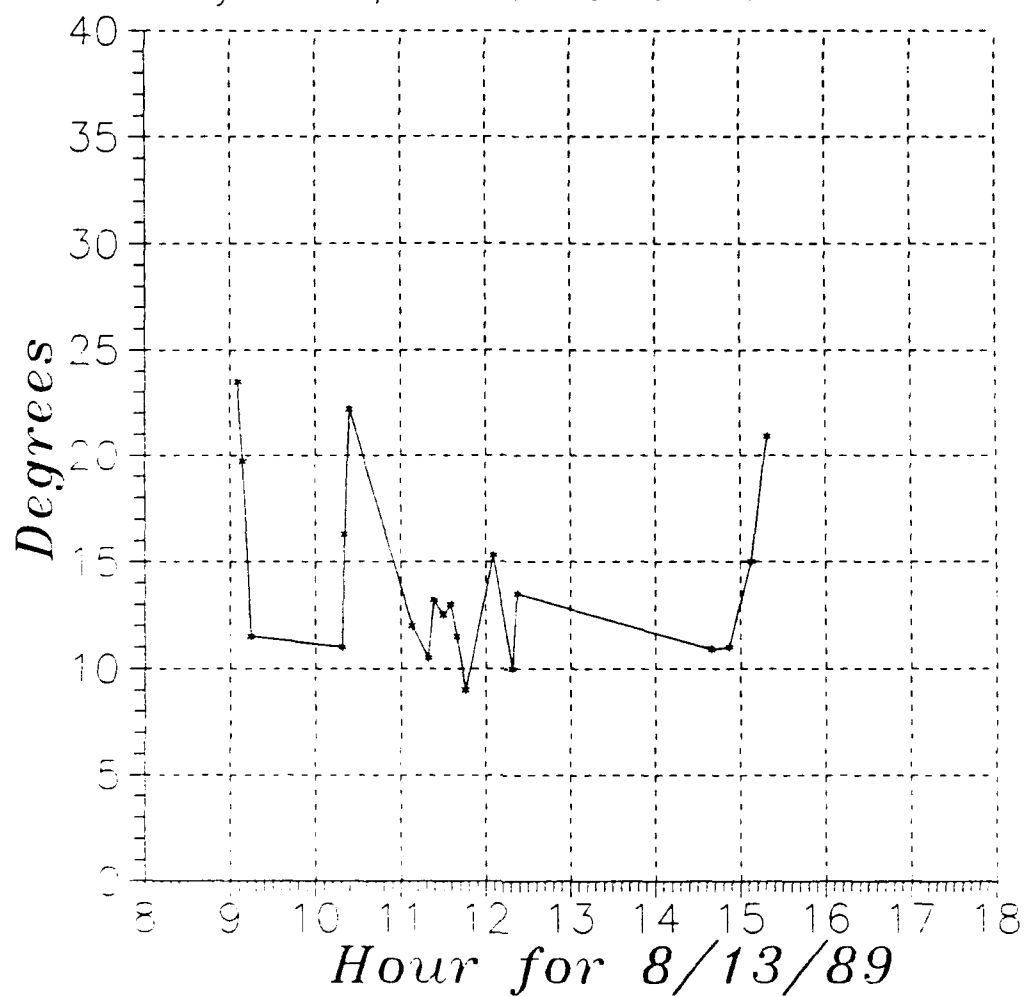
PLUME WIDTH (to 0.1 max conc.)

Van Analyzer data, SF6 Release from HSSF



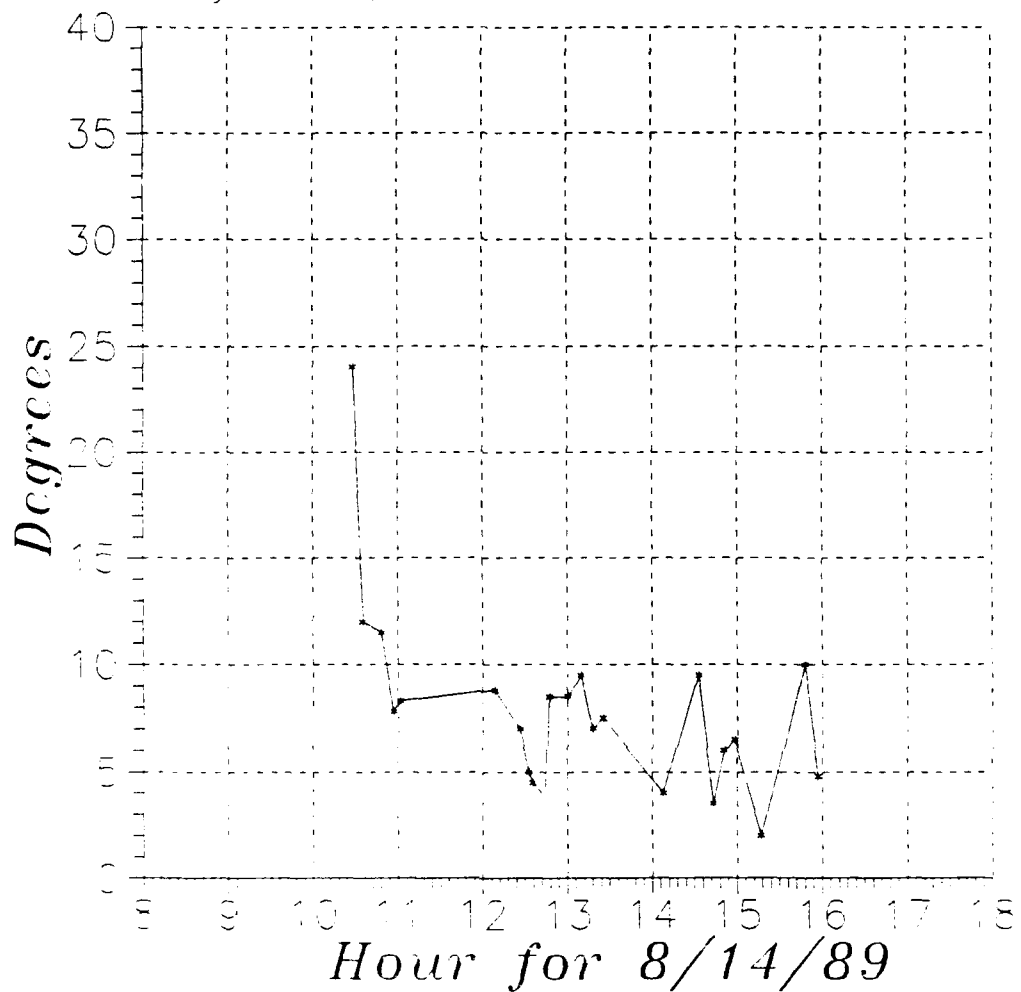
PLUME WIDTH (to 0.1 max conc.)

Van Analyzer data, SF6 Release from HSSF



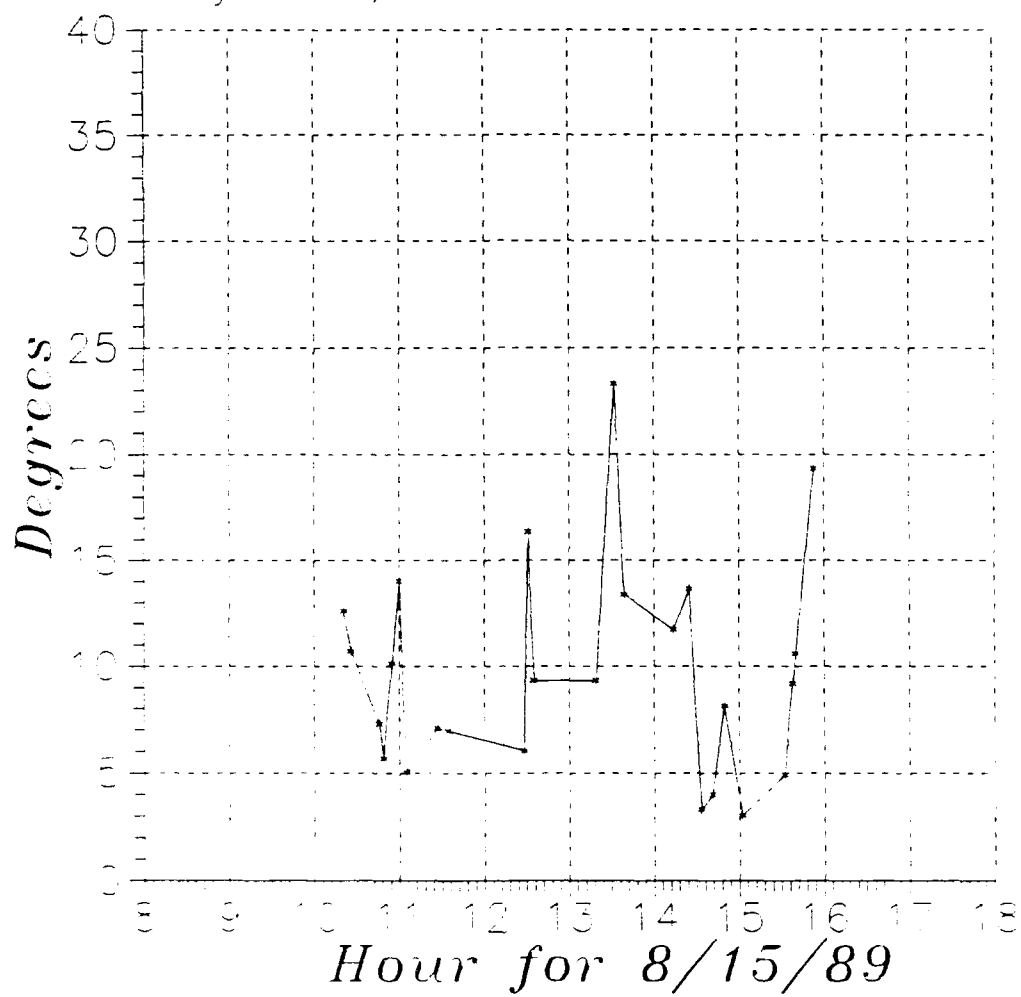
PLUME WIDTH (to 0.1 max conc.)

Van Analyzer data, SF6 Release from HSSF



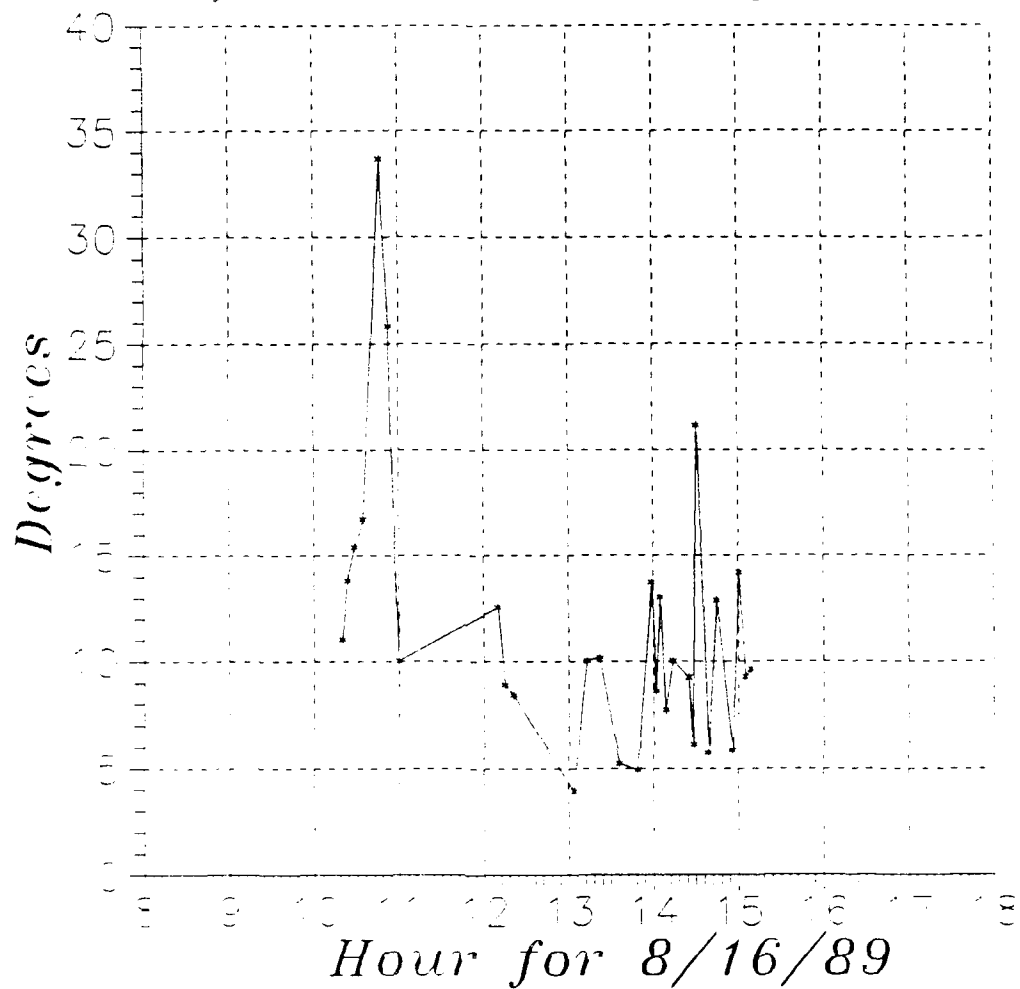
PLUME WIDTH (to 0.1 max conc.)

Van Analyzer data, SF6 Release from Ocean Park



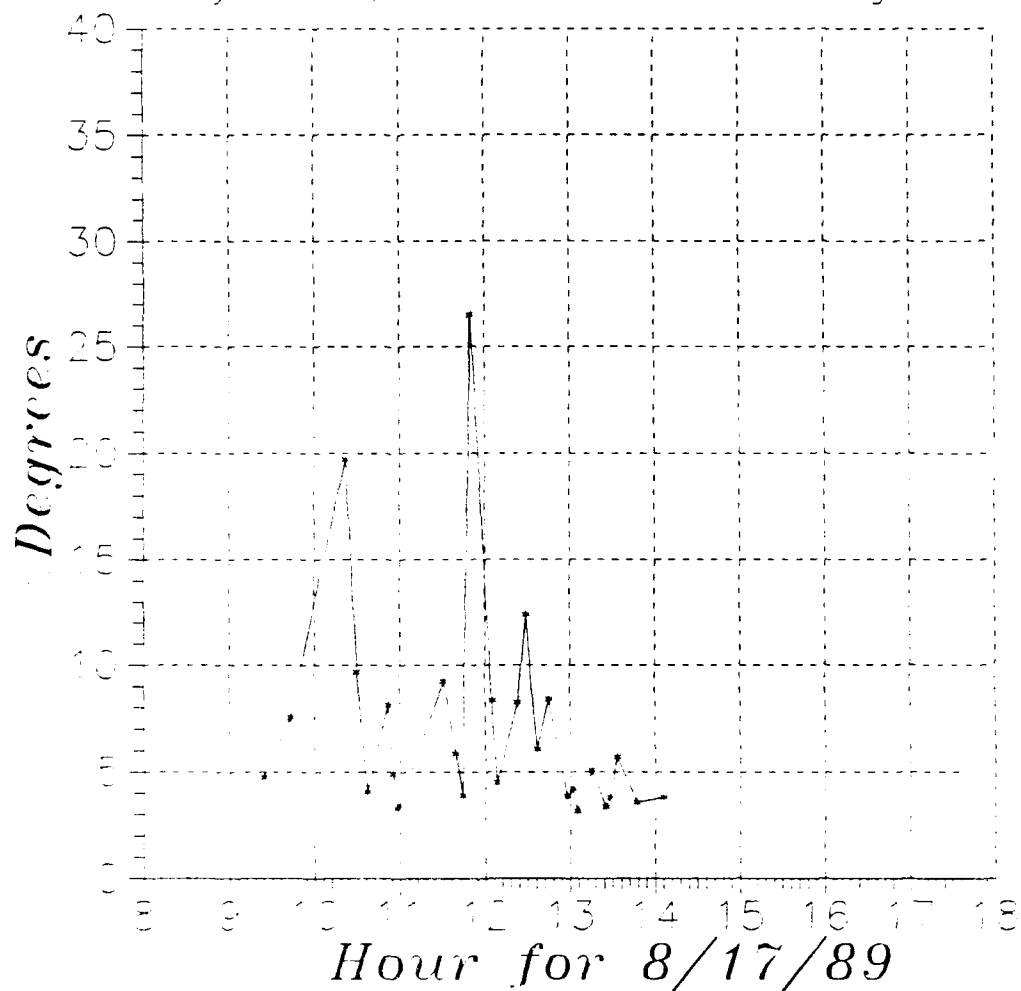
PLUME WIDTH (to 0.1 max conc.)

Van Analyzer data, SF6 Release from Arguello & 246



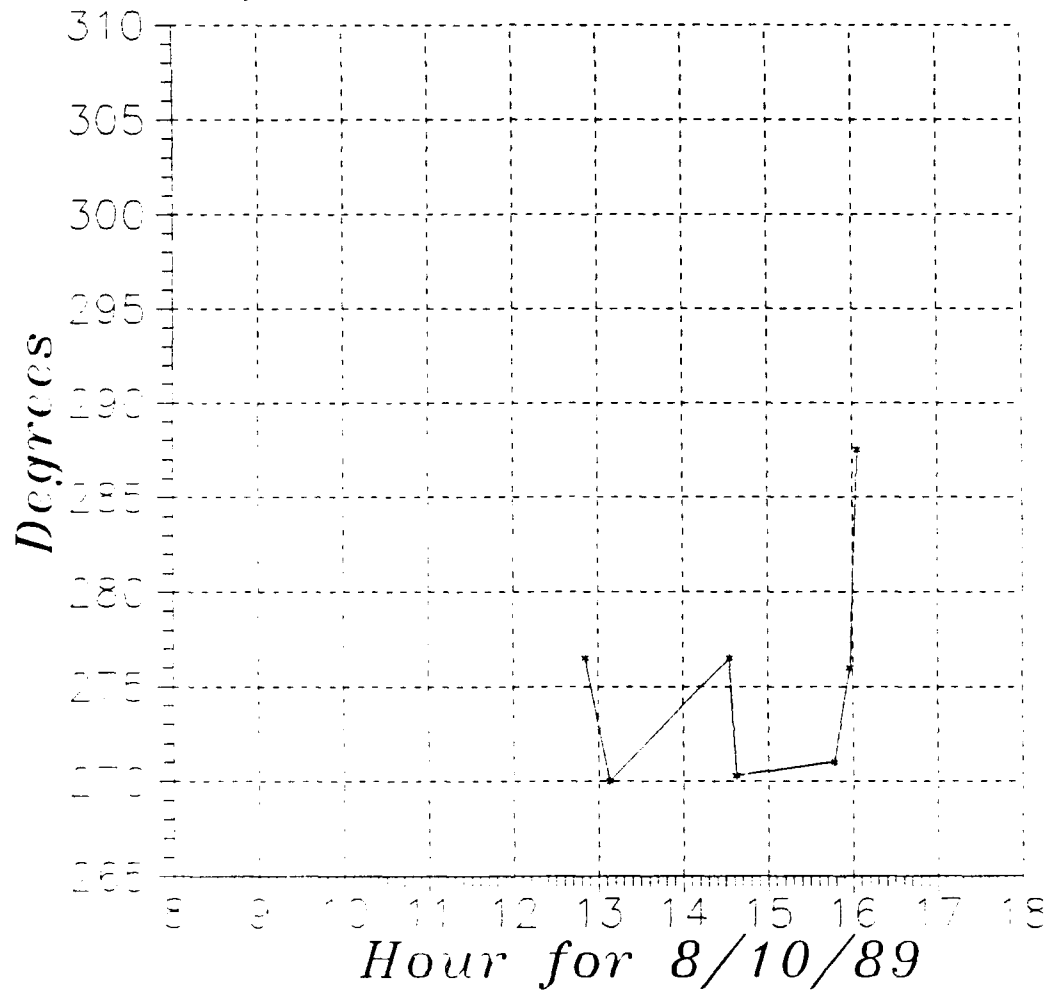
PLUME WIDTH (to 0.1 max conc.)

Var Analyzer data, SF6 Release from Union Sugar Rd



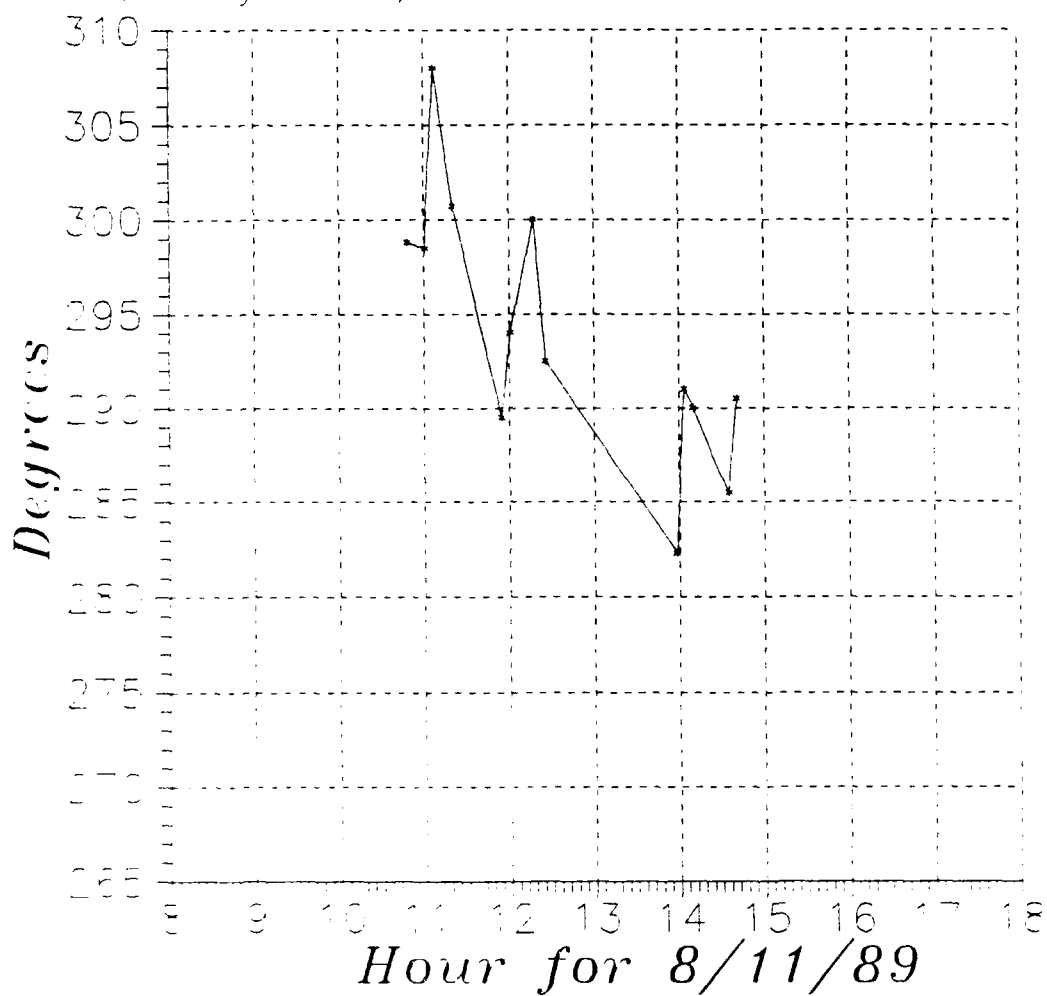
PLUME CENTERLINE DIRECTION

Van Analyzer data, SF6 Release from HSSF



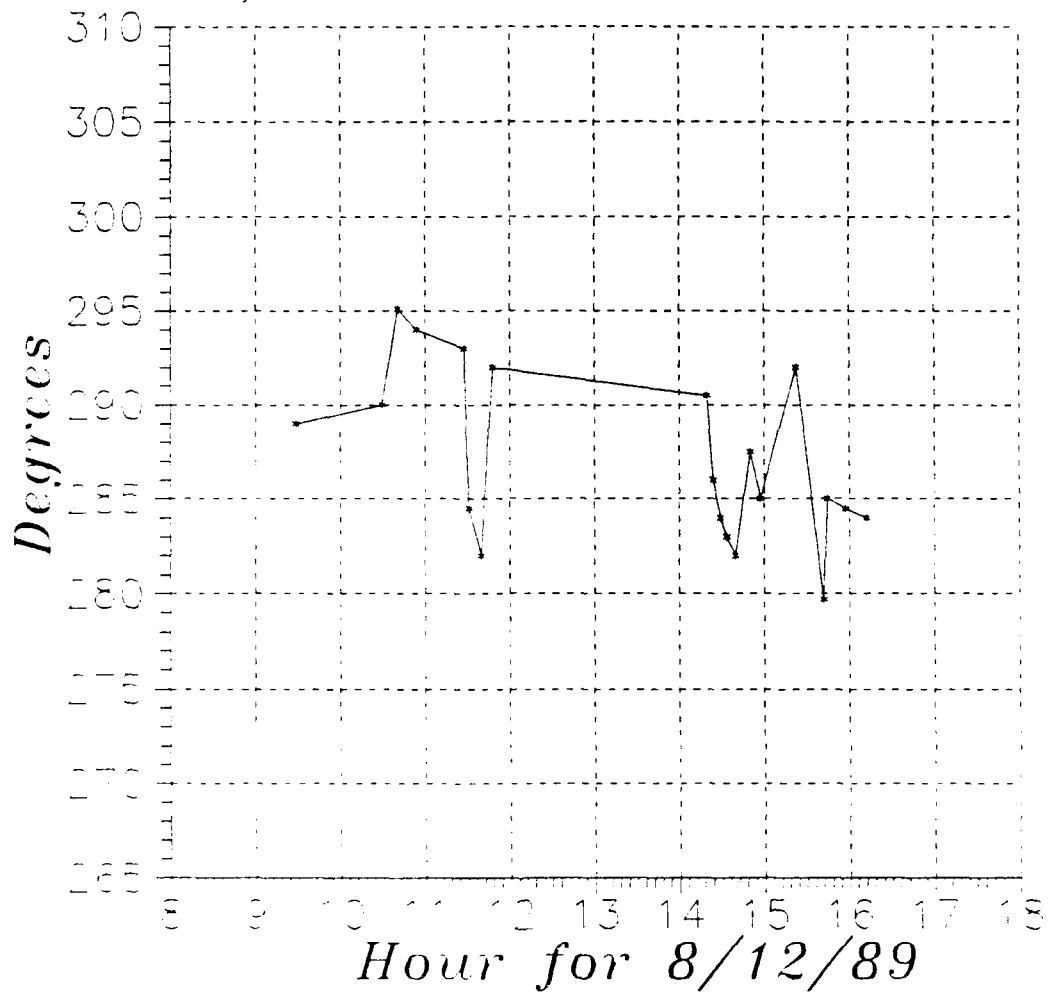
PLUME CENTERLINE DIRECTION

Van Analyzer data, SF6 Release from HSSF



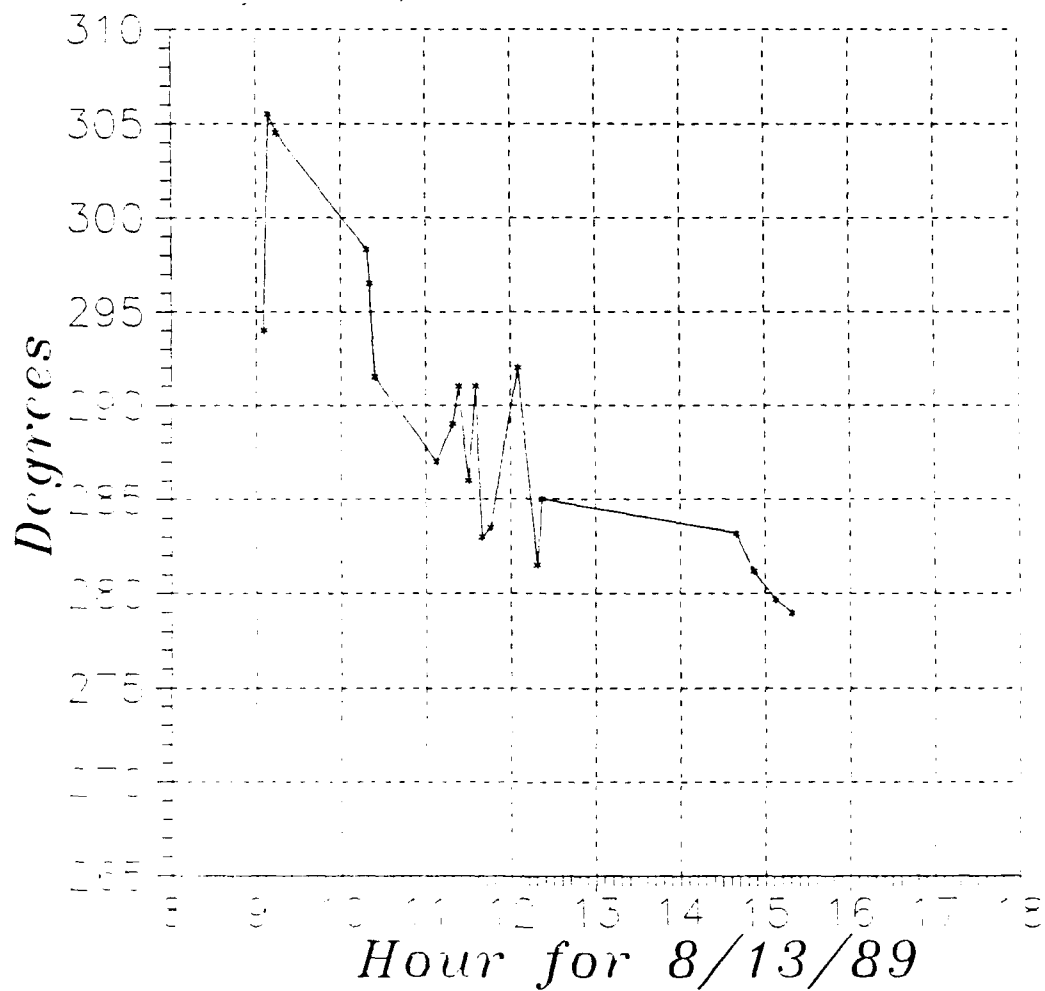
PLUME CENTERLINE DIRECTION

Van Analyzer data, SF6 Release from HSSF



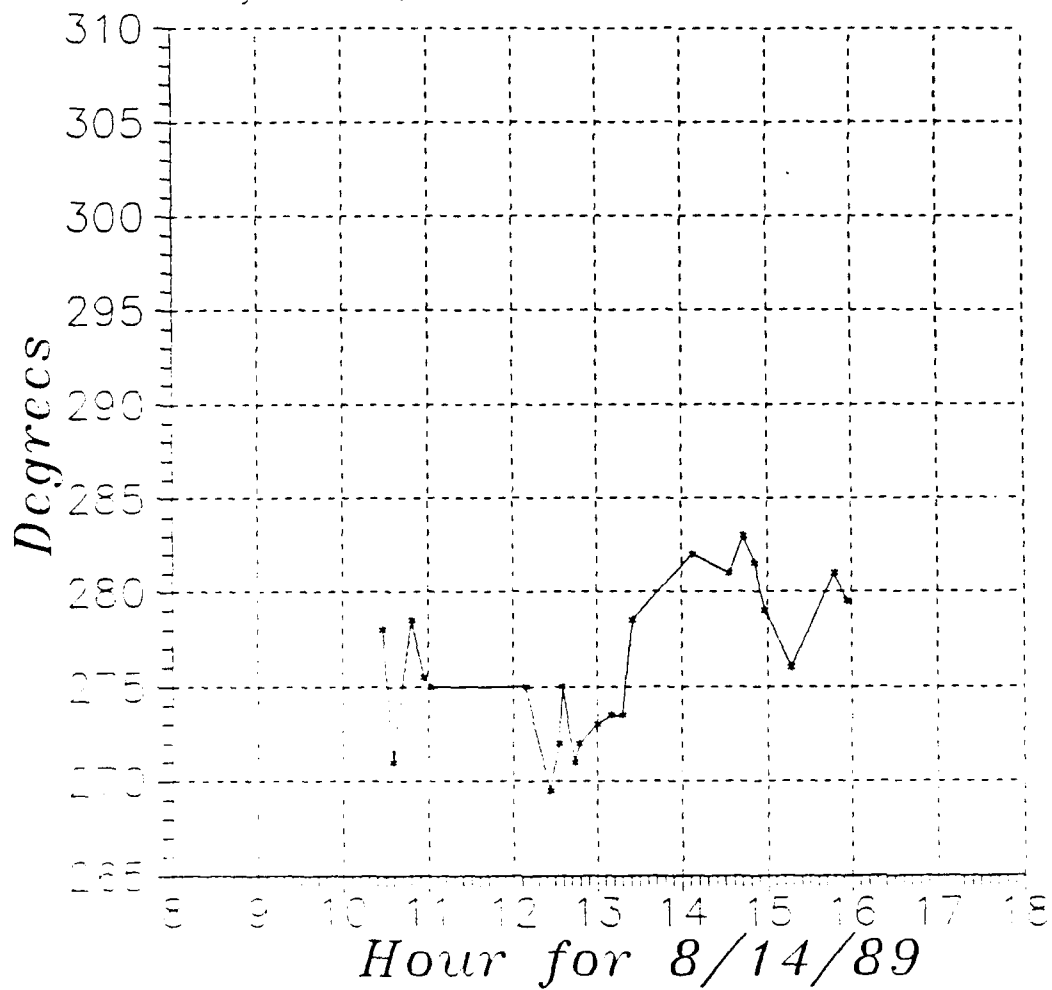
PLUME CENTERLINE DIRECTION

Van Analyzer data, SF6 Release from HSSF



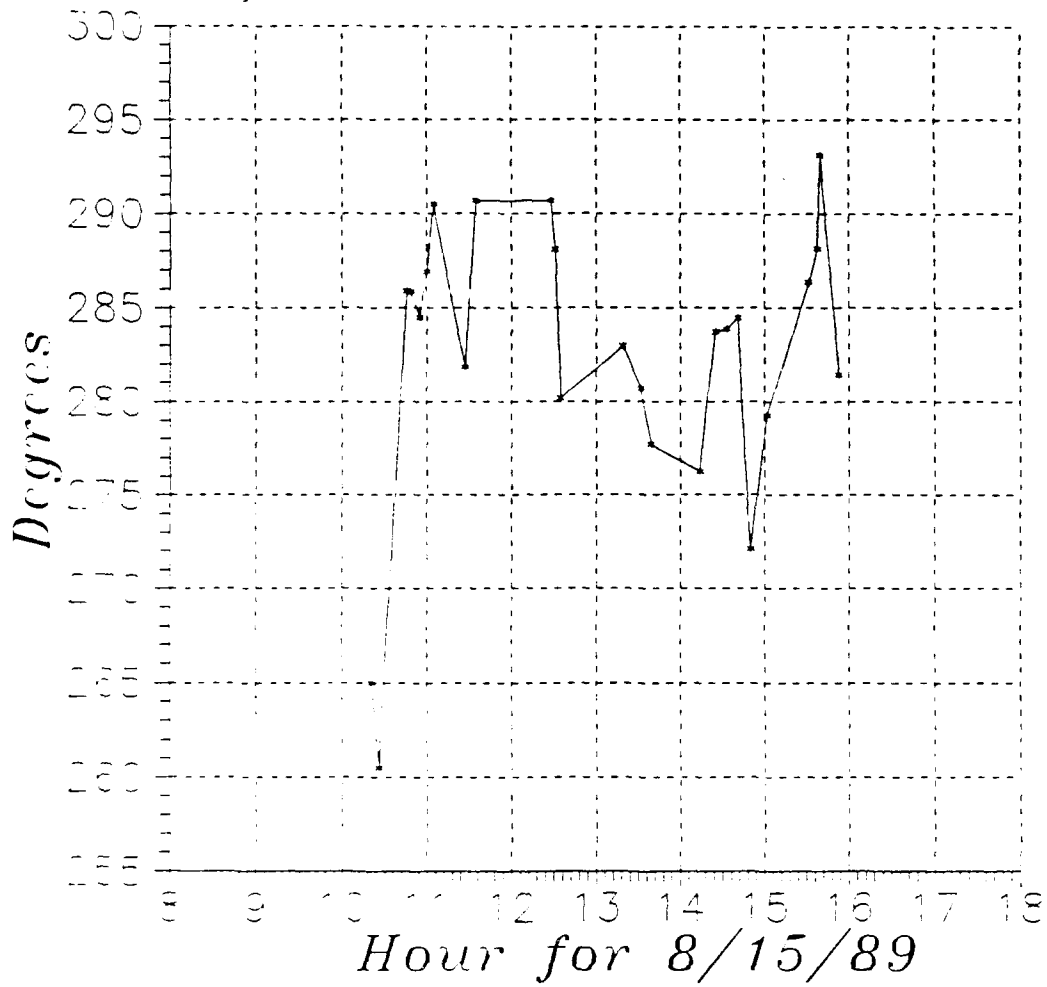
PLUME CENTERLINE DIRECTION

Van Analyzer data, SF6 Release from HSSF



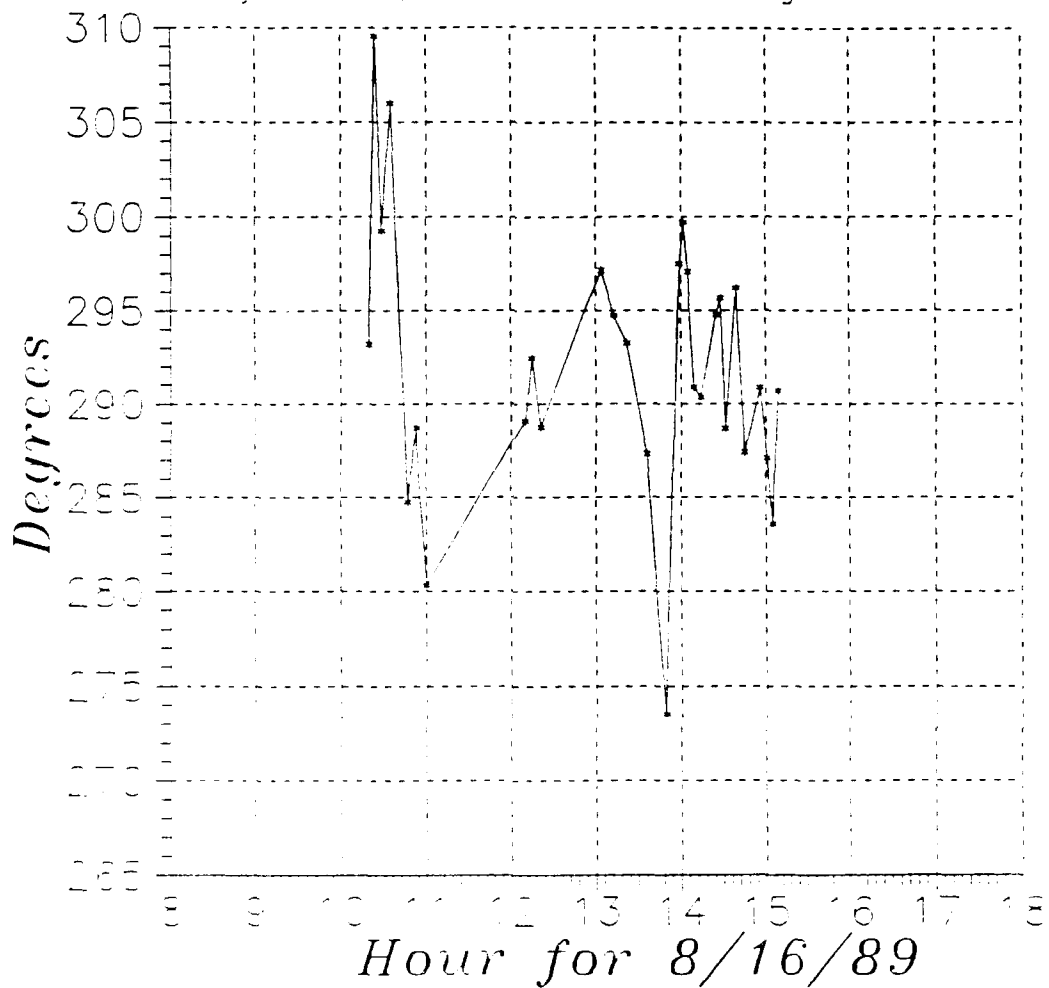
PLUME CENTERLINE DIRECTION

Van Analyzer data, SF6 Release from Ocean Park



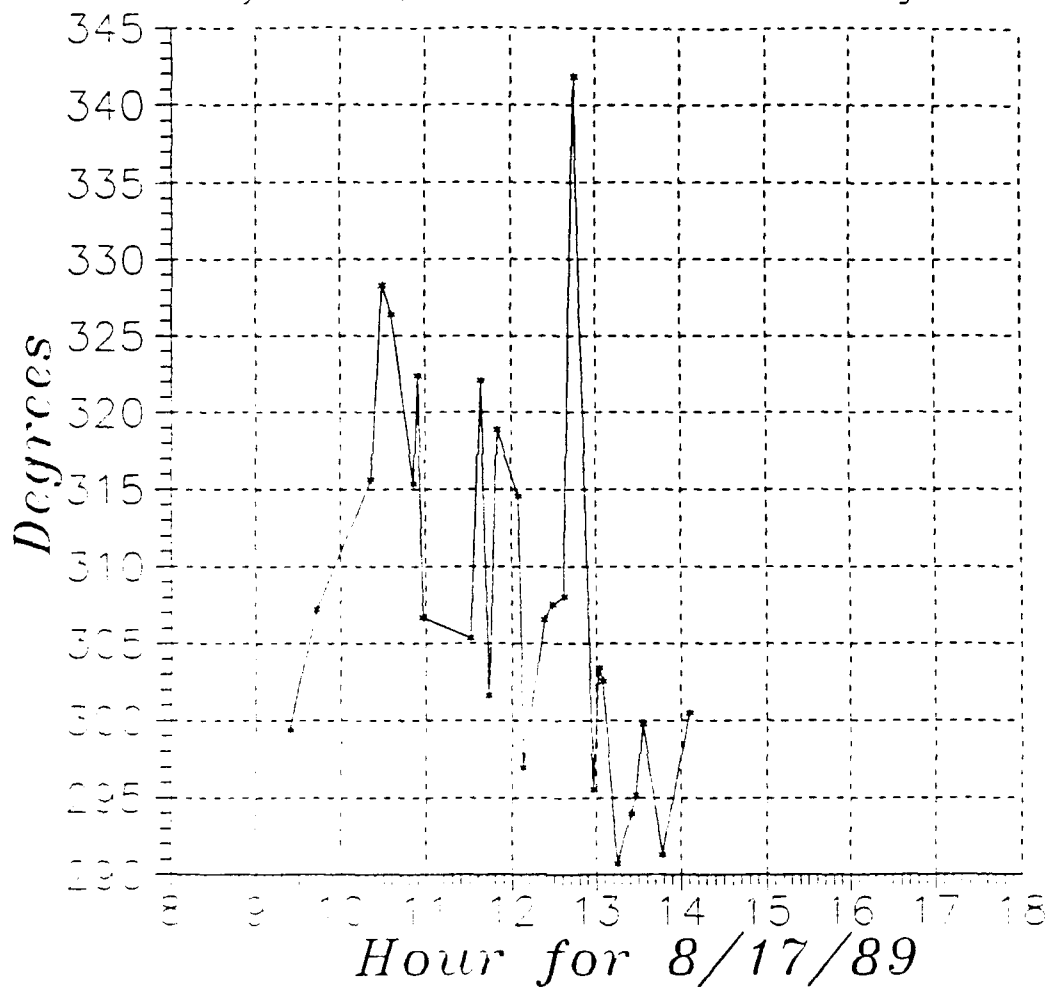
PLUME CENTERLINE DIRECTION

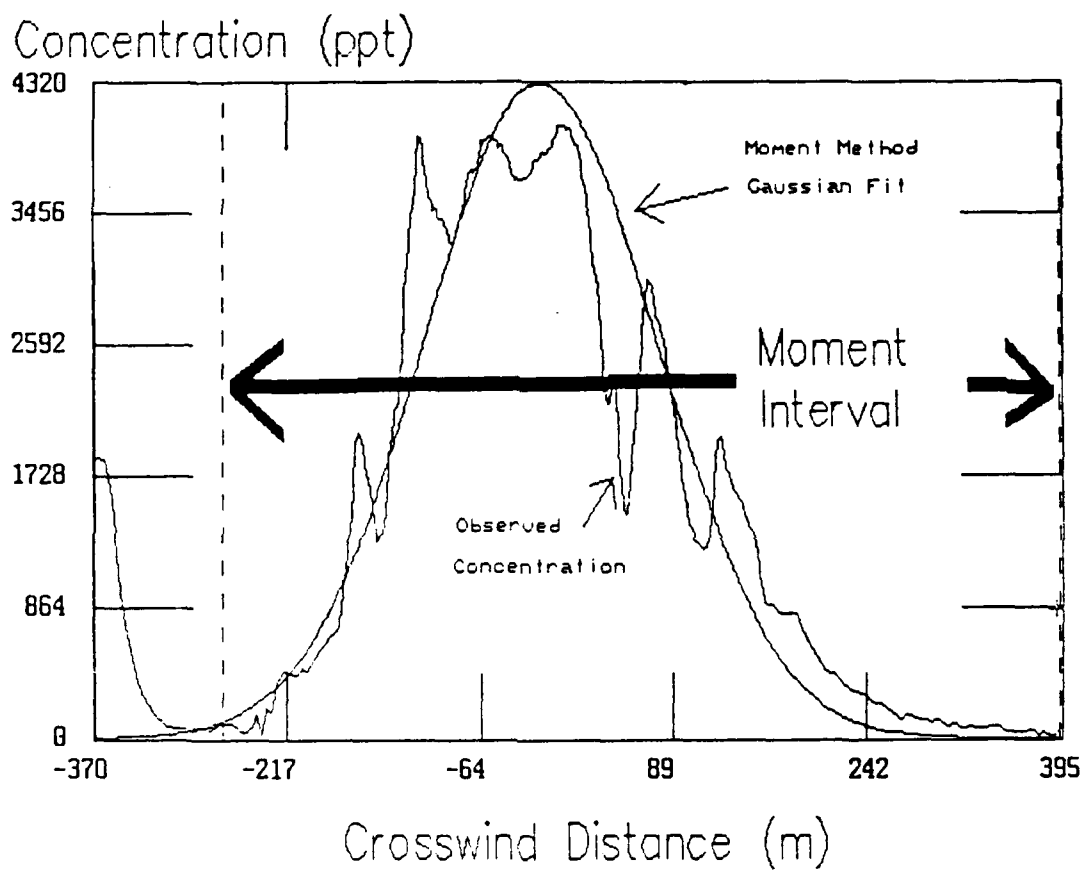
Van Analyzer data, SF6 Release from Arguello & 246

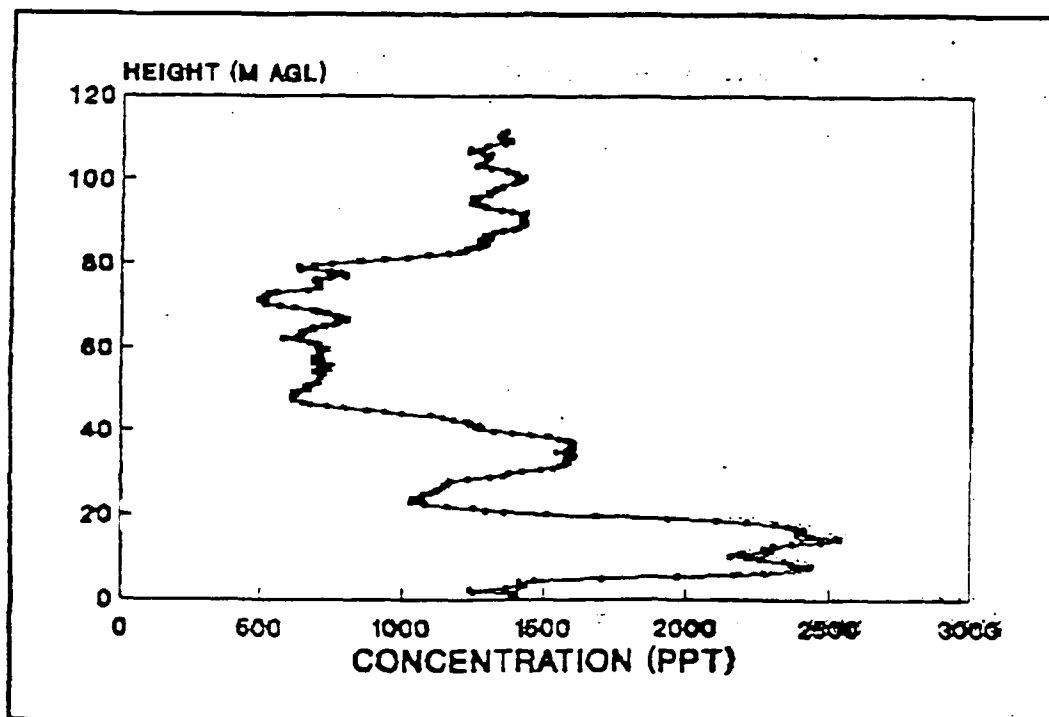


PLUME CENTERLINE DIRECTION

Van Analyzer data, SF6 Release from Union Sugar Rd







4. INFRARED MOLECULAR PLUME IMAGERY

On two of the sampling days, LCSP/AC operated a narrow-band infrared imaging camera from locations near the source and roughly perpendicular to the wind flow. This system produced a two-dimensional image of the SF6 molecular plume out to distances roughly 1 km from the source.

In order to image SF6 plumes, LCSP/AC has fitted an Inframetrics 525 infrared camera with a narrow-band filter, optimized to transmit infrared only in the SF6 absorption band. In an aerosol-free environment, the camera primarily detects infrared radiation that was emitted by SF6. Imagery from this camera was recorded on standard VHS videotape. The data was later digitized and averaged to enhance the signal to noise ratio. To further enhance the image of the molecular plume, a background average (taken immediately before the SF6 release) was subtracted from the plume imagery averages.

Figures 4.1-7 show imagery averaged over the puff releases described in section 2. For each case, a brightness temperature somewhat above background brightness levels was selected and the height of this temperature is listed as a function of distance from the source. This "plume height" is also plotted in fgs. 8-15.

The appearance of the infrared plume images is dependent upon the relative temperatures of the plume and the background against which it is viewed. After release, the SF6 quickly comes into thermal equilibrium with the air, which was typically colder than the ground, but warmer than the background sky during LVDE. When seen against the ground, the SF6 plume is darker than the background because the cooler SF6 absorbs radiation emitted by the warmer ground. When seen against the sky, the plume is brighter than the background, because the warmer SF6 emits more infrared radiation than the cooler sky.

It should be noted that conditions on 17 Aug were less than ideal for infrared imaging. The presence of high humidity and fog between the camera and plume drastically reduced the infrared signal to noise ratio. Further, the IR camera was looking at a background cloud bank rather than at clear skies. The clouds and the plume were at nearly the same temperature, so the plume signature was very weak above the horizon.

The raw data from these images is not supplied in the data archive, but is available upon request from LCSP/AC. The line integrated concentration at each pixel may be estimated with these images, the known absorption spectrum of SF6, the release mass, and the air-background temperature difference. With the

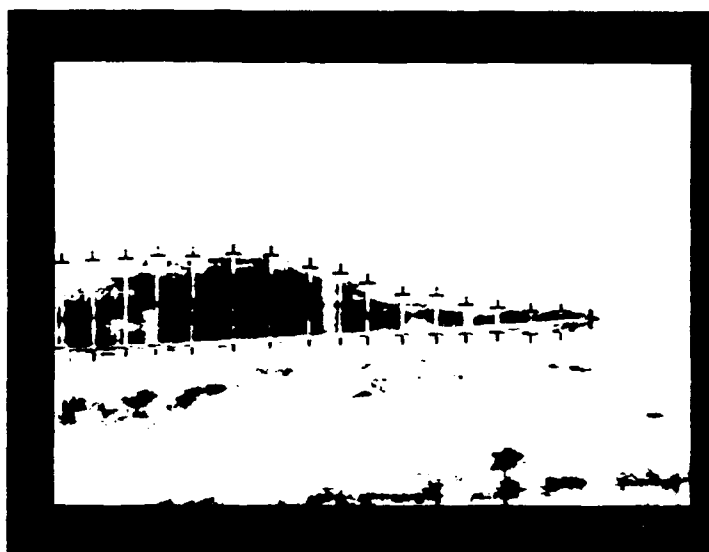
additional assumption of isotropy (or stability dependent anisotropy), vertical plume parameters may be estimated from the cross-image distributions.

SECTION 4 FIGURE CAPTIONS

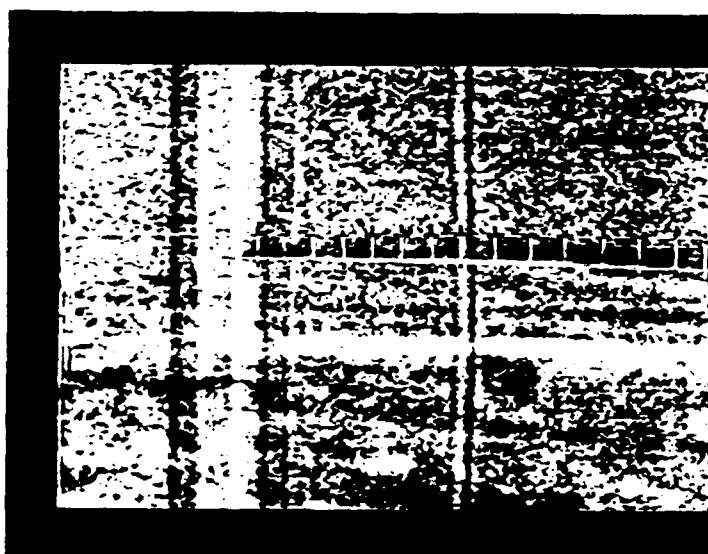
F4.1-7 Selected examples of infrared imaging of SF6 tracer. All images are of 3 minute puff releases (250 kg/hr), except fig. 3, which is an image of the continuous release. Images on 11 Aug were conducted from the HSSF under stratus conditions, while 17 Aug images were in clear sky conditions. Note that background features often include the horizon and terrain features.

F4.8-15 Plume heights derived from the infrared images, determined by selecting and tracking a brightness temperature near the visual edge of the SF6 image. Heights are roughly proportional to line-integrated concentration.

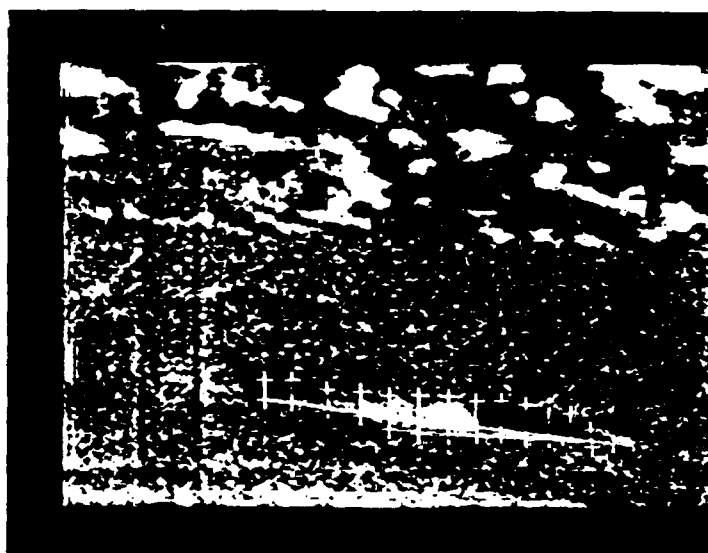
SF6 Release #1, 08/11/1989			
Distance from Camera to Release Site = 383 m			
<i>Distance from Release Site (deg)</i>	<i>Plume Height (deg)</i>	<i>Distance from Release Site (m)</i>	<i>Plume Height (m)</i>
0.900	0.832	6	6
1.526	0.979	10	7
2.201	1.077	15	7
2.903	1.273	19	9
3.579	1.714	21	11
4.340	1.763	29	12
5.144	2.351	34	16
5.757	2.792	38	19
6.470	3.086	43	21
7.399	3.723	49	25
8.248	3.919	55	26
9.220	3.968	62	27
10.058	4.018	67	27
10.789	3.919	72	26
11.508	4.066	77	27
12.198	3.821	82	26



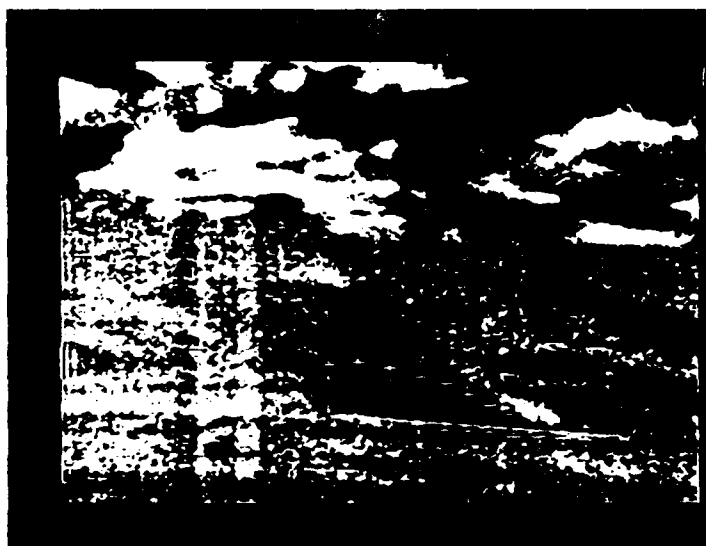
SF6 Release #4, 08/11/1989 Distance from Camera to Release Site = 2313 m			
<i>Distance from Release Site (deg)</i>	<i>Plume Height (deg)</i>	<i>Distance from Release Site (m)</i>	<i>Plume Height (m)</i>
0.651	1.028	26	41
1.274	1.077	51	43
1.924	1.077	78	43
2.635	1.028	106	41
3.285	1.028	133	41
3.968	1.077	160	43
4.680	1.028	189	41
5.331	1.077	215	43
6.107	1.077	247	43
6.913	1.126	279	45
7.688	1.126	310	45
8.558	1.175	345	47
9.427	1.224	381	49
10.297	1.175	416	47
10.982	1.175	443	47



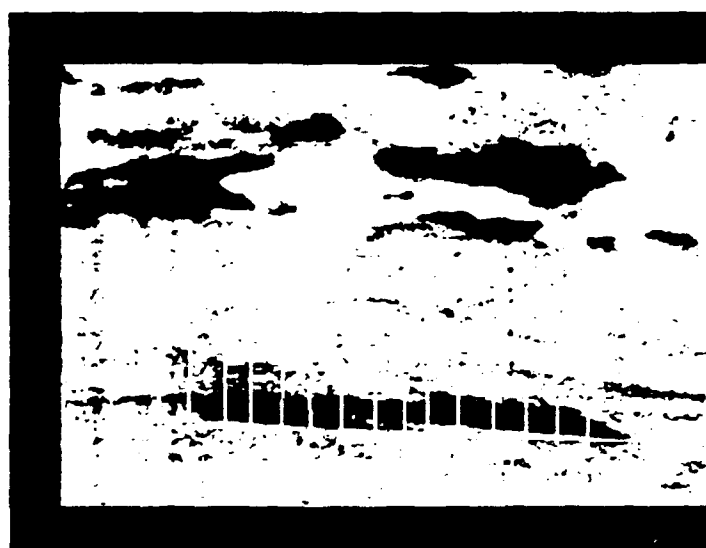
Continuous SF6 Release, 08/17/1989 Distance from Camera to Release Site = 1514 m			
<i>Distance from Release Site (deg)</i>	<i>Plume Height (deg)</i>	<i>Distance from Release Site (m)</i>	<i>Plume Height (m)</i>
0.532	0.734	14	19
0.992	1.224	26	32
1.500	1.420	40	38
2.029	1.420	54	38
2.602	1.420	69	38
3.155	1.420	83	38
3.802	1.616	100	43
4.481	1.665	118	44
5.179	1.469	137	39
5.914	1.028	156	27
6.704	0.832	177	22
7.585	0.930	200	25
8.290	0.881	217	23



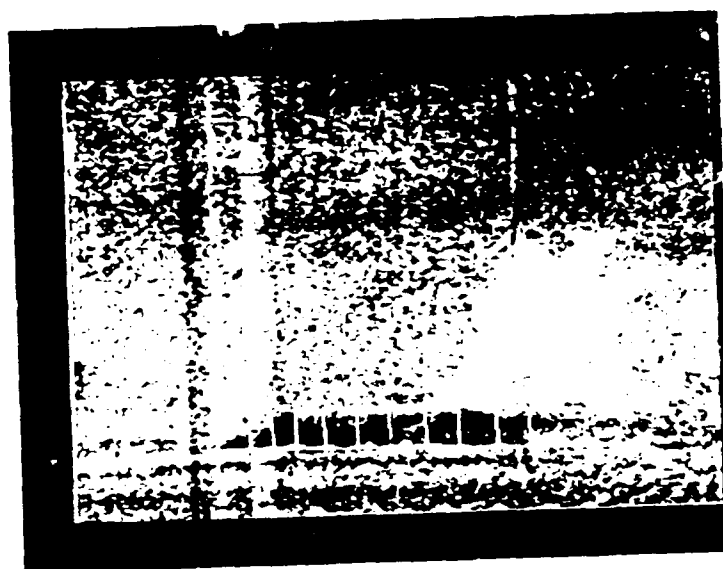
SF6 Release #1, 08/17/1989			
Distance from Camera to Release Site = 1514 m			
<i>Distance from Release Site (deg)</i>	<i>Plume Height (deg)</i>	<i>Distance from Release Site (m)</i>	<i>Plume Height (m)</i>
0.828	0.538	22	14
1.340	0.587	35	16
1.860	0.587	49	16
2.449	0.979	65	26
3.010	1.175	80	31
3.508	1.616	93	43
4.037	2.057	107	54
4.657	2.106	124	56
5.375	2.302	142	61
6.170	2.352	163	62
6.701	2.204	179	58



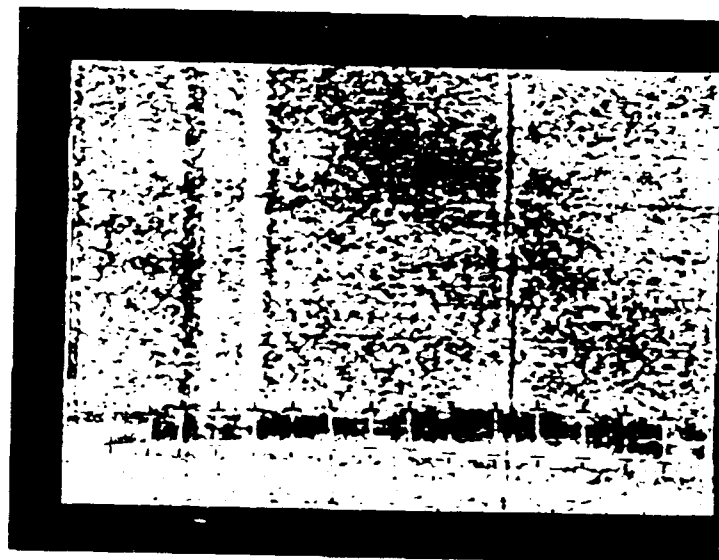
SF6 Release #2, 08/17/1989			
Distance from Camera to Release Site = 1514 m			
<i>Distance from Release Site (deg)</i>	<i>Plume Height (deg)</i>	<i>Distance from Release Site (m)</i>	<i>Plume Height (m)</i>
1.115	1.126	29	30
1.831	1.518	48	40
2.555	1.469	68	39
3.303	1.518	87	40
4.133	1.469	109	39
4.846	1.616	128	43
5.340	1.616	141	43
6.015	1.861	159	49
6.795	1.812	180	48
7.512	2.008	198	53
8.201	2.645	217	70
8.927	2.792	236	74
9.515	2.792	252	74
10.346	3.331	273	88
11.026	3.380	291	89



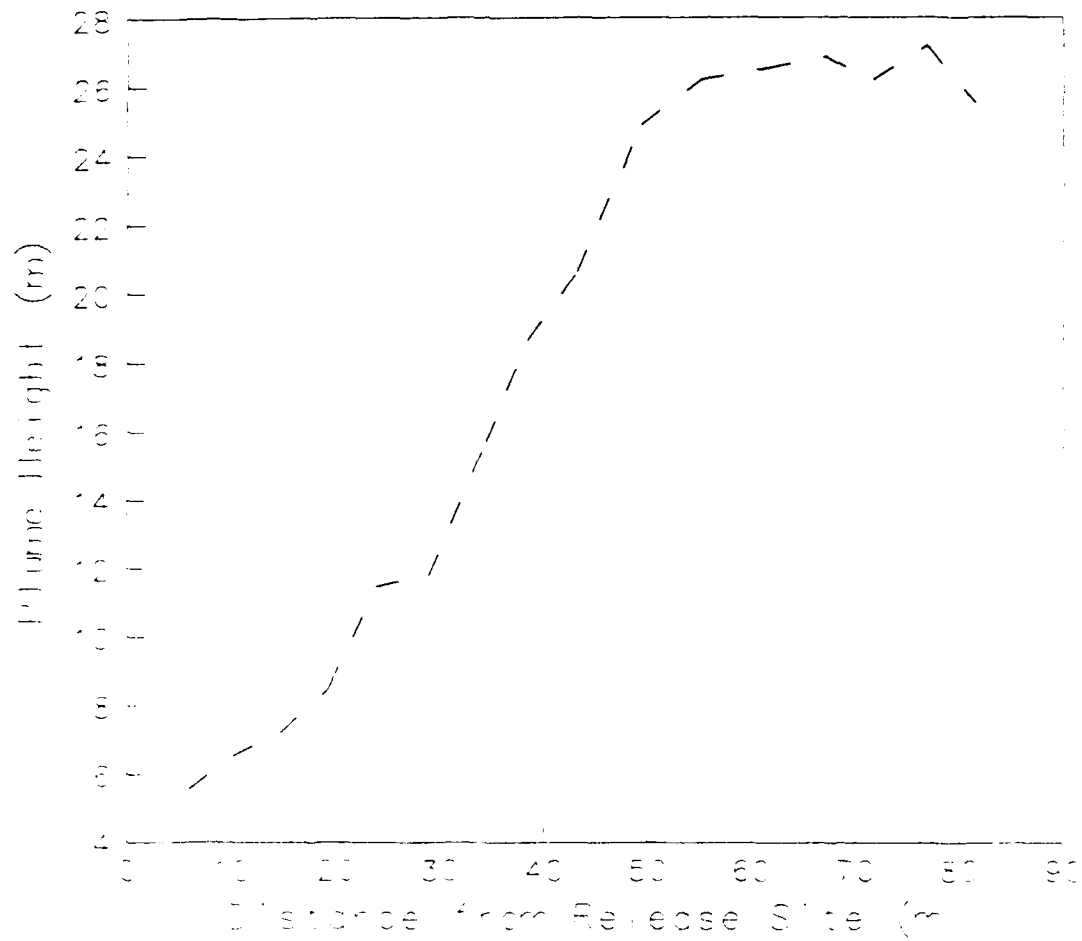
SF6 Release #3, 08/17/1989			
Distance from Camera to Release Site = 2072 m			
<i>Distance from Release Site (deg)</i>	<i>Plume Height (deg)</i>	<i>Distance from Release Site (m)</i>	<i>Plume Height (m)</i>
0.061	0.832	35	30
1.485	1.420	54	51
2.017	1.567	73	57
2.666	1.714	96	62
3.410	1.763	123	64
4.185	1.605	151	60
5.022	1.567	182	57
5.766	1.567	209	57
6.603	1.518	241	55
7.411	1.469	268	53



SF6 Release #4, 08/17/1989			
Distance from Camera to Release Site = 2072 m			
<i>Distance from Release Site (deg)</i>	<i>Plume Height (deg)</i>	<i>Distance from Release Site (m)</i>	<i>Plume Height (m)</i>
0.868	1.273	31	46
1.581	1.665	57	60
2.417	1.567	87	57
3.285	1.616	119	58
4.153	1.665	150	60
5.052	1.763	183	64
5.952	1.665	215	60
6.851	1.714	248	62
7.750	1.910	280	69
8.805	1.959	318	71
9.797	2.106	354	76
10.820	2.057	391	74
11.816	2.008	427	73
12.714	1.959	460	71

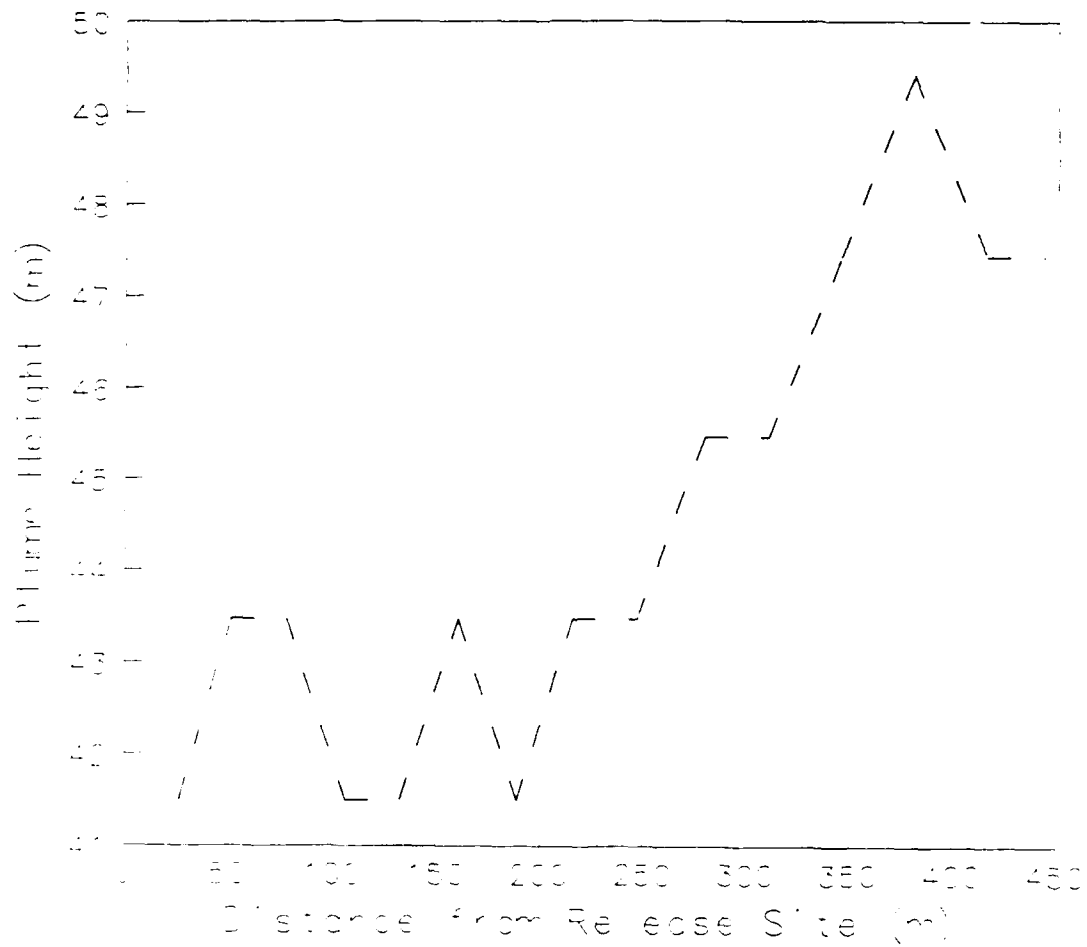


SF6 Release #1, 08/11/89



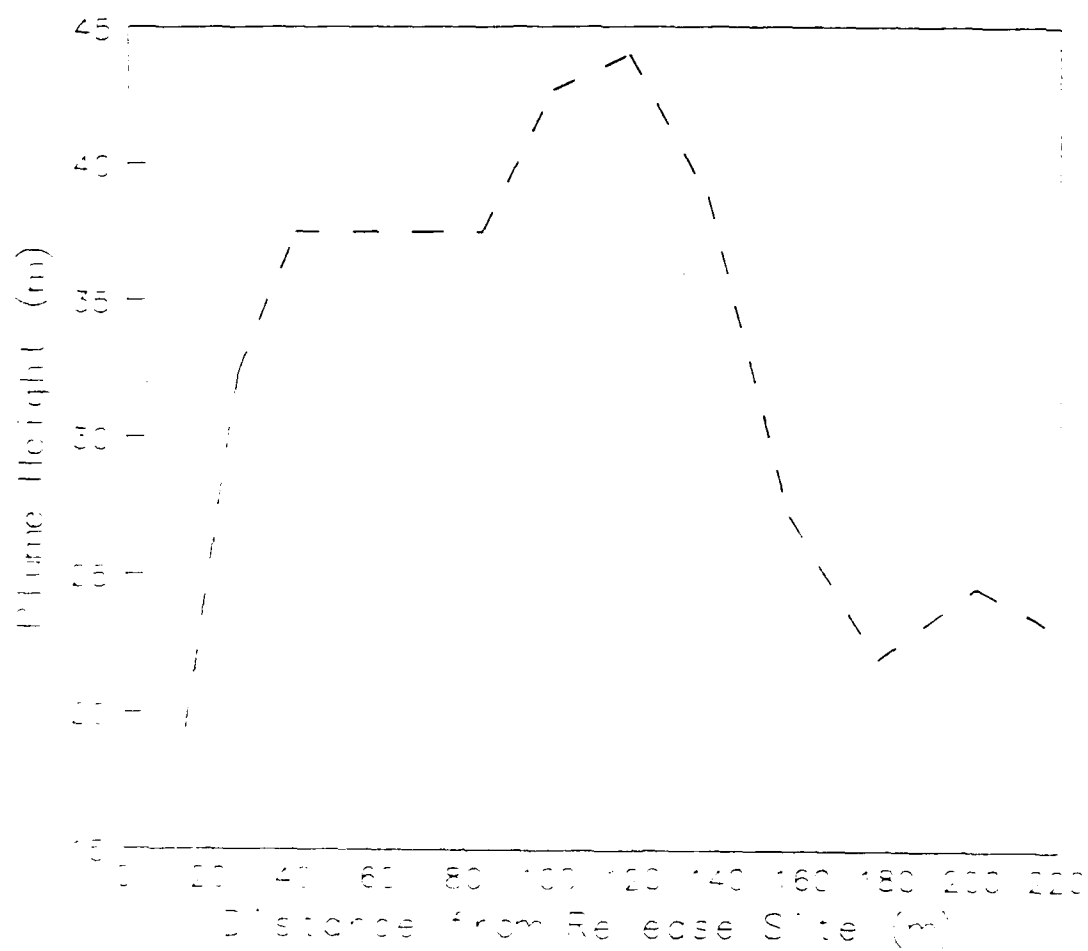
Distance from Camera to Release Site = 383 m

SF6 Release #4, 08/11/89



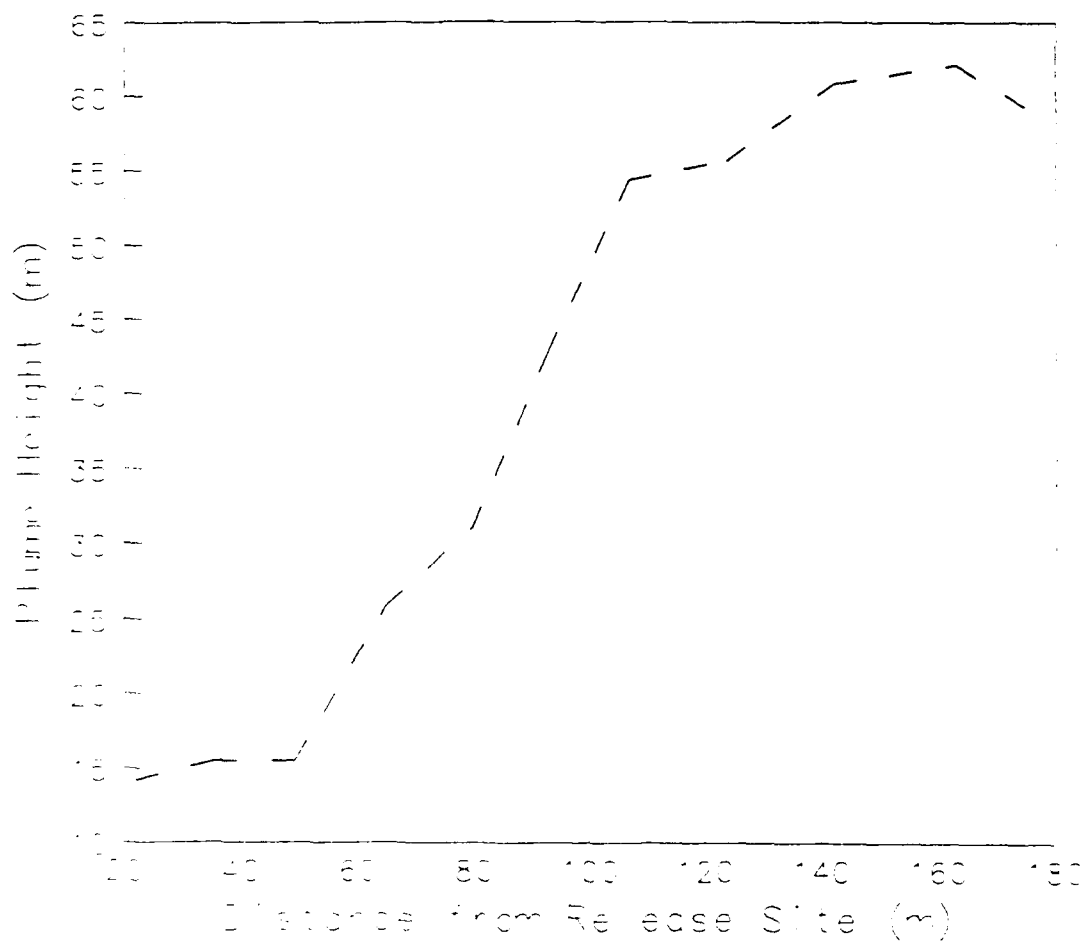
Distance from Camera to Release Site = 2313 m

Continuous SF6 Release, 08/17/89



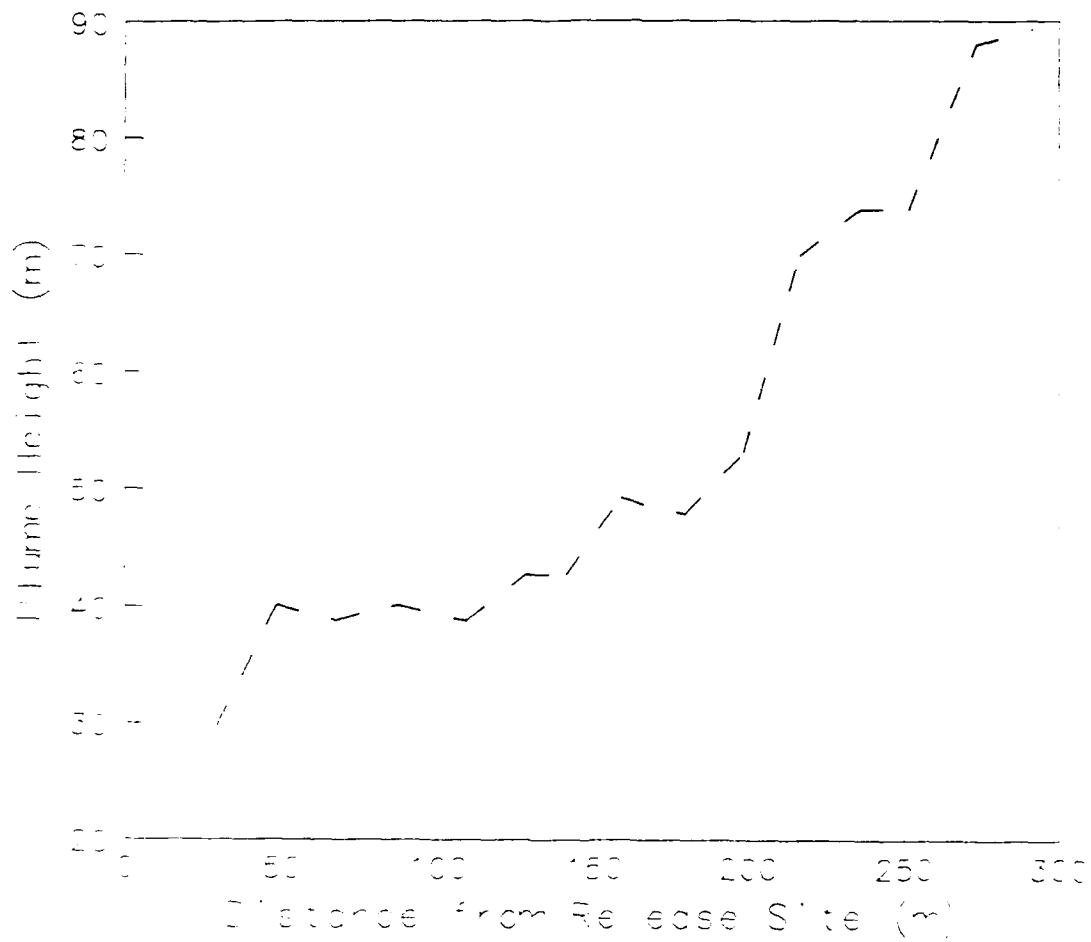
Distance from Camera to Release Site = 1514 m

SF6 Release #1, 08/17/89



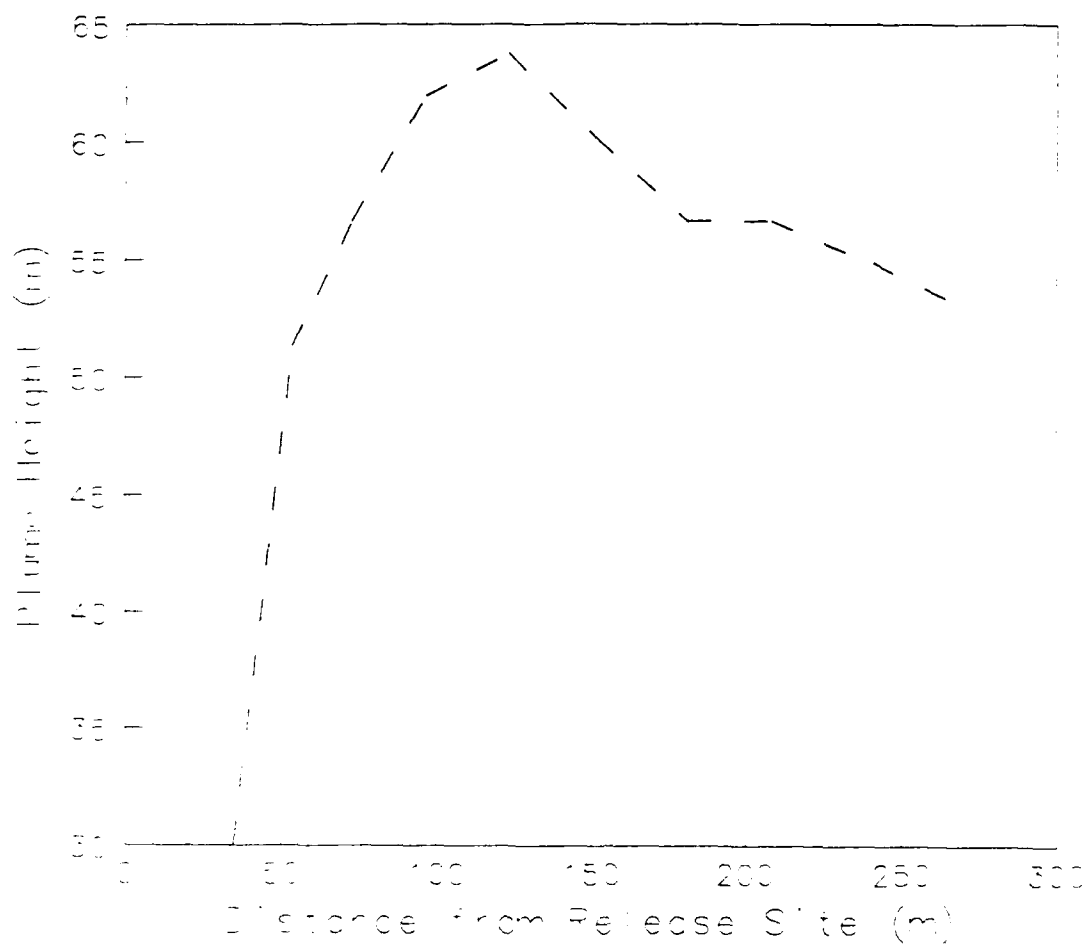
Distance from Camera to Release Site = 1514 m

SF6 Release #2, 08/17/89



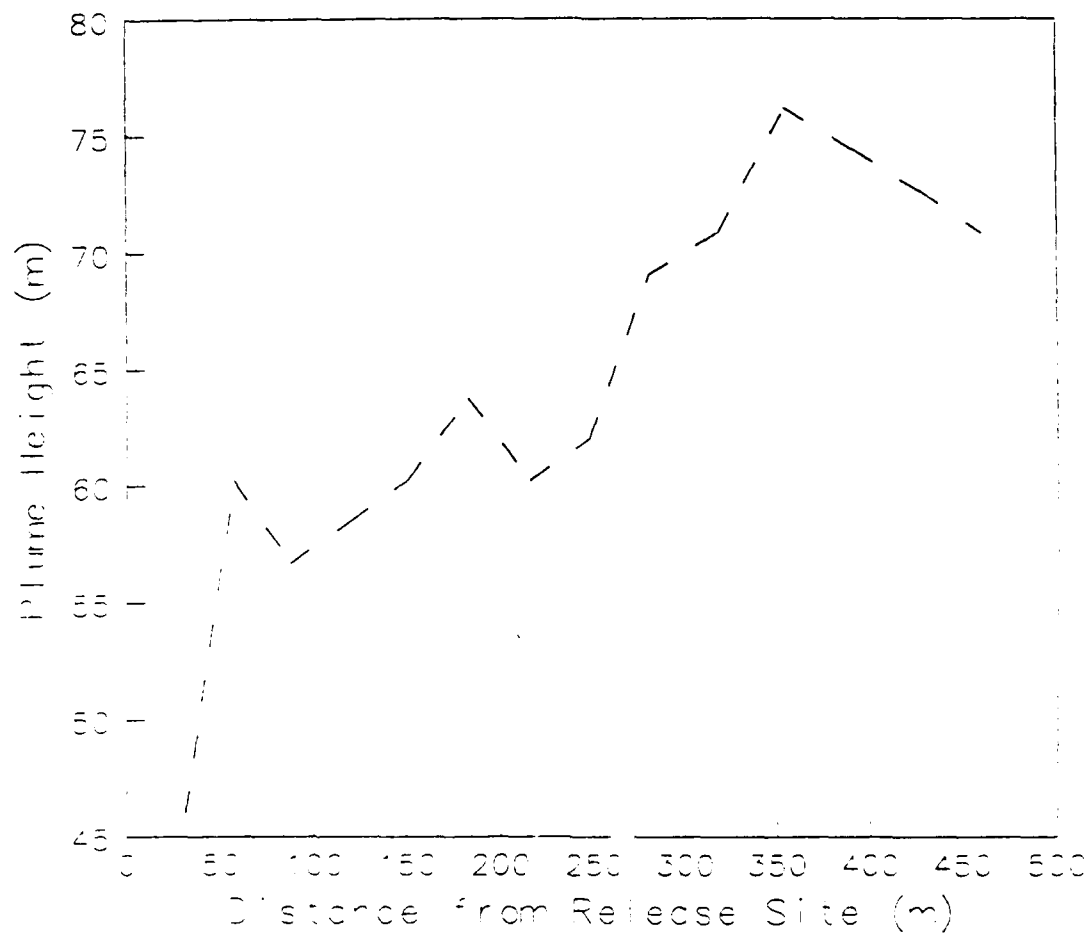
Distance from Camera to Release Site = 1514 m

SF6 Release #3, 08/17/89



Distance from Camera to Release Site = 2072 m

SF6 Release #4, 08/17/89



Distance from Camera to Release Site = 2072 m

5. DASS DATA

Data collected by the three VBG DASS systems are supplied for the time period 4-19 Aug, and data collected by two NPS DASS systems are supplied for 9-17 Aug. The DASS data is organized into separate sets of 10 min and 1 hour averages. Both sets include mean and turbulent wind quantities. Range gates are 50 m for the base system and 25 m for the NPS data. The 1 hour means are vectorized averages of the 10 min records. The standard deviations are true 1 hour statistics in that they include the contributions of variance in the mean values as well as the 10 min standard deviations. 1 hour averages were calculated only if more than 30 minutes of data were valid for the hour. An example of a DASS record is supplied in table 5.1.

Kamada et al. (1990a,b) established the importance of properly measuring the boundary layer height for defining flow and diffusion at VAFB. Four boundary layer heights are supplied in the VBG data sets as determined from the echo shadowgraphs. For each of these heights, the mean and turbulent wind statistics are calculated from 100 m to the boundary layer top. This reduces the data to one value of boundary layer averaged wind and turbulence. The boundary layer heights are defined as follows: BL1 is the maximum height of the surface based echo layer. Since the backscattered power as displayed on the shadowgraphs is system

dependent, this height is somewhat qualitative. BL2 is the center altitude of the first elevated echo layer. BL3 is the upper boundary of the first elevated echo layer. BL4 is the height of the horizontal wind speed minimum above 150 m.

Boundary layer applications often use the center of the elevated echo layer as the assumed boundary layer height. This corresponds to the value of BL2. We choose to define BL3 because the presence of stratus dramatically affects the echo profile. The elevated echo layer will often be very thin with stratus present. Thus, BL2 will often be very close to the value of BL3. As thermal activity develops and clouds dissipate, the elevated echo layer becomes diffused, i.e., thicker. Due to the increased turbulence within this layer, the boundary layer height for applications may be set more appropriately to BL3. While BL1-3 are thermodynamic measures of the boundary layer, we regard BL4 as a dynamical measure of the altitude at which boundary layer flow is most balanced against the dominant flow above the boundary layer. For similar reasons BL4 is usually located in a region of strong wind shear.

TABLE 5.1 Example of a 1 Hour VBG DASS Data Record

hour date location							
13 809 900							
height	direct.		mean	v.v.	standard deviation		
(m)	(deg)	(deg)	(m/s)	(m/s)	(deg)	(m/s)	(m/s)
0.00	271.64		3.93	0.22	14.16	1.02	0.39
50.00	280.08		3.76	0.05	32.20	2.19	1.38
100.00	280.91		3.92	0.02	31.07	1.91	1.58
150.00	279.87		3.09	-0.04	32.60	1.97	1.75
200.00	280.58		2.36	-0.04	36.62	1.61	1.41
250.00	255.58		1.08	-0.05	58.71	1.64	1.15
300.00	182.16		0.87	-0.04	67.84	1.79	1.44
350.00	212.45		0.69	-0.04	77.96	1.72	1.51
400.00	199.58		1.28	0.02	62.27	1.86	1.08
450.00	200.78		1.74	0.06	63.92	1.99	0.76
500.00	199.36		1.86	0.07	60.49	2.22	0.72
550.00	199.25		2.22	0.18	51.84	2.24	1.05
600.00	214.02		1.16	0.15	72.93	2.40	1.07
650.00	305.22		0.32	0.20	105.70	2.34	1.01
700.00	174.41		0.62	0.11	87.05	2.08	0.77
750.00	119.83		0.74	0.27	76.88	1.93	1.20
800.00	131.86		0.62	0.23	79.03	2.13	0.98
850.00	199.55		0.68	0.22	88.81	2.49	1.14
900.00	111.08		0.68	0.12	85.62	2.14	1.12
950.00	90.00		0.38	0.03	90.95	1.90	1.18
BL1	217	280.32	3.59	0.01	31.97	2.07	1.58
BL2	275	278.53	2.82	-0.01	40.86	2.21	1.47
BL3	336	275.01	2.34	-0.02	56.98	2.28	1.46
BL4	650	248.11	1.56	0.03	67.90	2.26	1.28

10 Minute VBG Record Specifics

Suggested Input Format: (fixed) field, binary

field 1: TIME, DATE, ID, N (4A2 , FORTRAN convention)
(2 byte integers)

TIME = Local Daylight Time of launch (hour * 100 + minute)

DATE = date in 1989 (month * 100 + day)

ID = DASS identifier

1764 = building 1764 (north base by airfield)

900 = building 900 (south base near release site)

301 = SLC6 near Tower 301

N = record number (arbitrary)

field 2: Z, D, U, W, SD, SU, SW (7A4)
(4 byte single-precision floating point)

Z = height of range gate (m)

(Z=0 data is from a 12 ft Gill cup anemometer)

D = wind direction (deg)

U = horizontal wind speed (m/s)

W = vertical wind speed (m/s)

SD = standard deviation of wind direction (deg)

SU = standard deviation of horizontal wind speed (m/s)

SW = standard deviation of vertical wind speed (m/s)

field 3-21: same as field 2

field 22: BL1, D1, U1, W1, SD1, SU1, SW1 (7A4)
(4 byte single-precision floating point)

BL1 = boundary layer height #1

D1 = average wind direction from 100 m to BL1

U1 = average horizontal wind speed from 100 m to BL1

W1 = average vertical wind speed from 100 m to BL1

SD1 = standard deviation of wind direction from 100 m to BL1
SU1 = st. dev. of horizontal wind speed from 100 m to BL1
SW1 = st. dev. of vertical wind speed from 100 m to BL1
field 23: same as field 22, except for BL2
field 24: same as field 22, except for BL3
field 25: same as field 22, except for BL4
record delimiter: none
total record size: 680 bytes

1 Hour VBG Record Specifics

Suggested Input Format: {fixed} or free field, ASCII, space delimited

line 1: TIME, DATE, ID, N {4I5 , FORTRAN convention}
line 2-21: Z, D, U, W, SD, SU, SW {7F6.2}
line 22: BL1, D1, U1, W1, SD1, SU1, SW1 {7F6.2}
line 23: same as line 22, except for BL2
line 24: same as line 22, except for BL3
line 25: same as line 22, except for BL4
record delimiter: [CRLF]

NPS assembled and operated a DASS at the Lompoc Water Treatment Plant (WTP) continuously from 9-17 Aug. This data acquisition system also recorded data from two upward looking radiometers at the Lompoc site. Hence we include these data in the WTP DASS data set. The radiometer measurements are further described in section IX, and values are also available (upon

request) in a stand-alone data set.

10 Minute NPS WTP Record Specifics

Suggested Input Format: {fixed} field, binary

field 1: TIME, DATE, SW, LW {4A2 , FORTRAN convention}
(2 byte integers)

SW = visible radiation in W/m^2

LW = infrared radiation in W/m^2

field 2-25: same as 10 Minute VBG records, except no surface data

record delimiter: none

total record size: 680 bytes

1 Hour NPS WTP Record Specifics

Suggested Input Format: {fixed} or free field, ASCII, space delimited

line 1: TIME, DATE, SW, LW {4I5 , FORTRAN convention}

line 2-25: same as 1 Hour VBG records, except no surface data

record delimiter: [CRLF]

NPS also operated a second, trailer-mounted NPS DASS at various sites within the domain. During HSSF releases, the NPS trailer DASS location was selected to be roughly downwind of the release and half way between the Building 900 DASS and the WTP DASS. During the valley floor releases (15-17 Aug) the trailer was the release point, and the DASS and tower measurements supplied

release point meteorology. This DASS only operated during daylight hours near the release times. The location of the trailer during each data record is given as a code which corresponds to Table 5.2. No hourly averages are supplied for the trailer DASS data because of the short periods of operation and the mobile mission of the platform.

This vehicular platform also included a 8 m mast with a Kaijo Denki Dat300 sonic anemometer and a surface weather station from which mean and turbulent surface layer quantities were measured. See Skupniewicz et al. (1990) for complete description of the equipment and data analysis techniques. In summary, the sonic standard deviation and covariances quantities supplied in the data set have been properly calibrated and rotated into Cartesian coordinates. Time series were screened for dramatic wind shifts, but no further editing has been performed. Since these records are 10 minutes in length, the sonic turbulent statistics will be highly variable from record to record due to in stationarity in the boundary layer which occurs at time scales larger than 10 minutes. Also, some records at the more topographically complex sampling locations may be contaminated by obstructions, etc. Until further editing is performed, we recommend only using sonic turbulent statistics from locations known to be flat, such as the Lompoc Valley floor, and averaging over many 10 minute records to gain statistical confidence.

10 Minute NPS Trailer Record Specifics

Suggested Input Format: {fixed} field, binary

field 1: TIME, DATE, LC {3A2 , FORTRAN convention}
(2 byte integers)

LC = location code (see Table 5.2)

field 2: H, T0, P0, RH0, D0, U0, UT, SU, SV, SW, ST,
UW, WT, VW, UT, VT, UV {17A4}
(4 byte floating point)

H = compass heading of the trailer (deg)

T0 = surface (3.6 m) temperature (deg C)

P0 = surface (3.6 m) pressure (mb)

RH0 = surface (3.6 m) relative humidity (%)

D0 = surface (3.6 m) wind direction (deg)

U0 = surface (3.6 m) horizontal wind speed (m/s)

UT = sonic (7.7 m) total wind speed (m/s)

SU = sonic standard deviation of the longitudinal wind
vector component (m/s)

SV = sonic standard deviation of the lateral wind
vector component (m/s)

SW = sonic standard deviation of the vertical wind
vector component (m/s)

ST = sonic standard deviation of the temperature
(deg C)

UW = sonic covariance of the longitudinal and vertical
wind vector components (m^2/s^2)

WT = sonic covariance of the vertical wind vector
component and temperature (m/s * deg C)

VW = sonic covariance of the lateral and vertical
wind vector components (m^2/s^2)

UT = sonic covariance of the longitudinal wind vector
component and temperature (m/s * deg C)

VT = sonic covariance of the lateral wind vector
component and temperature (m/s * deg C)

UV = sonic covariance of the longitudinal and lateral
wind vector components (m^2/s^2)

field 3-26: same as 10 Minute VBG records, fields 2-25,
except no surface data

record delimiter: none

total record size: 746 bytes

TABLE 5.2 Location Code Coordinates for NPS Trailer DASS
10 Minute Data Files

<u>LC</u>	<u>latitude</u>	<u>longitude</u>	<u>location</u>
1	34 39.6"	120 34.7"	Bldg. 900
2	34 40.0	120 34.0	Tower 009
3	34 40.2	120 33.7	South Gate
4	34 38.4	120 34.3	Bear Creek/Arguello
5	34 39.7	120 30.3	Hwy 246/Douglas
6	34 40.1	120 33.8	Santa Ynez/Arguello (by South Gate)
7	34 37.8	120 30.6	Santa Ynez/Arguello
8	34 39.8	120 30.6	Santa Ynez/UHF
9	34 39.3	120 32.2	Union & 246
10	34 35.7	120 28.0	Miguelito (Filtration plant, RR Xing)
11	34 41.4	120 36.0	Ocean Park
12	34 38.9	120 31.6	Artesia/246
13	34 40.2	120 30.6	Douglas (between 246 & Central)
14	34 35.4	120 28.8	Miguelito
15	34 38.0	120 27.6	Olive/South P St.
16	34 38.7	120 31.2	LaSalle Canyon/246
17	34 39.9	120 33.2	near Tower 009
18	34 39.5	120 34.2	Mesa/Arguello
19	34 39.8	120 33.0	NRL Lab/Santa Ynez Rd.
20	34 38.5	120 29.0	Bailey Rd. (RR tracks 246/Central)
21	34 38.6	120 34.8	Bear Creek & Manzanita (near SLC 3)
22	34 39.8	120 33.0	NRL Lab/Santa Ynez Rd. (same as 19)
23	34 39.7	120 32.2	Union/Central
24	34 40.4	120 33.3	13th St (south of N Gate)
25	34 39.2	120 32.2	1.6 mile marker on Union Sugar

6. WINDS SYSTEM DATA

Data collected by the VBG WINDS system are supplied for the time period 5-20 Aug. Only data graded as "good" by the VBG winds system was included. This does not guarantee that all data are correct, since the WINDS system only screens for reasonable ranges and subtle errors may not be detected. Data is organized into two sets: a 10 min "raw" data dump and a calibrated 1 hour average. VBG assigns a quality code to each number, and we have included only those data with the highest grade.

10 Minute Record Summary

Data records represent single sensor values. Sensors are identified in Table 6.1. Values must be divided by the scale factors listed in Table 6.2. Every data record will have a time tag and valid mean value. In some cases the mean is given a good grade, while the standard deviation is graded below top quality. For those cases, we have assigned the standard deviation a value of (-99). A final word of caution, in some cases wind speed or direction sensor mean and standard deviations are given a good grade, but the standard deviations are 0 and the mean is suspiciously constant. We therefore suggest invoking an additional criteria for winds which only accepts mean values if

the standard deviation is non-zero. Since temperatures can be very slow changing, this technique will not work for thermodynamic quantities. The pressure and short and long wave radiation sensors at Tower 301 were not operating during LVDE.

10 Minute Record Specifics

Suggested Input Format: {fixed} field, binary

field 1: DATE, TIME, ID, MEAN, SD {5A4 , FORTRAN convention}
(4 byte integers)

DATE = date in 1989 (month * 100 + day)

TIME = Local Daylight Time of launch (hour * 100 +
minute)

ID = sensor identifier (see tables xx-xx)

MEAN = scaled 10 min mean value (see table xx)

SD = scaled 10 min standard deviation (see table xx)
record delimiter: none

TABLE 6.1 Sensor Identifiers

ID	TOWER#	LEVEL(ft)	SENSOR	LATITUDE	LONGITUDE
1	004	12	1	34N41"50.8'	120W33"58.2'
4	004	12	2		
7	005	12	1	45"12.6'	34"16.4'
10	005	12	2		
13	007	12	1	43 51.1	32 23.0
16	007	12	2		
19	008	6	3	49 31.6	30 30.7
20	008	12	1		
23	008	12	2		
26	009	12	1	39 53.8	33 17.7
29	009	12	2		
32	014	12	1	36 30.7	31 31.4
35	014	12	2		
38	015	6	3	46 15.4	31 52.0
39	015	12	1		
42	015	12	2		
45	017	12	1	52 56.1	38 12.6
48	017	12	2		
51	018	12	1	50 41.7	34 57.6
54	018	12	2		
57	019	6	3	33 56.1	30 5.0
58	019	12	1		
61	019	12	2		
64	050	6	3	48 2.2	35 55.5
65	050	12	1		
68	050	12	2		
71	050	54	1		
74	050	54	2		
77	050	54	4		
78	051	6	3	42 35.5	33 55.2
79	051	12	1		
82	051	12	2		
85	051	54	1		
88	051	54	2		
91	051	54	4		
92	052	6	3	44 8.8	35 43.2
93	052	12	1		
96	052	12	2		
99	052	54	1		
102	052	54	2		
105	052	54	4		
106	053	6	3	33 19.1	36 38.1
107	053	12	1		
110	053	12	2		
113	053	54	1		
116	053	54	2		
119	053	54	4		

TABLE 6.1 Continued

ID	TOWER#	LEVEL(ft)	SENSOR	LATITUDE	LONGITUDE
120	054	6	3	38 31.1	35 29.0
121	054	12	1		
124	054	12	2		
127	054	54	1		
130	054	54	2		
133	054	54	4		
134	055	6	3	35 14.8	35 43.2
135	055	40	1		
138	055	40	2		
141	055	40	4		
142	056	6	3	34 60.0	33 40.9
143	056	40	1		
146	056	40	2		
149	057	6	3	40 0.5	35 21.9
150	057	12	1		
153	057	12	2		
156	057	54	1		
159	057	54	2		
162	057	54	4		
163	058	6	3	41 49.6	32 17.2
164	058	12	1		
167	058	12	2		
170	058	54	1		
173	058	54	2		
176	058	54	4		
177	059	6	5	49 7.4	34 52.0
178	059	6	6		
179	059	6	3		
180	059	12	1		
183	059	12	2		
186	059	54	1		
189	059	54	2		
192	059	54	4		
193	059	54	5		
194	060	6	5	50 58.7	35 57.7
195	060	6	6		
196	060	6	3		
197	060	12	1		
200	060	12	2		
203	060	54	1		
206	060	54	2		
209	060	54	4		
210	060	54	5		
211	101	6	3	36 38.2	33 58.8
212	101	12	1		
215	101	12	2		
218	101	54	1		

TABLE 6.1 Continued

ID	TOWER#	LEVEL(ft)	SENSOR	LATITUDE	LONGITUDE
221	101	54	2		
224	101	54	4		
225	102	6	3	45 29.6	37 18.2
226	102	12	1		
229	102	12	2		
232	102	54	1		
235	102	54	2		
238	102	54	4		
239	102	102	1		
242	102	102	2		
245	200	6	3	36 27.4	37 35.2
246	200	12	1		
249	200	12	2		
252	200	54	1		
255	200	54	2		
258	200	54	4		
259	200	102	1		
262	200	102	2		
265	200	204	1		
268	200	204	2		
271	200	204	4		
272	300	6	3	38 1.1	36 50.6
273	300	12	1		
276	300	12	2		
279	300	54	1		
282	300	54	2		
285	300	54	4		
286	300	102	1		
289	300	102	2		
292	300	102	4		
293	300	108	1		
296	300	108	2		
299	300	204	1		
302	300	204	2		
305	300	204	4		
306	300	300	1		
309	300	300	2		
312	300	300	4		
313	301	6	7	34 48.2	37 57.9
314	301	6	8		
315	301	6	9		
316	301	6	3		
317	301	6	10		
318	301	6	6		
319	301	6	5		
320	301	12	1		
323	301	12	2		

TABLE 6.1 Continued

ID	TOWER#	LEVEL(ft)	SENSOR	LATITUDE	LONGITUDE
326	301	54	1		
329	301	54	2		
332	301	54	4		
333	301	54	5		
334	301	102	1		
337	301	102	2		
340	301	102	4		
341	301	102	5		
342	301	204	1		
345	301	204	2		
348	301	204	4		
349	301	204	5		
350	301	300	1		
353	301	300	2		
356	301	300	4		
357	301	300	5		

TABLE 6.2 Sensor Types and Scale Factors

SENSOR	Scale		TYPE
	MEAN	SD	
1	1	10	wind speed (kts)
2	1	10	wind direction (deg)
3	1	10	temperature (F)
4	10	10	temperature-temperature(6 ft)
5	1	10	dew point depression (F)
6	10	10	pressure-914.2 (mb)
7	100	100	long wave radiation (Ly/min)
8	10	10	precipitation (none observed)
9	100	100	short wave radiation (Ly/min)
10	10	10	visibility (nmi)

Hourly Averages Summary

Hourly averages of selected WINDS mean variables are supplied in a separate data set. The purpose of this reduction was to provide easily accessible wind or temperature fields for the base. Additionally, wind data from all operating 12 ft sensors (maximum of 24 towers) was averaged into a "base average" and the variance between the towers was calculated. This allows for a quick look at the mean flow across the base and the variability of that flow.

Figure 6.1 shows the hourly averages flow at two times during the third day of releases, conditions typical of the experiment. The 900-1000 LDT flow represents flow before the passage of the sea breeze front; light winds speeds and directions ranging from north to northwest over most of the base, implying that releases from HSSF would travel well south of Lompoc. After the sea breeze front passes, the 1200-1300 LDT flow field shows stronger wind speeds and more westerly directions, offering improved chances for impact at Lompoc from HSSF releases. Judging from the centerline positions shown in section 3, the more northerly winds along the coast are local, and do not represent the general flow between HSSF and Lompoc.

Hourly Record Specifics

Suggested Input Format: free or {fixed} field, ASCII, space delimited

field 1: DATE {I5 , FORTRAN convention}

field 2: BS12(24), BSS12(24), BD12(24), BSD12(24)
{24F6.1,24F5.2,24I5,24F5.1}

field 3: TWR12, LATM12, LATS12, LONM12, LONS12, S12(24),
D12(24) {I5,4F5.1,24F6.1,24I5}

field 4-27: same as field 3

field 28: TWR23, HT23, LATM23, LATS23, LONM23, LONS23,
S23(24), D12(24) {2I5,4F5.1,24F6.1,24I5}

field 29-32: same as field 28

field 33: TWR6, LATM6, LATS6, LONM6, LONS6, T6(24)
{I5,4F5.1,24F6.1}

field 34-52: same as field 33

field 53: TWR54, LATM54, LATS54, LONM54, LONS54, DT54(24)
{I5,4F5.1,24F6.1}

field 54-67: same as field 53

field 68: TWR301, LATM301, LATS301, LONM301, LONS301,
PR(24), DP(24), SW(24), LW(24)
{I5,4F5.1,24I5,24F6.1,24I5,24I5}

DATE = date in 1989 (month * 100 + day)

*** Each variable array of 24 elements contains hour averages (or standard deviations) for the 24 hours of DATE. Element 1 corresponds to 0000-0100 LDT, element 2 is 0100-0200 LDT, etc.

BS12(24) = (24 element array) base average 12 ft wind speed (m/s)

BSS12(24) = standard deviation of the 12 ft mean wind speeds across the base

BD12(24) = base average 12 ft wind direction

BSD12(24) = standard deviation of the 12 ft mean
wind directions across the base

TWR12 = tower number with 12 ft wind sensors

LATM12 = latitude minutes past 34 N of the tower

LATS12 = latitude seconds past LATM12 of the tower

LONM12 = longitude minutes past 120 W of the tower

LONS12 = longitude seconds past LONM12 of the tower

S12(24) = average 12 ft wind speed at the tower

D12(24) = average 12 ft wind direction at the tower

*** The sequence TWR12 through D12(24) is repeated 24
times for each of the towers with 12 ft wind sensors.

TWR23 = "tall" tower number

HT23 = height of the tall tower sensor (ft)

LATM23 = latitude minutes past 34 N of the tall tower

LATS23 = latitude seconds past LATM23 of the tall tower

LONM23 = longitude minutes past 120 W of the tall tower

LONS23 = longitude seconds past LONM23 of the tall tower

S23(24) = average 12 ft speed at HT23 on the tall tower

D12(24) = average 12 ft direction at HT23 on the tower

*** The sequence TWR23 through D12(24) is repeated 5
times for each of the tall tower wind sensors.

TWR6 = tower number with 6 ft temperature sensor

LATM6 = latitude minutes past 34 N of the tower

LATS6 = latitude seconds past LATM6 of the tower

LONM6 = longitude minutes past 120 W of the tower

LONS6 = longitude seconds past LONM6 of the tower

T6(24) = average 6 ft temperature (deg C) at the tower

*** The sequence TWR6 through T6(24) is repeated 19 times for each of the towers with 6 ft temperatures.

TWR54 = tower number with 54-6ft temperature difference

LATM54 = latitude minutes past 34 N of the tower

LATS54 = latitude seconds past LATM54 of the tower

LONM54 = longitude minutes past 120 W of the tower

LONS54 = longitude seconds past LONM54 of the tower

DT54(24) = average 54 ft - 6 ft temperature difference
(deg C) at the tower

*** The sequence TWR54 through DT54(24) is repeated 14 times for each of the towers with differential temp
TWR301 = tower number 301

LATM301 = latitude minutes past 34 N of the tower

LATS301 = latitude seconds past LATM6 of the tower

LONM301 = longitude minutes past 120 W of the tower

LONS301 = longitude seconds past LONM6 of the tower

PR(24) = no valid data

DP(24) = average 54 ft dew point temperature at tower 301

SW(24) = no valid data

LW(24) = no valid data

SECTION 6 FIGURE CAPTIONS

F6.1 Average 12 ft wind vectors from the VBG WINDS system for (left) 900-1000 LDT, and (right) 1200-1300 LDT. Labels indicate tower identifiers. Contours are in meters above sea level and coordinates are UTMS.

7. REGIONAL TOWER NETWORK

The Santa Barbara Regional Air Pollution Control District operates a network of meteorological masts over an area ranging from Santa Maria to Santa Barbara. A catalog of 12 ft winds at selected towers for 1 hour averaging periods has been acquired. Most of these tower data sets also include 12 ft temperatures. Even though the network domain is much larger than the domain of tracer measurements for LVDE, these data should be useful for initiating or validating regional scale flow models and compliment the higher density WINDS data. These data are supplied for the entire month of August 1989. Tower locations correlating with the site number listed in the data set are given in Table 7.1.

Regional Tower Network Specifics

Suggested Input Format: {fixed} field, ASCII

*** For all data, ASCII text identifies the variables.
Therefore, line by line format is not supplied.

TABLE 7.1 Regional Tower Locations

#	<u>site</u>	<u>latitude</u>	<u>longitude</u>
1	Battles	34 56.09	120 24.24
2	Pt Arguello	34 34.30	120 38.45
3	Lompoc HSP	34 43.31	120 25.36
5	Paradise Rd	34 32.15	119 48.00
7	Bonita School	35 59.22	120 30.47
9	Casmalia Hills	34 55.54	120 36.26
12	VAFB STS	34 35.41	120 37.39
16	Pt Conception	34 27.12	120 27.27
17	Jalama Beach	34 30.40	120 29.21
19	Gaviota West	34 28.40	120 12.49
20	Gaviota East	34 28.40	120 12.15
21	Odor West	34 28.10	120 13.10
22	Odor East	34 28.20	120 10.40
26	LFC 1	34 29.24	120 02.45
27	LFC 2	34 28.50	120 01.58
28	LFC 3	34 28.18	120 02.22
29	LFC 4	34 28.57	120 02.35
30	LFC 10	34 24.56	119 52.47

8. RAWINSONDE DATA

Rawinsonde data consists of the 27 VBG operational launches (0000 UTC, 1200 UTC) over the days 6-20 Aug, and 12 supplemental launches performed by EPG/NPS during the tracer experiments. The supplemental rawinsonde data has significantly higher vertical resolution than the VBG data because the instruments reports every 5 seconds versus 15 seconds for the base system. The VBG data includes only significant levels (NWS standard), while the EPG/NPS data includes all measurements. Only data at heights below 10 km are listed. Because of hardware problems, the EPG/NPS rawinsonde system's wind estimates were unreliable, so only surface winds are reported. For similar reasons, all supplemental launch attempts on 10,11 Aug were total failures. Successful launches were completed only after 12 Aug.

Rawinsonde Record Specifics

Suggested Input Format: free-field, space-delimited

line 1: ID, ASCENT, N, LAT, LON, ZS, DATE, TIME

ID = station identifier

1764 = building 1764 (north base by airfield)

900 = building 900 (south base near release site)

1 = EPG/NPS mobile laboratory

ASCENT = sequential launch number (EPG/NPS use a different sequence than VBG)

N = number of measurement levels in the current record

LAT = latitude (north) in decimal degrees
LON = longitude (west) in decimal degrees
ZS = height (m) of station
DATE = date in 1989 (month * 100 + day)
TIME = Local Daylight Time of launch (hour*100 + minute)

line 2-end: Z, P, T, RH, TD, MIX, DD, FF

Z = height (m)
P = pressure (mb)
T = temperature (deg C)
RH = relative humidity (%)
TD = dew point temperature (deg C)
MIX = mixing ratio (g/kg)
DD = wind speed (m/s)
FF = wind direction (deg)

record delimiter = empty line [CRLF]

9. SURFACE-LAYER PROFILE MAST

A surface layer profile mast was located 100 m upwind (west) of Building 900, and was operated continuously during LVDE. Four anemometers and four temperature sensors were mounted at the positions shown in fig. 9.1. The mast could be rotated to a horizontal position for maintenance and calibration then raised to a vertical orientation for data acquisition. Measurements were collected at 50 hz, then averaged and stored at ten minute intervals.

The profile mast was rotated to a horizontal orientation (between 8/08/89 15:00 and 8/09/89 15:00) and the wind speed and temperature measurements from each of the sensors were recorded for a 24 hour period. Temperature and wind speed measurements from each sensor were compared with the average temperature and wind speed for all four sensors and linear correlations were determined. These linear regressions were averaged to find an average linear regression. Each sensor was then calibrated by adding the difference in y-intercept between the sensor and the average and then multiplying by the ratio of the two slopes. For wind velocity,

$$u_{i \text{ cal}} = (u_i + y_i - y_{\text{ave}}) * m_i / m_{\text{ave}} \quad i \rightarrow 1, 4, \quad (9.1)$$

where $u_{i \text{ cal}}$ is the calibrated wind speed, y is the y-intercept and

m is the slope of the linear regression corresponding to the individual sensor (i) or the average of the sensors (ave). An analogous equation applies to the temperature sensors. Linear regressions for the calibrated anemometers and the calibrated temperature sensors in fig. 9.2 validate this calibration algorithm. Note that the calibration is so precise all four linear regressions overlap in both cases.

The wind vane on the profile mast was calibrated by comparing ten minute averaged wind directions with those recorded by the DASS Gill anemometer at Building 900 during brisk constant winds.

The friction velocity, (u_*), surface temperature scaling term, (T_*), and Monin-Obukhov length, (L), were calculated utilizing Monin-Obukhov surface-layer theory. Parameterizing a few variables and utilizing dimensional analysis, one can develop equations which derive some relevant quantities which are difficult to measure directly; i.e., surface heat flux (see Panofsky and Dutton, 1984).

The friction velocity is defined as

$$u_* \equiv (\tau_o / \rho_o)^{1/2} , \quad (9.2)$$

where τ_o and ρ_o are surface values for Reynolds stress and air density. Assuming a first-order closure, the Reynolds stress can be defined as

$$\tau = K_m \rho \partial u / \partial z \quad (9.3)$$

where K_m is the kinematic viscosity and is proportional to the product of the eddy size and the eddy velocity.

If we further assume that the eddy size is proportional to height z and eddy velocity is proportional to u_* , K_m can be described as

$$K_m = k_a u_* z \quad (9.4)$$

where k_a is von Karman's constant. Since K_m does not vanish at the surface, one can define a height, z_o , the roughness height, below which the horizontal wind speed equals zero. So at the surface,

$$K_m = k_a u_* z_o. \quad (9.5)$$

Equations 9.2, 9.3, and 9.5 can be combined and integrated to yield a logarithmic wind profile which can be used to determine u ;

$$u_* = u / k_a \ln(z/z_o) + \phi_m \quad (9.6)$$

where ϕ_m is a stability correction factor applied when the vertical temperature profile is either slightly unstable or slightly stable. An analogous equation for T is

$$T_* = T/k_g \ln(z/z_{0T}) + \phi_T. \quad (9.7)$$

The level of stability (required to determine $\phi_{m,T}$) is defined by the Monin-Obukhov length,

$$L = T_0 u_*^2 / (k_g g T_*) \quad (9.8)$$

where T_0 is the surface temperature and g is acceleration due to gravity.

Equations 9.6 and 9.7 were iterated utilizing the graphical technique of plotting $\ln z$ against u and T to determine u_* , T_* , and a statistically reliable value for z_0 . This z_0 value was then used to recompute u_* and T_* .

We determined z_0 to be $5.1 \text{ cm} \pm 0.5 \text{ cm}$ for westerly to northwesterly winds. This was also consistent with the rule of thumb that z_0 be $1/7$ the height of the scrub brush vegetation canopy.

Although the general upwind fetch was relatively level compared with other South Vandenberg terrain there were significant slopes dropping into the Lompoc Valley to the north of the mast. Prevailing theory indicates that these slopes would only cause kinks in the wind and temperature profiles at heights above the top

level of the profile mast, and z_0 estimates for northerly winds were consistent with values for more westerly flow.

Profile Mast Data Specifics

Suggested Input Format: free field, space delimited

*** Bad or missing data indicated as -99 except for L = 99

Column 1 - Begin time for data run in Pacific
Standard Time

Column 2 - End time for data run

Column 3 - Derived 12 ft wind speed (m/s)

Column 4 - 12 ft wind direction (degrees)

Column 5 - Derived 6 ft temperature (deg C)

Column 6 - Ustar (m/s)

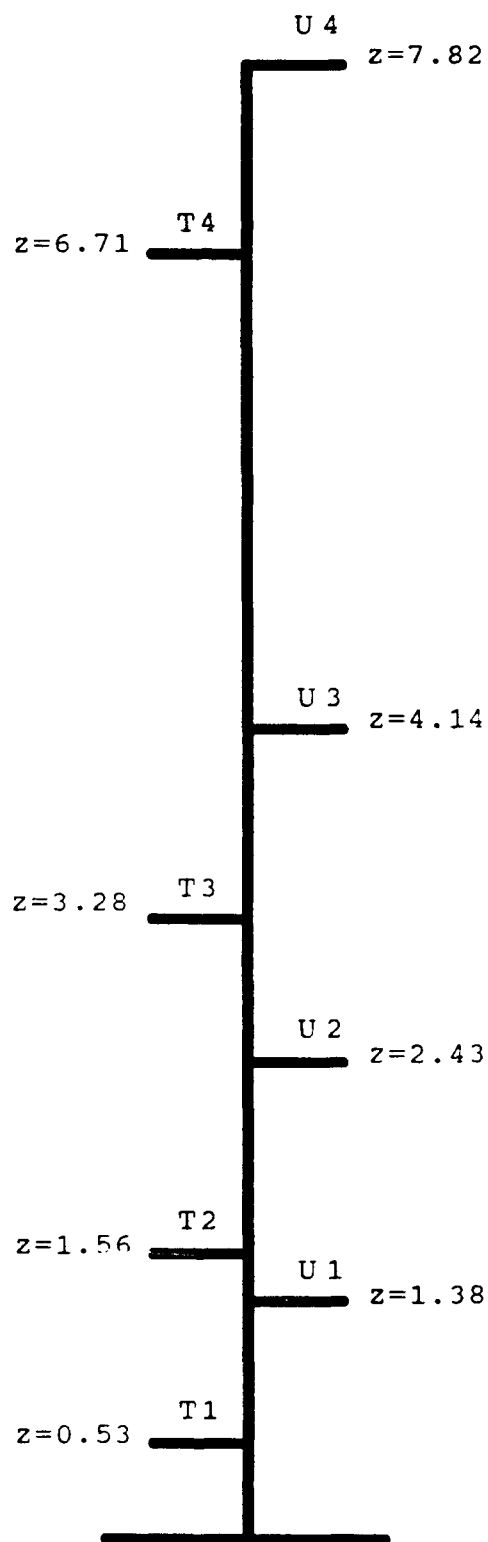
Column 7 - Tstar (deg C)

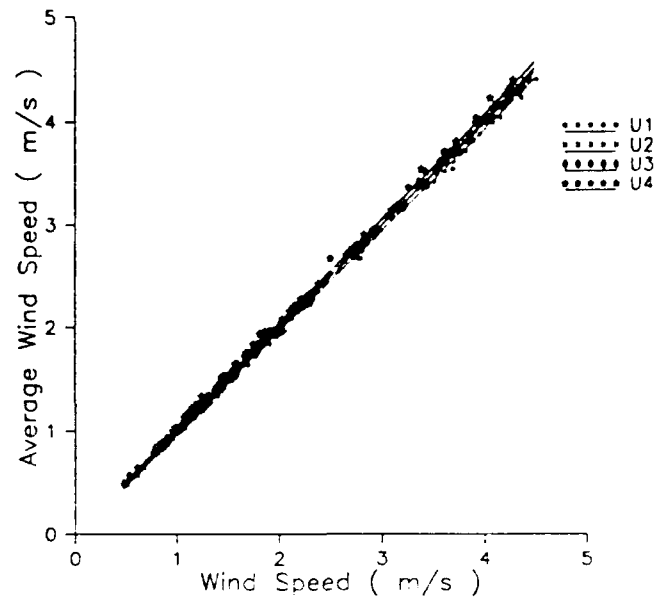
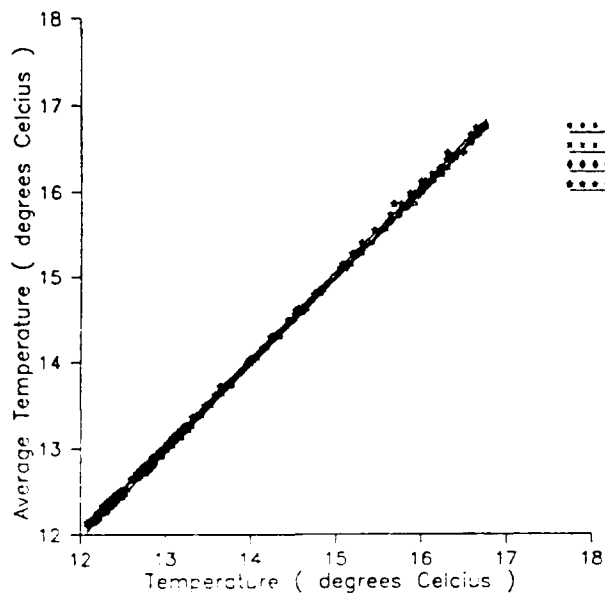
Column 8 - L, the Monin - Obukhov length (m)

SECTION 9 FIGURE CAPTIONS

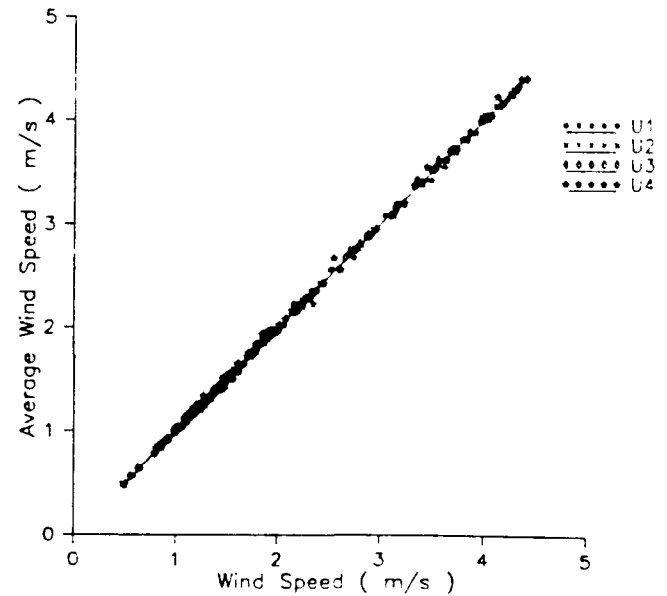
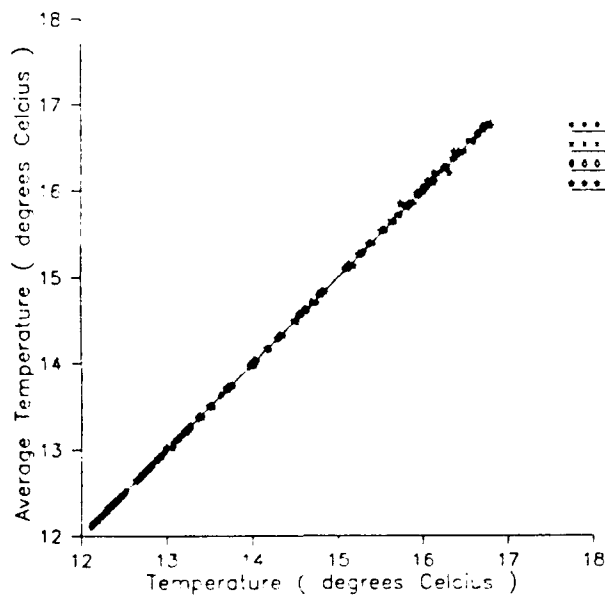
F9.1 Profile mast with wind sensors (U 1-4) and temperature sensors (T 1-4) at the indicated heights in meters.

F9.2 Linear regressions of profile mast wind and temperature sensors a) before, and b) after application of eq. 9.1.





(a)



(b)

10. RELEASE SITE SURFACE-LAYER DATA AND RADIATION

We obtained data from two sources at Tower 57, the HSSF release point for the LVDE experiment. The first source was the standard WINDS equipment: cup anemometers and wind direction vanes at 12 and 54 feet, and temperature sensors with aspirators at 6 and 54 feet. The communications link between the WINDS master computer and Tower 57 was not working for the majority of LVDE but we were able to intercept and store the data with an IBM PC.

The second source was equipment temporarily installed for the experiment: a Weathertronics (model 8152-A) temperature sensor with aspirator, a Young bivane anemometer at 54 feet, and upward looking Eppley shortwave and longwave radiation sensors.

By inspection of the 54 - 6 ft temperature differences, it was determined that the WINDS 54 ft temperature sensor was unreliable. Therefore, the 54 - 6 ft temperature differences required for heat flux calculations were derived from the NPS 54 ft sensor and the WINDS 6 ft sensor. (The WINDS temperature difference has subsequently been repaired.)

To insure accurate temperature differences for heat flux calculations, the 6 ft temperature sensor was calibrated by temporarily moving the NPS 54 ft temperature sensor to 6 ft and

determining a linear correlation between the two sensors. The NPS temperature sensor was factory calibrated and measurements with this sensor were treated as true values. Figure 10.1 compares the two sensors after calibration.

The bivane wind speed and radiometers were calibrated prior to the experiment. The bivane wind direction was calibrated by comparison with the 54 foot WINDS vane. Because the bivane frequently goes out of balance, the true wind speed will often be greater than the measured wind speed. The bivane wind speeds were therefore further calibrated by treating the capture wind speed as the true value (Fig. 10.2).

The bivane measurements were recorded at 2 hz between 8/10/89 and 8/14/89 and 3 hz thereafter. Standard deviations for the three wind components were derived over 10 minute periods. Horizontal wind components were calibrated to match 54 ft WINDS measurements before mean wind speeds and standard deviations were determined. No further vertical wind speed calibration was made.

Two sets of radiometers were used during the experiment; one located at Tower 057 and the other sited at the Water Treatment Plant in Lompoc (N45 39.0', W120 27.1'). Each set included an Eppley pyrgeometer (model PIR) to measure longwave radiation, an Eppley pyranometer (model PSP) to measure shortwave radiation and a Weathertronics amplifier (model series 1300). During calibration

and the experiment the radiometers and amplifiers were treated as a matched sets.

The radiometer calibration procedure was fairly involved and will only be outlined. Factory specified calibrations were applied to the radiometers and amplifiers. The two sets of amplifiers were compared against a third set by operating all three several days in a sunny location. Linear correlations of the results were generated to establish a common value based on the third, freshly calibrated radiometer set. Adjustments were made for solar heating of the pyrgeometer domes. No adjustments were made for differential heating of the pyrgeometer dome and body for either set.

Tower 57 values of u_* , T_* , and L were determined utilizing temperatures at 54 and 6 ft, 54 ft wind speeds, and the z_0 determined at the profile mast. As with the profile mast, stability functions were used to iteratively determine u_* and T_* . Since the two temperature sensors were widely spaced and the surface roughness estimate was made approximately 1 km downwind of the tower, we recommend that these surface stress, heat flux, and stability should only be used as a back-up to the profile mast estimates. For applications which require surface-layer turbulent statistics, we recommend using the bivane measurements over applying surface-layer similarity to the profile mast data. A second source of surface-layer turbulent statistics is the ground-

level ($z=0$) range bin from the Building 900 DASS (see section IV). These data are derived from a Gill-type three-axis propeller anemometer. We recommend avoiding the use of the WINDS turbulence statistics (e.g. sigma theta) since these data are based on 1 min averages (see section 13). Turbulence statistics at the WINDS tower locations have been parameterized by Skupniewicz et al. (1989) to include the effects of averaging time. This method may be used to adjust the WINDS turbulent statistics to greater averaging times, or when WINDS data is unavailable.

Release Site Meteorological Data Specifics

Suggested Input Format: free field, space delimited

*** Bad or missing data is demarked -99 except for L = 99.

- Column 1 - Begin time for a data run in Pacific Standard Time
- Column 2 - End time for a data run
- Column 3 - 54 ft East - west (u) wind speed component from bivane anemometer (m/s)
- Column 4 - 54 ft North - south (v) wind speed component from bivane anemometer (m/s)
- Column 5 - 54 ft vertical wind speed (m/s)
- Column 6 - Standard deviation of u (m/s)
- Column 7 - Standard deviation of v (m/s)
- Column 8 - Standard deviation of w (m/s)
- Column 9 - Downward shortwave radiation (W/m^2)
- Column 10 - Downward longwave radiation (W/m^2)
- Column 11 - 6 ft temperature (deg C)
- Column 12 - 12 ft wind speed (m/s)

Column 13 - 12 ft wind direction (degrees)

Column 14 - Ustar (m/s)

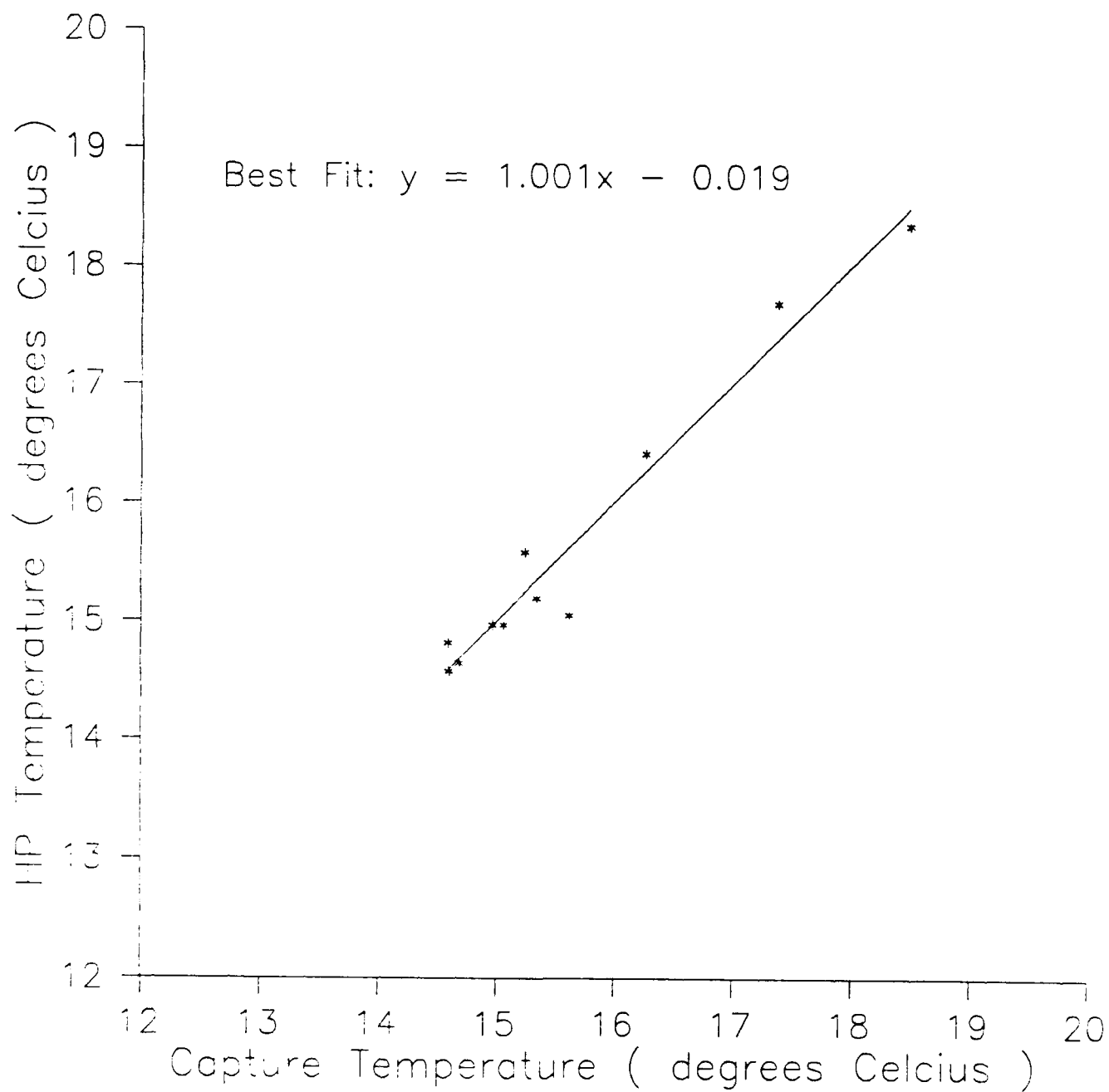
Column 15 - Tstar (deg C)

Column 16 - L, Monin - Obukhov length (m)

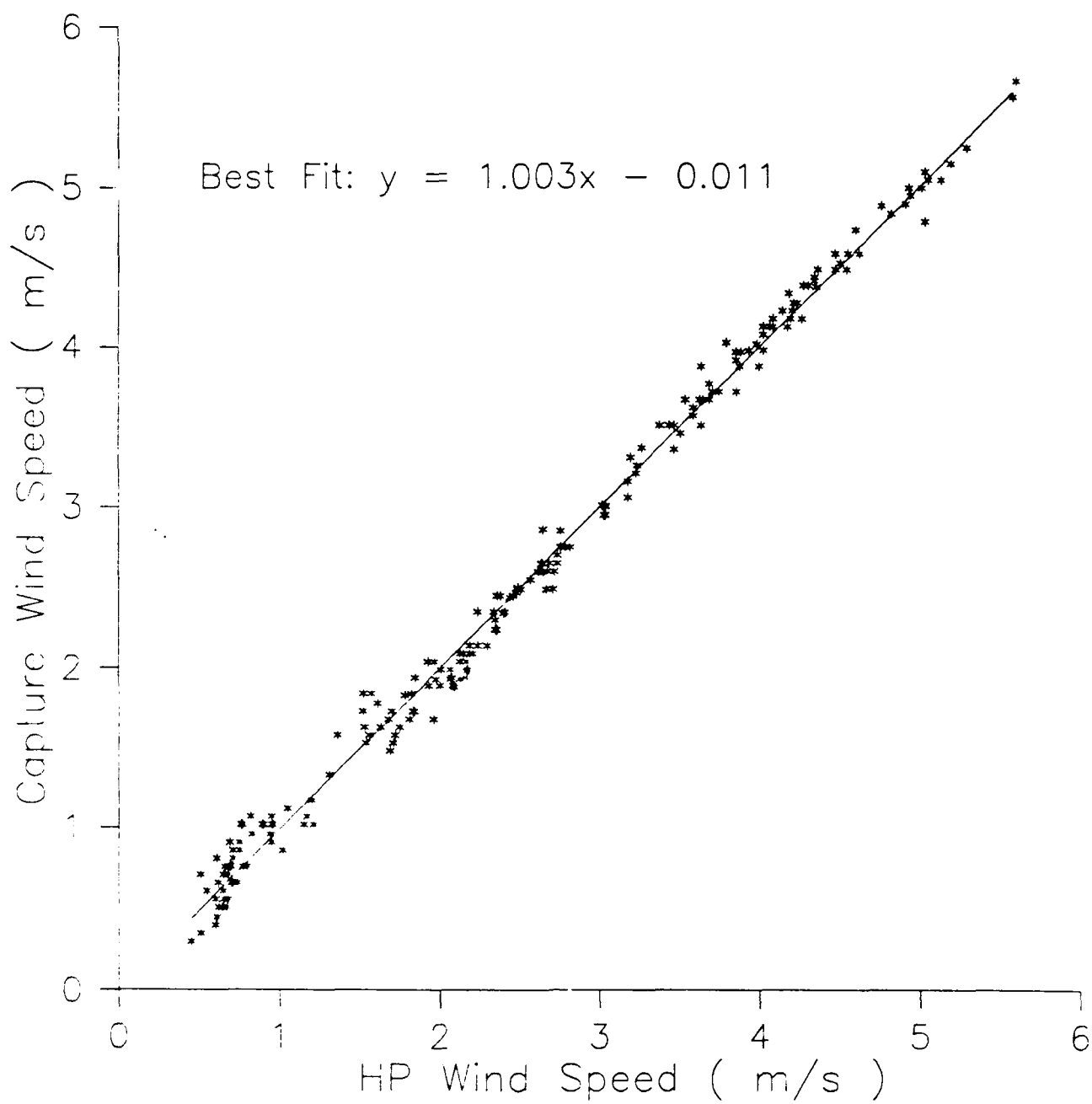
SECTION 10 FIGURE CAPTIONS

F10.1 Linear regressions comparing the 6' WINDS temperature sensor with the factory calibrated NPS temperature sensor.

F10.2 Comparison of calibrated bivane wind speeds with 54' WINDS wind speeds.



F10.1



11. CLOUD COVERAGE ANALYSIS

Determination of the stratus cloud edge is critical in determining boundary layer flow and turbulence at VAFB (Skupniewicz et al., 1990a). We obtained hourly visible image data from the 4 km resolution NOAA GOES-7 geostationary satellite, parked at 35,000 km in geostationary orbit, and also twice a day 1 km resolution images from the 850 km polar orbiting NOAA AVHRR. Since our releases began after 9:00 PDT, this coincides with the 8:22 - 9:40 PDT flyby times of the AVHRR satellite. This period is also shortly before inland heating begins to erode the stratus base and burn its edges back toward the coastline (Skupniewicz et al., 1990b). The second flyby period: 13:45 - 15:05 PDT is also quite useful, since it coincides with the period of maximal westward burn-off. For these reasons the HRPT data were selected for the initial analysis included in this report.

In figs. 11.1-11 complete or nearly complete stratus coverage is to the left of the dashed line and stars denote the day's release site (the HSSF is always marked). Lompoc and base boundaries are outlined. The domain was totally stratus covered during morning flybys on the 13th, 16th, and 17th and totally clear for the afternoon flybys on the 16th and 17th. Hence, we omit the corresponding figures.

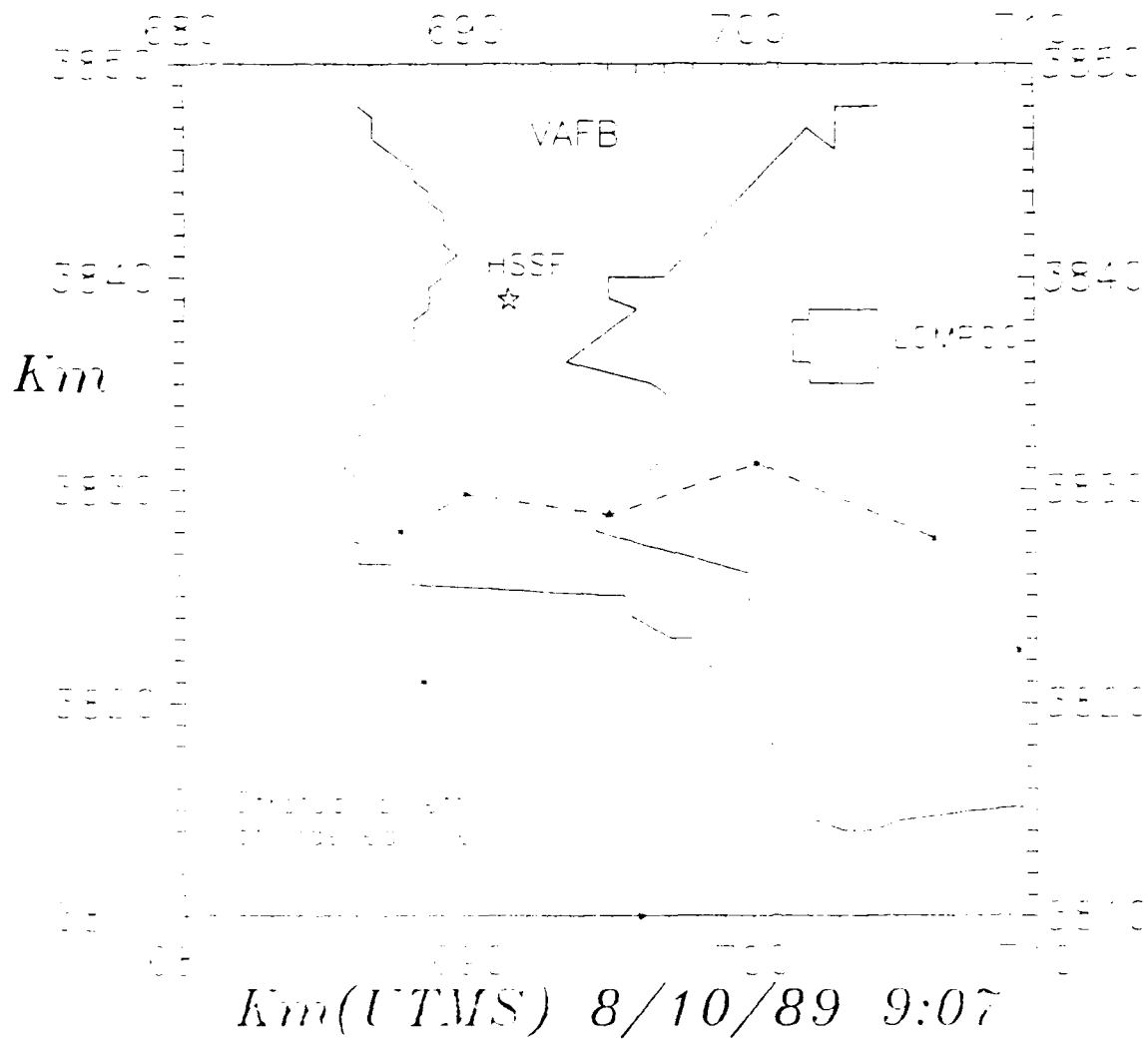
The figures show that the waters south of Pt. Concepcion and the mountains to the north and west are usually clear. We attribute this to the high ground rising above the nocturnal inversion and to the chronic nocturnal northwesterlies which appear as offshore winds with respect to the coastline south of Pt. Arguello. The morning and afternoon flybys make the daily westward migration of the stratus edge quite clear. During most afternoons the stratus edge tends to parallel the coast north of Pt. Arguello, remaining slightly east of the HSSF, while a stratus tongue sometimes extends eastward up the Lompoc Valley. These points are entirely consistent with our ground based observations.

Copies of the satellite data tapes are available from NPS upon request.

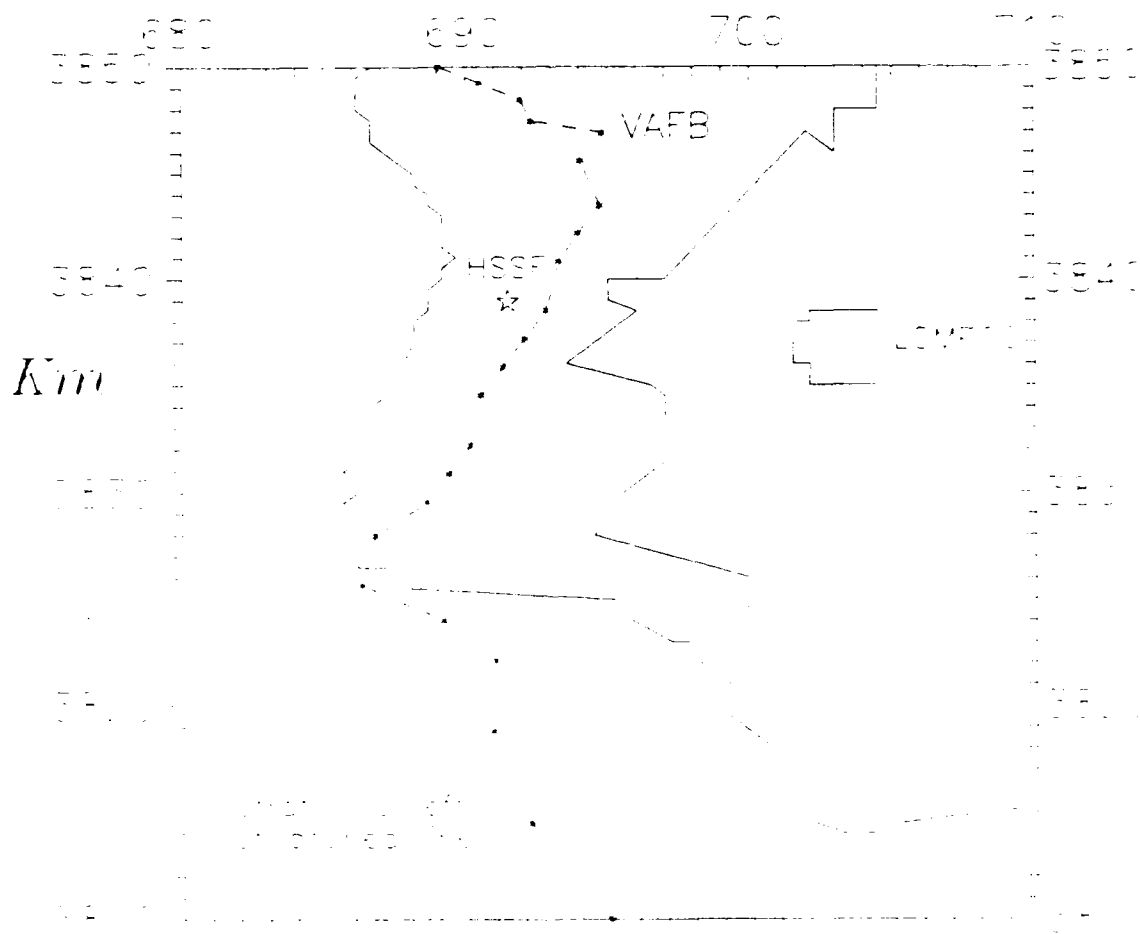
SECTION 11 FIGURE CAPTIONS

F11.1-11 Stratus cover as determined from NOAA AVHRR high resolution visual imagery (1 km). Images were landmarked to Pt. Concepcion, and are accurate to approximately 2 km. Times are in PDT.

STRATUS CLOUD BOUNDARIES

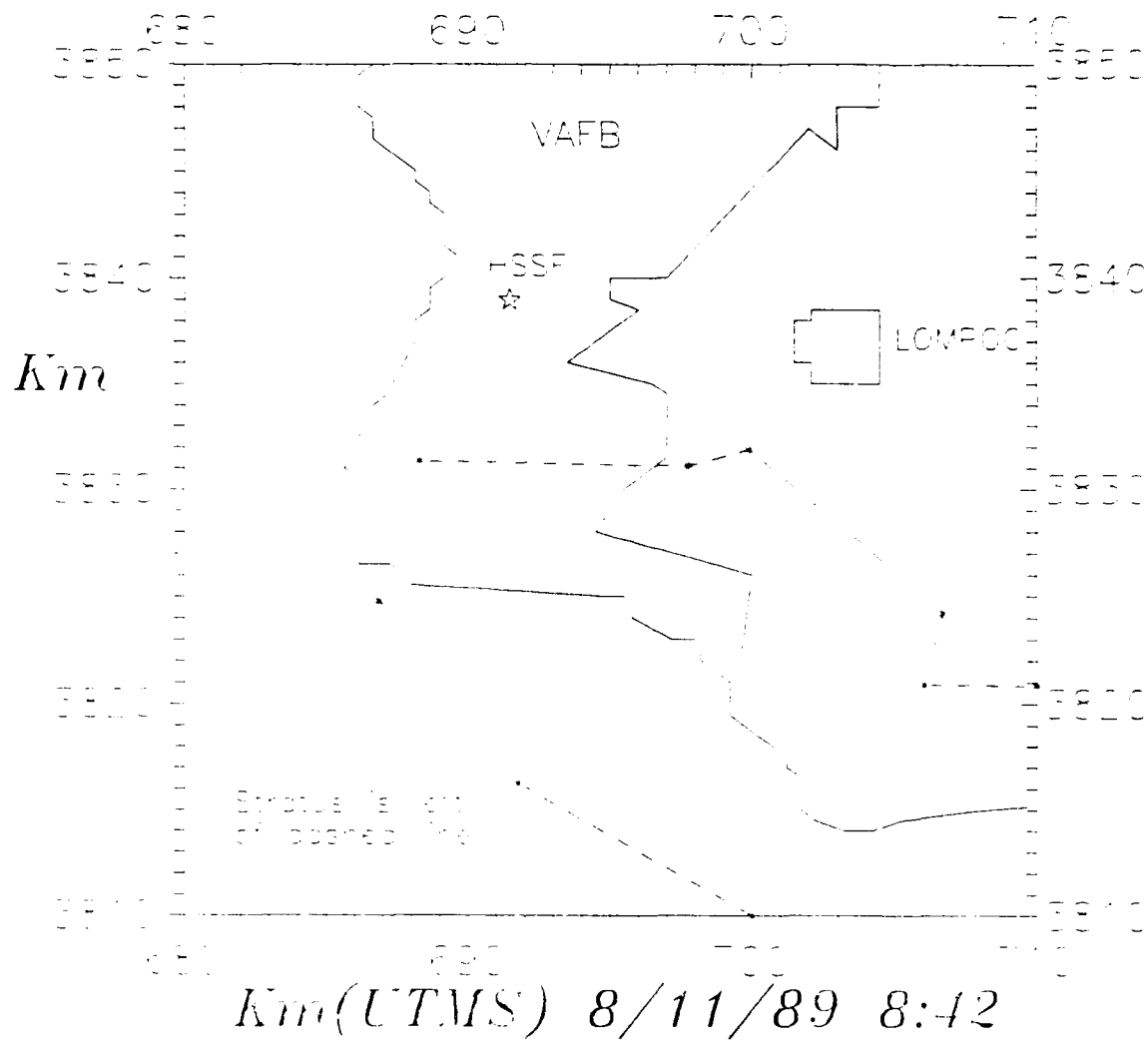


STRATUS CLOUD BOUNDARIES

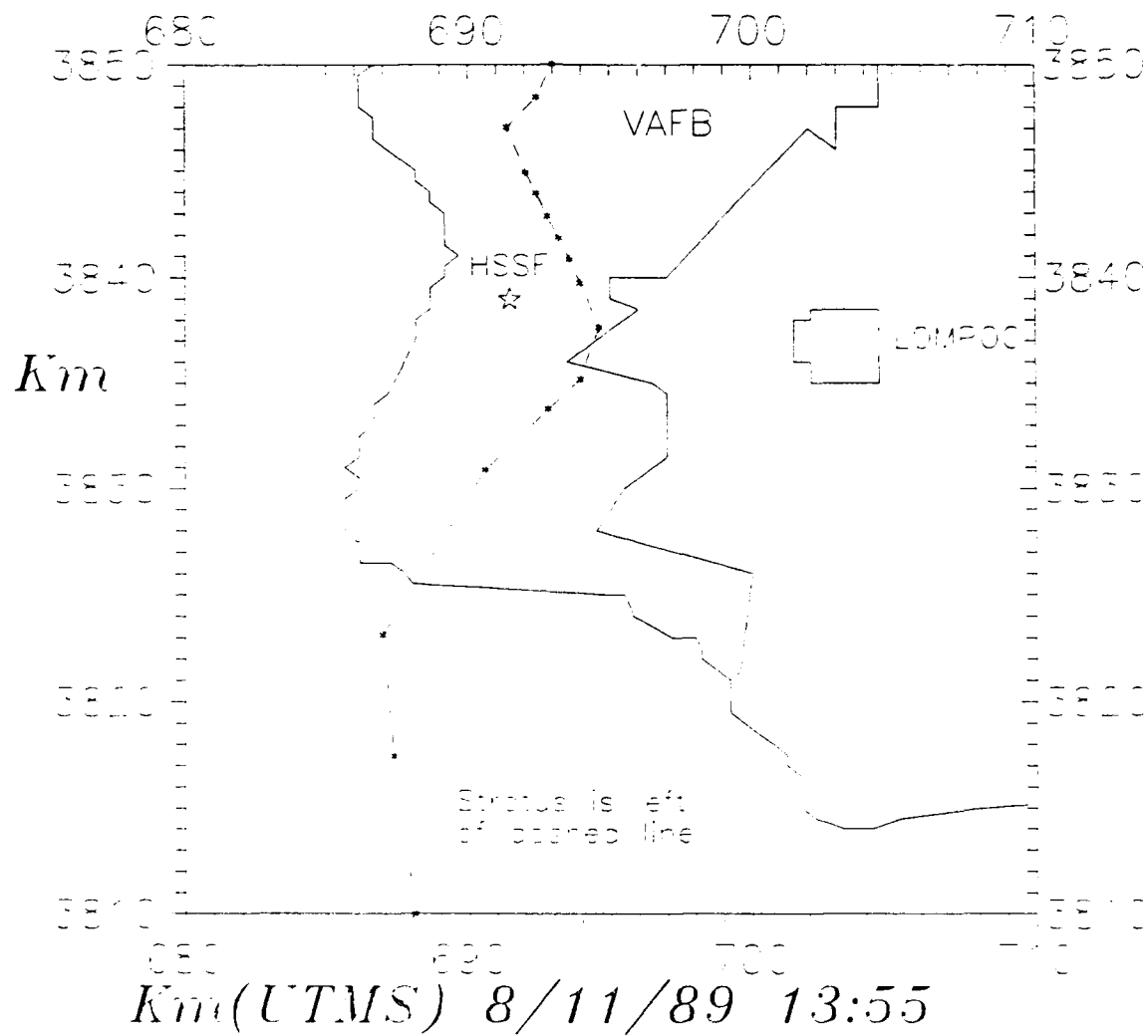


Km(UTMS) 8/10/89 14:06

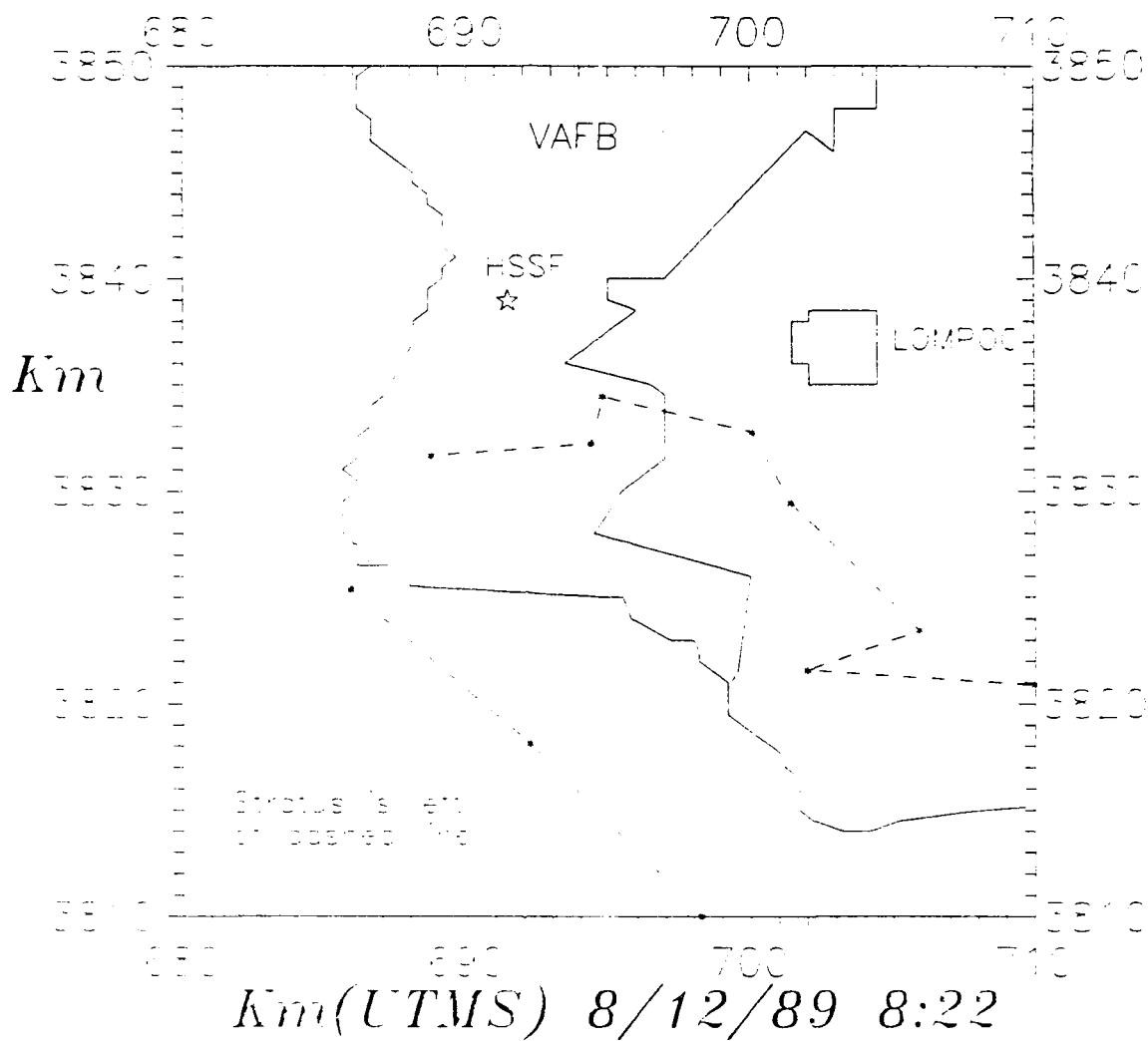
STRATUS CLOUD BOUNDARIES



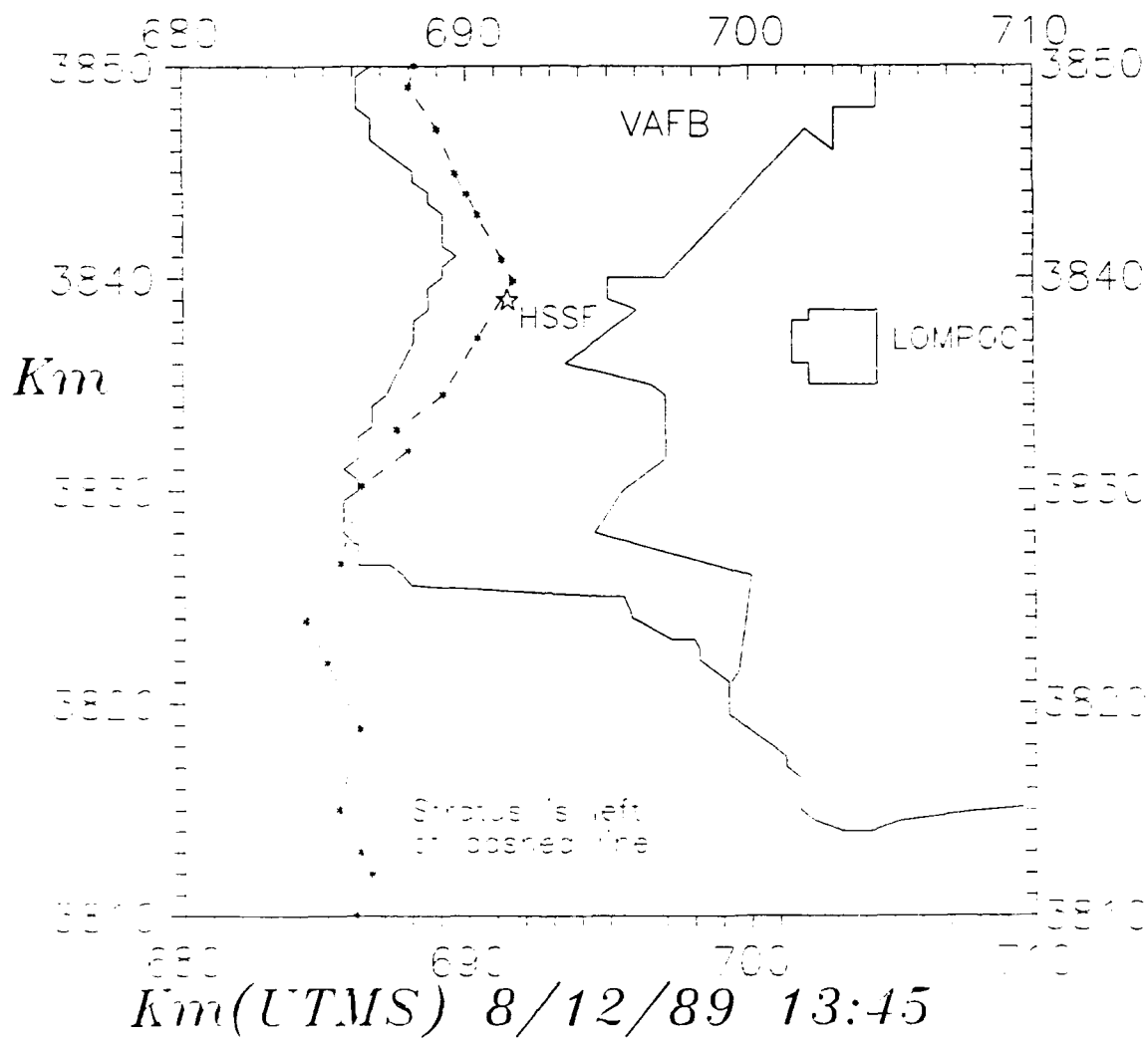
STRATUS CLOUD BOUNDARIES



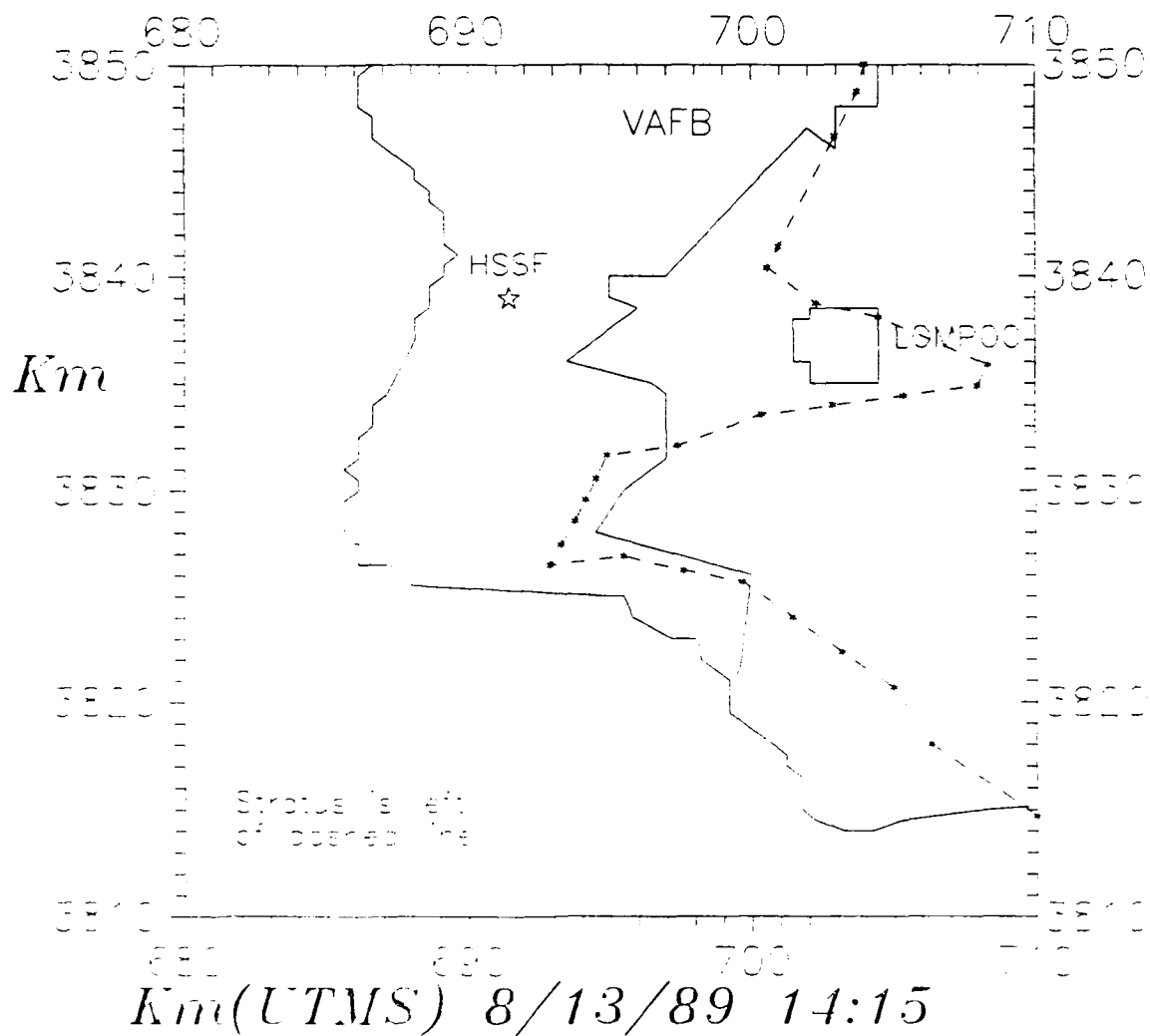
STRATUS CLOUD BOUNDARIES



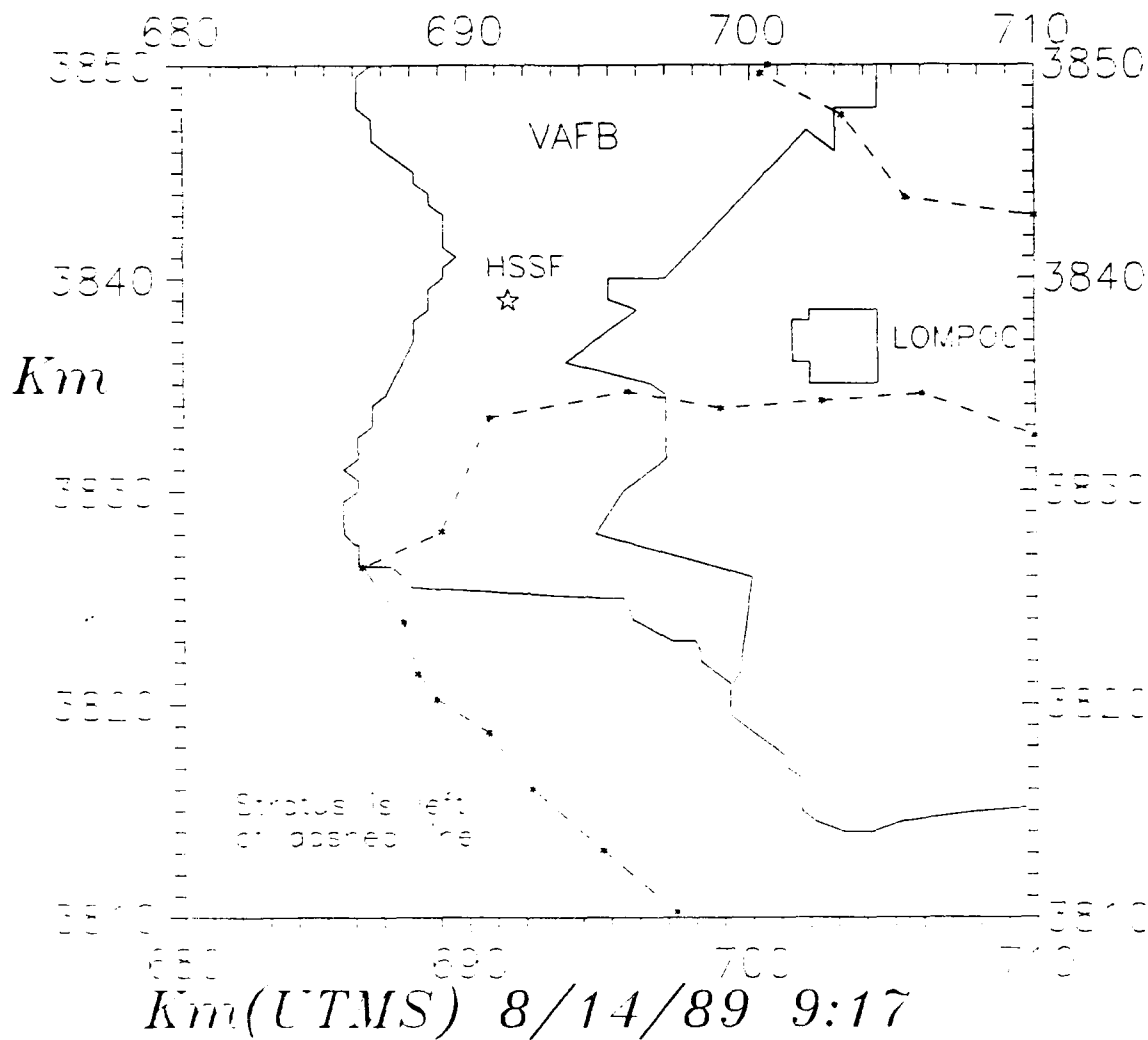
STRATUS CLOUD BOUNDARIES



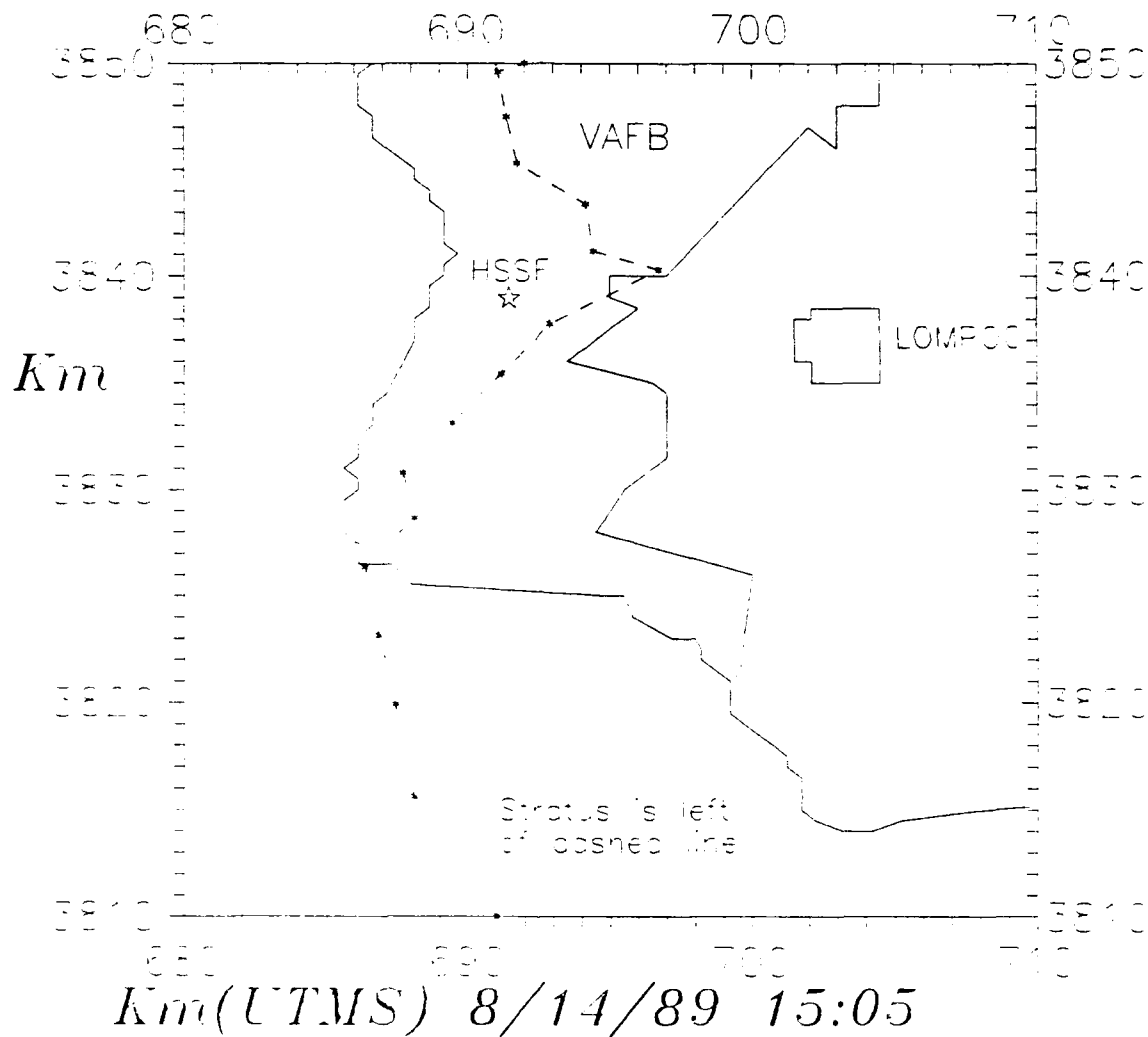
STRATUS CLOUD BOUNDARIES



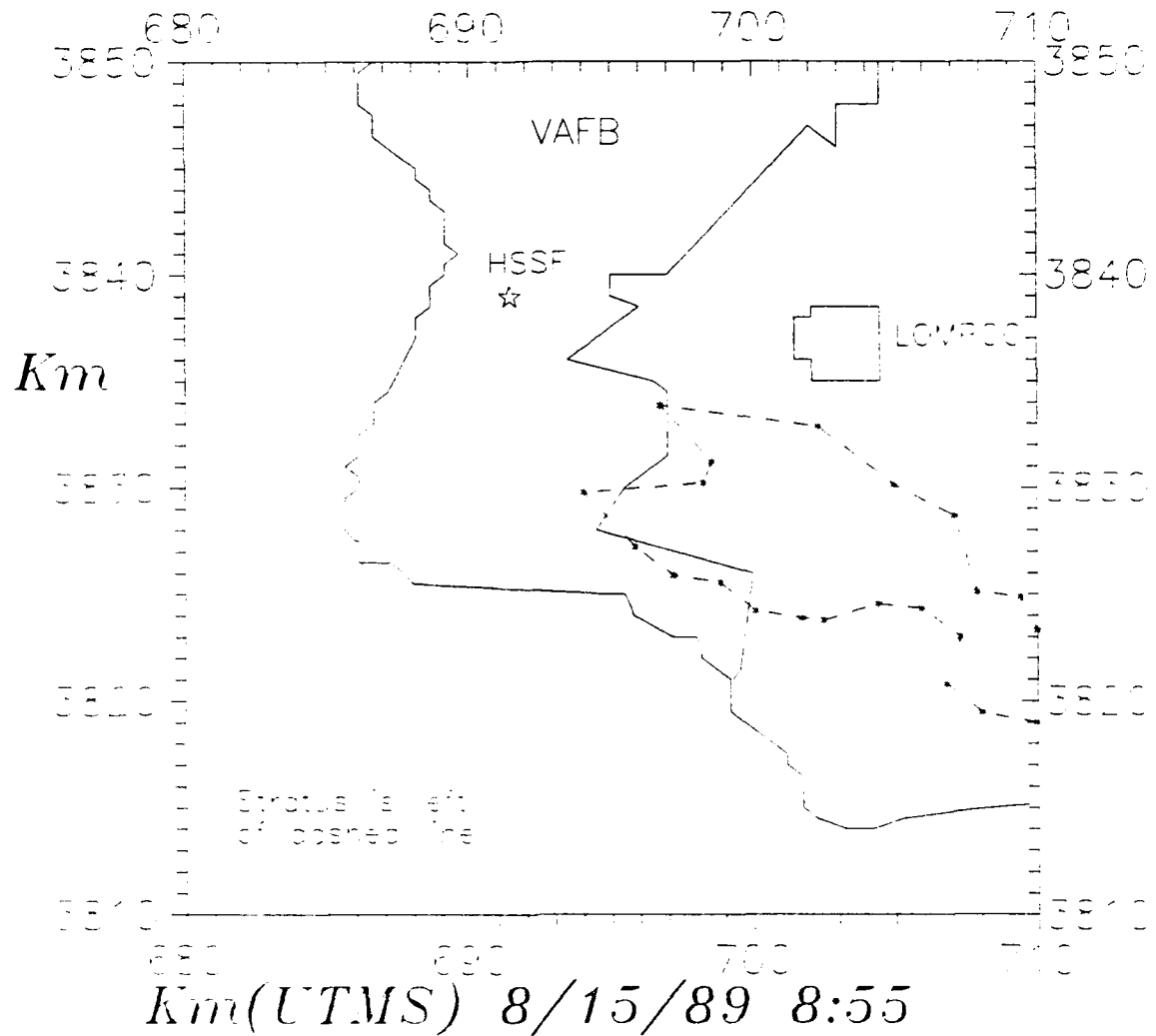
STRATUS CLOUD BOUNDARIES



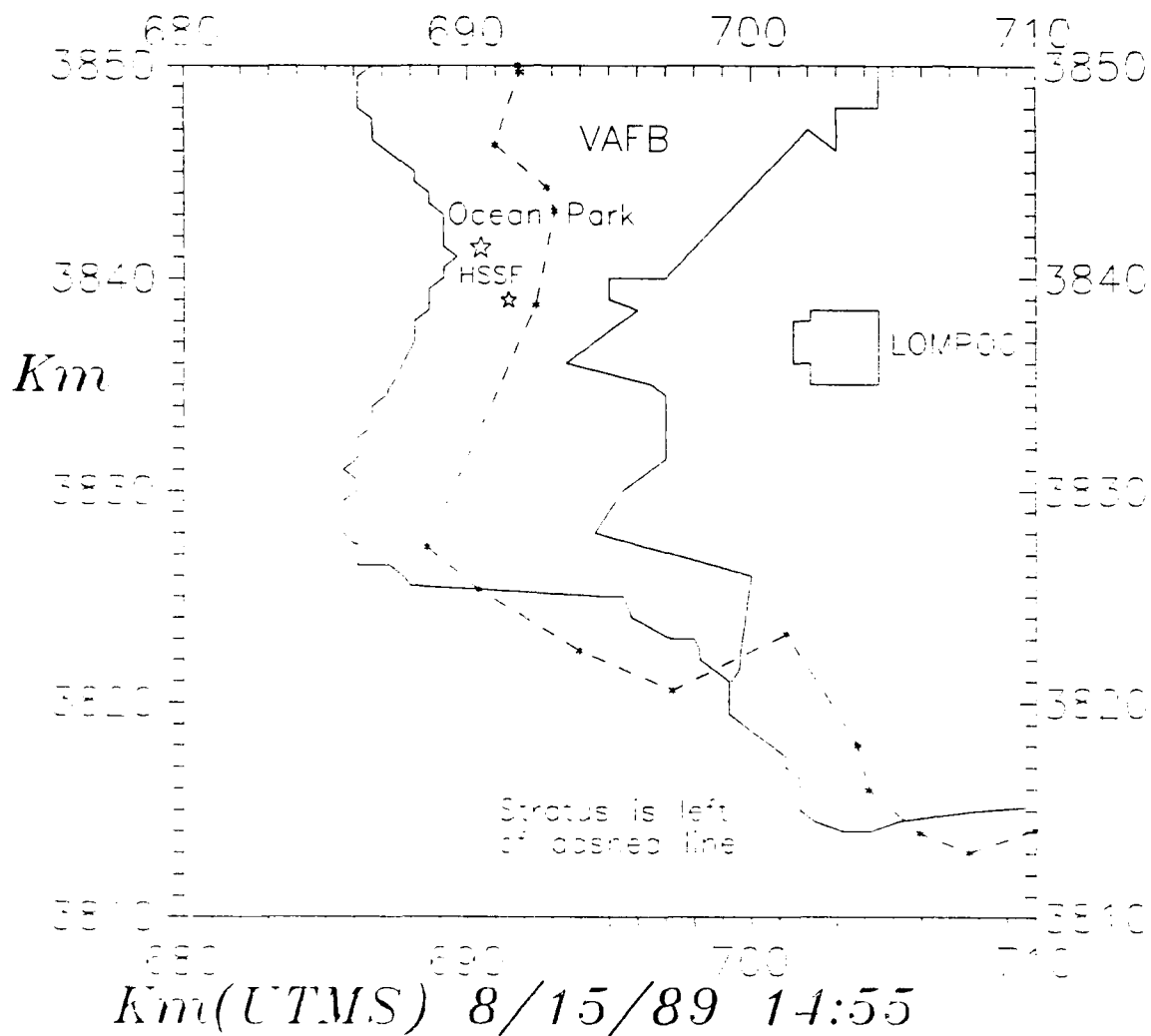
STRATUS CLOUD BOUNDARIES



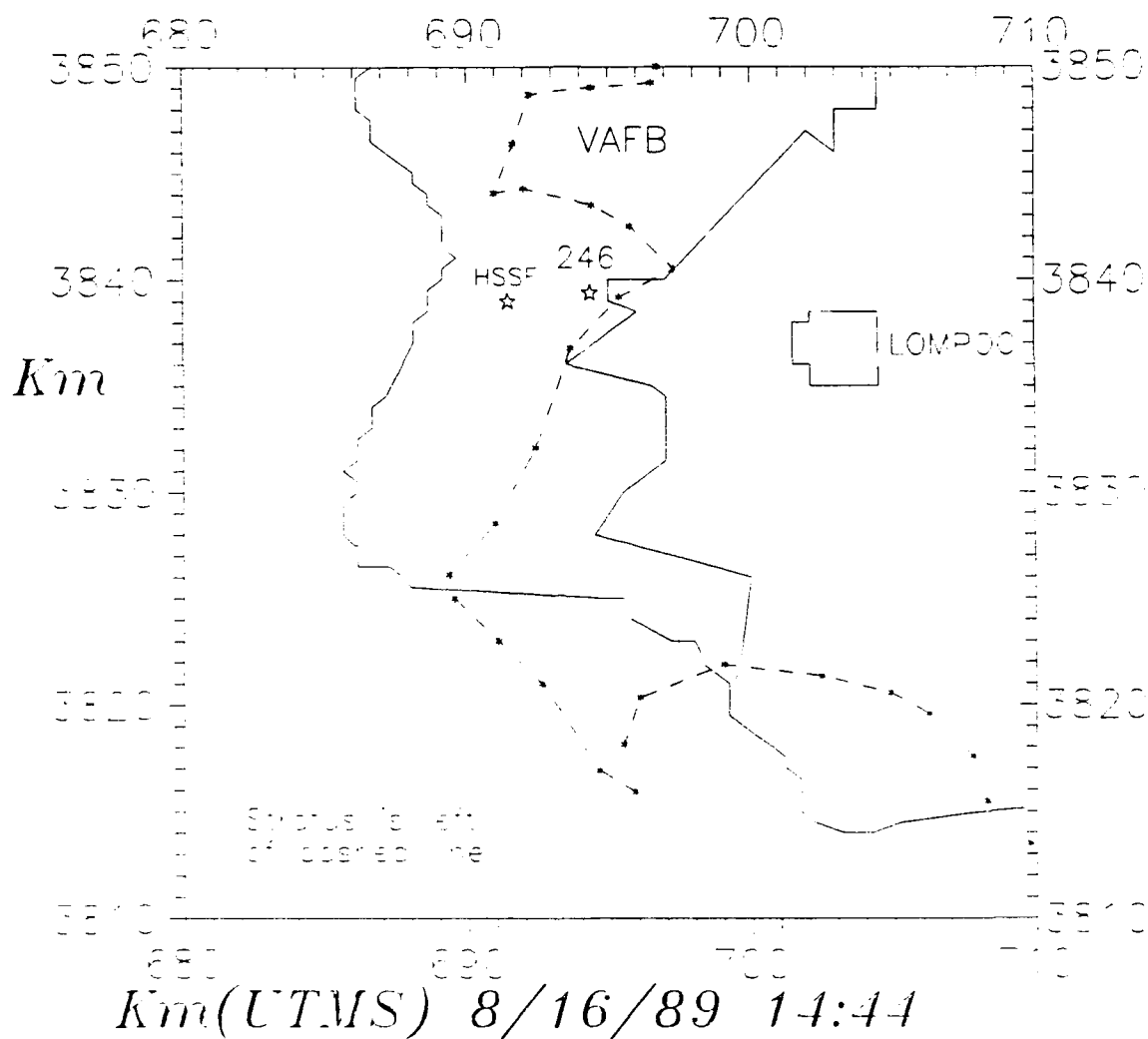
STRATUS CLOUD BOUNDARIES



STRATUS CLOUD BOUNDARIES



STRATUS CLOUD BOUNDARIES



12. SYNOPTIC METEOROLOGY

Selected NWS charts are supplied in figs. 12.1-11 summarizing the background synoptic-scale weather during LVDE. Tapes of all standard NWS chart data for the period are archived at NPS, and copies are available upon request. A short synopsis follows.

A typical summer sea breeze pattern prevailed during LVDE. The 500 mb pressure gradient was southwesterly before the test (fig. 12.1) and remained so through the entire experiment until the last day, 17 Aug, when a trough passed through California (fig. 12.2). The upper level northwesterly flow on the back side of the trough caused the boundary layer flow to veer more (rotate clockwise) on the last day of the experiment.

Fig. 12.3 shows the dominant 850 mb semi-permanent pattern. A subtropical high pressure center remained near 40 N, 145 W during all of LVDE. A complimentary thermal low is seen over California in fig 12.3. Note that the uniform southwesterly flow at 500 mb is not evident at 850 mb. The thermal low is actually centered slightly off the coast, resulting in strong northerly flow out to sea and weaker southerly flow along the coast of California. At the surface, the thermal low is centered over the California Central Valley (e.g. fig. 12.6). This

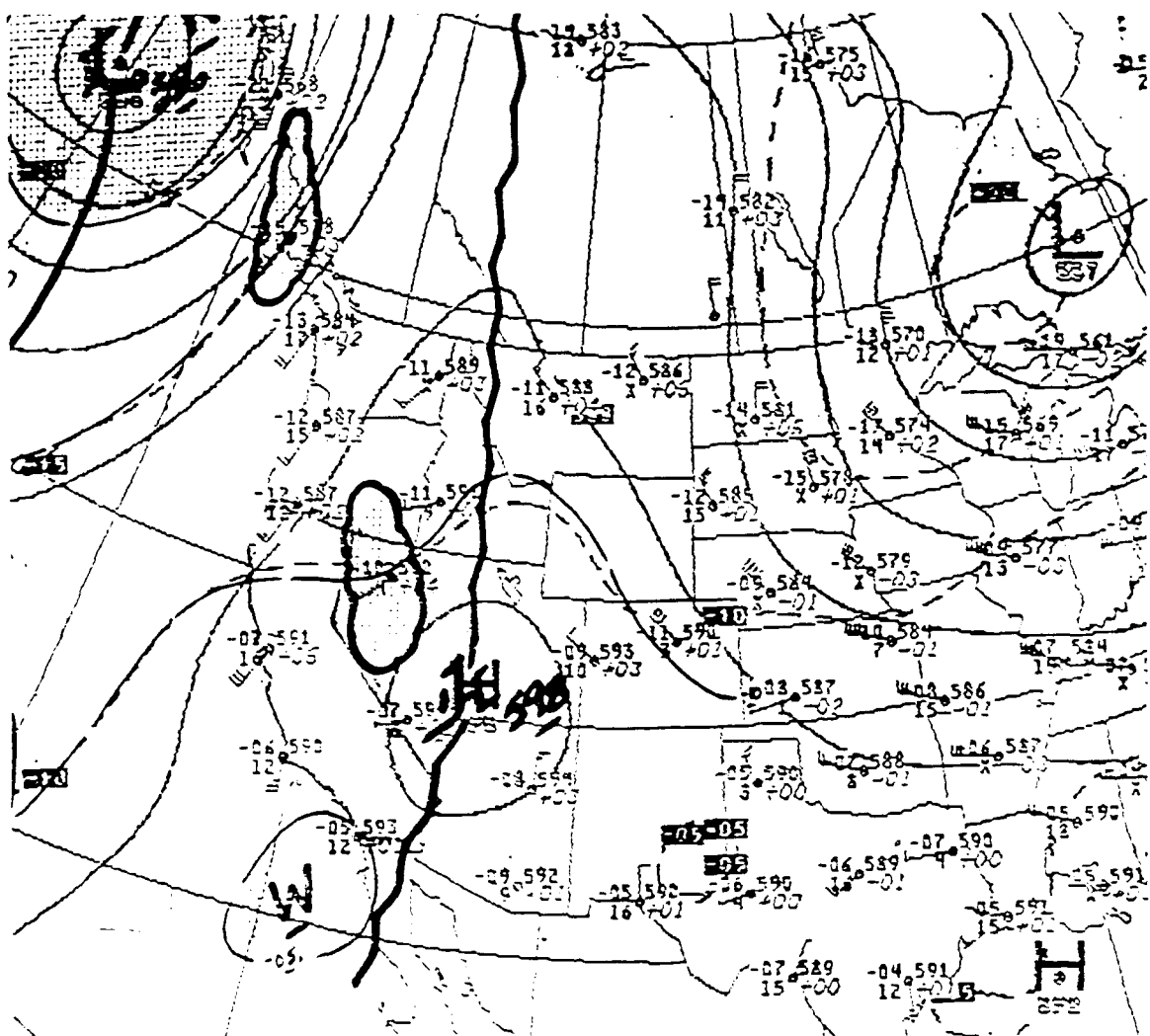
tilting of the trough axis is most likely due to the coastal temperature gradient, and is analogous to the characteristic westward tilt of troughs in developing baroclinic storm systems.

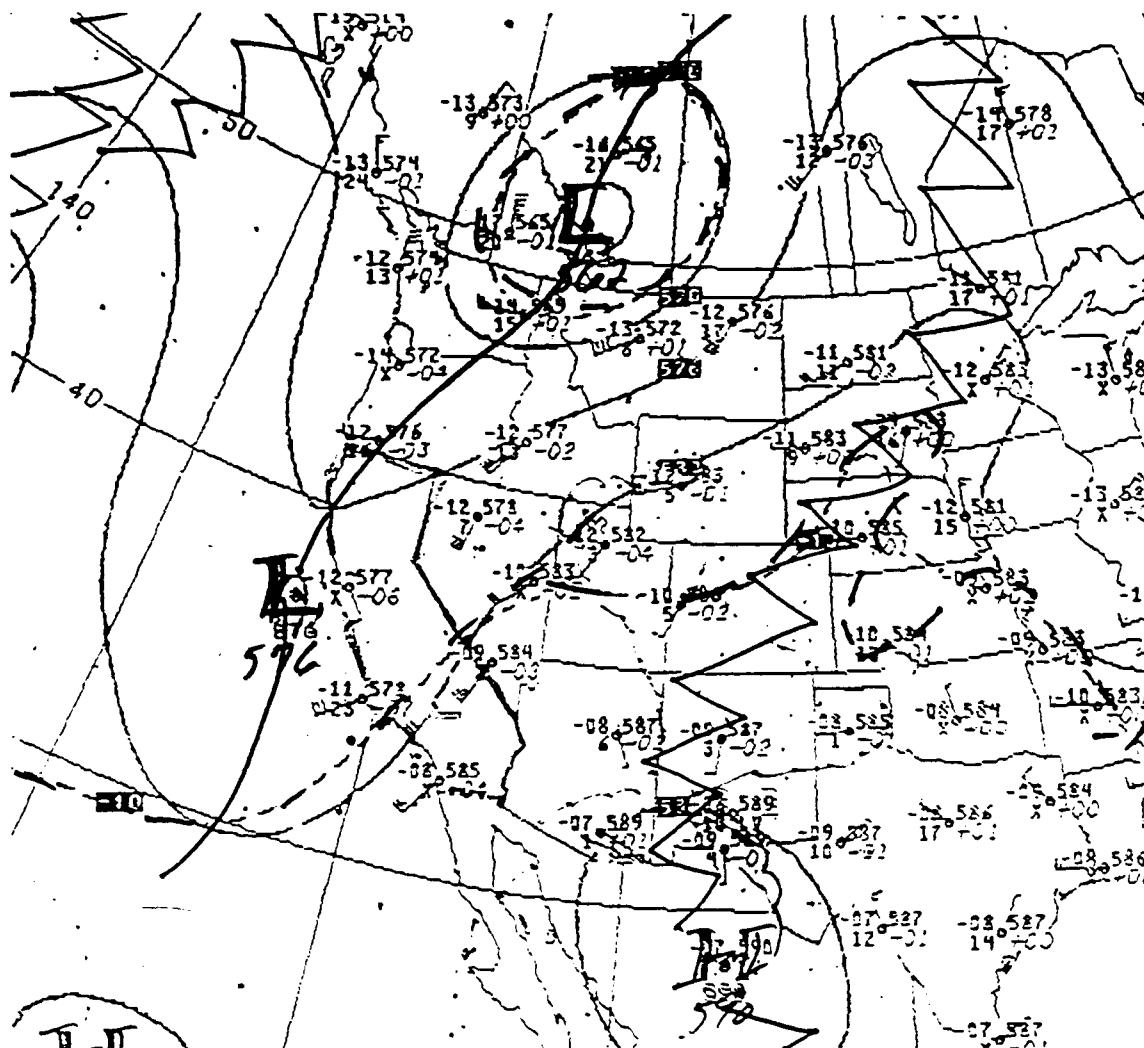
A weak trough passed VBG on 15 Aug (fig. 12.4) which displaced the thermal low, but weak southerly flow at 850 mb remained at VBG. On the final experimental day (fig. 12.5), another stronger trough passed VBG, and a northerly pressure gradient replaced the southerly gradient over VBG for 17 Aug.

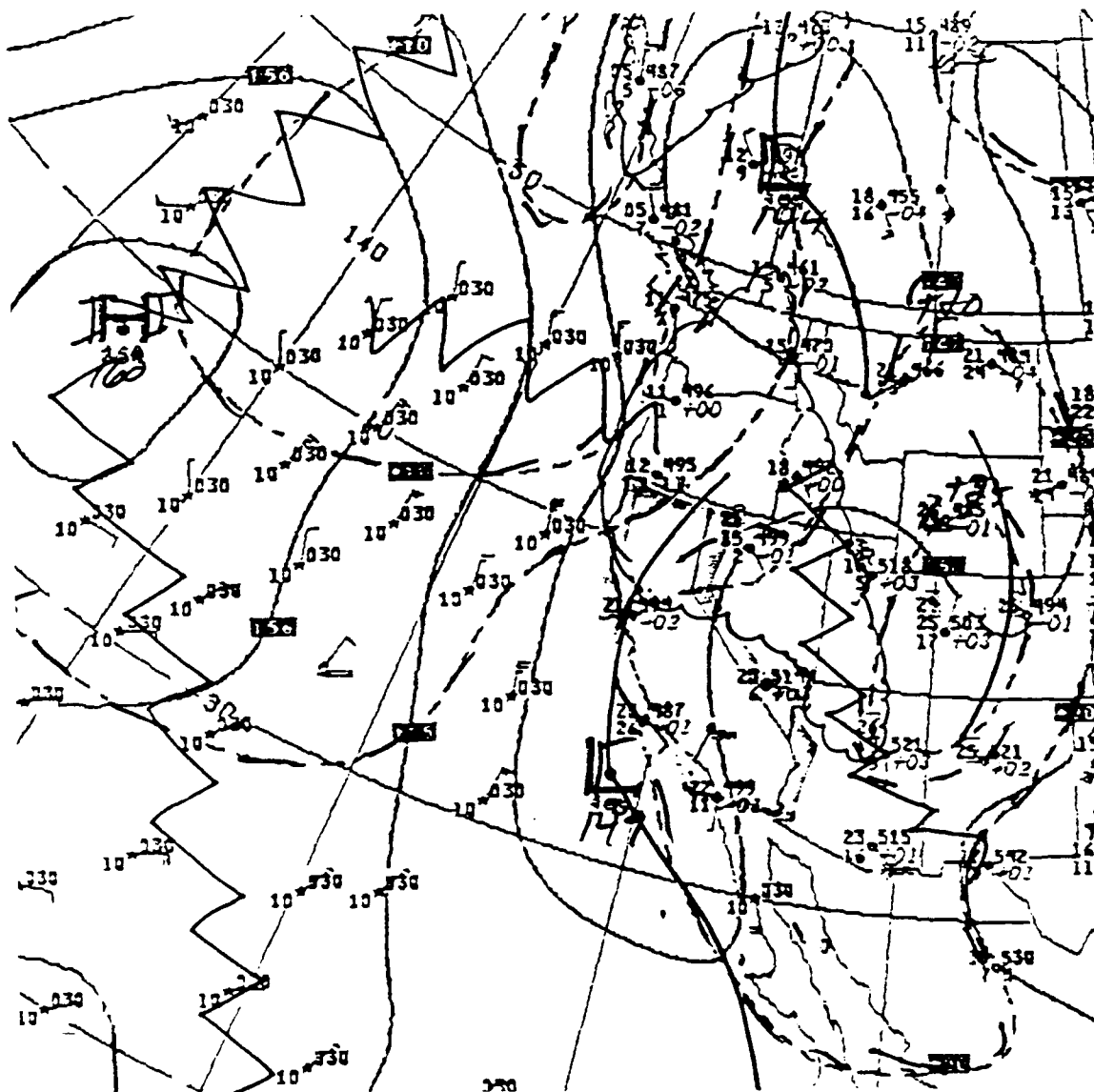
At the surface, a stationary front developed over northern California on 10 Aug (fig. 12.7) and remained through the entire experiment (figs. 12.7-11). As noted earlier, significant pressure troughs passed VBG at levels above the boundary layer on 17 Aug, but the surface front stalled in northern California. The only sign of the trough passage was slightly veered boundary layer winds on 17 Aug.

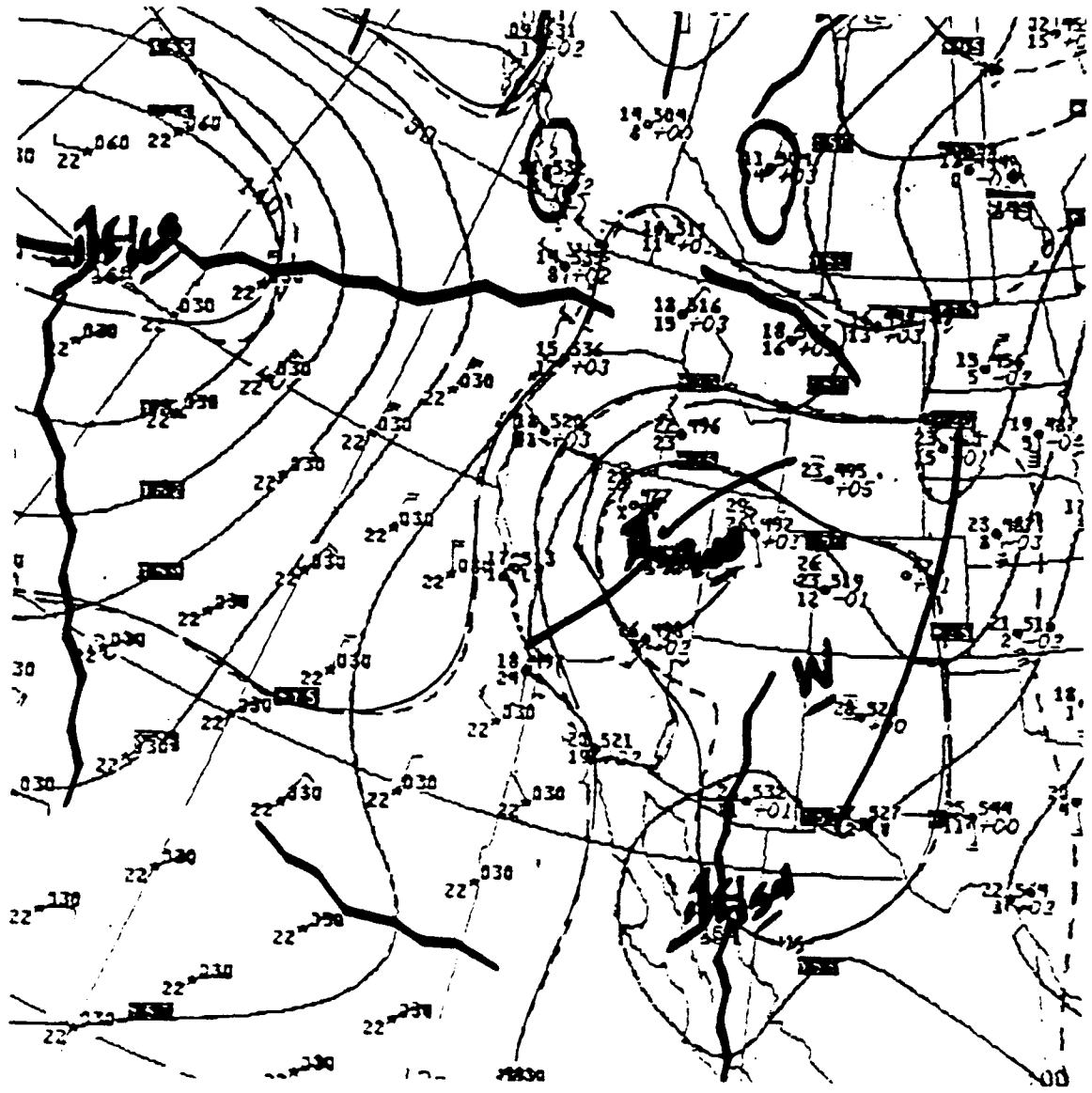
SECTION 12 FIGURE CAPTIONS

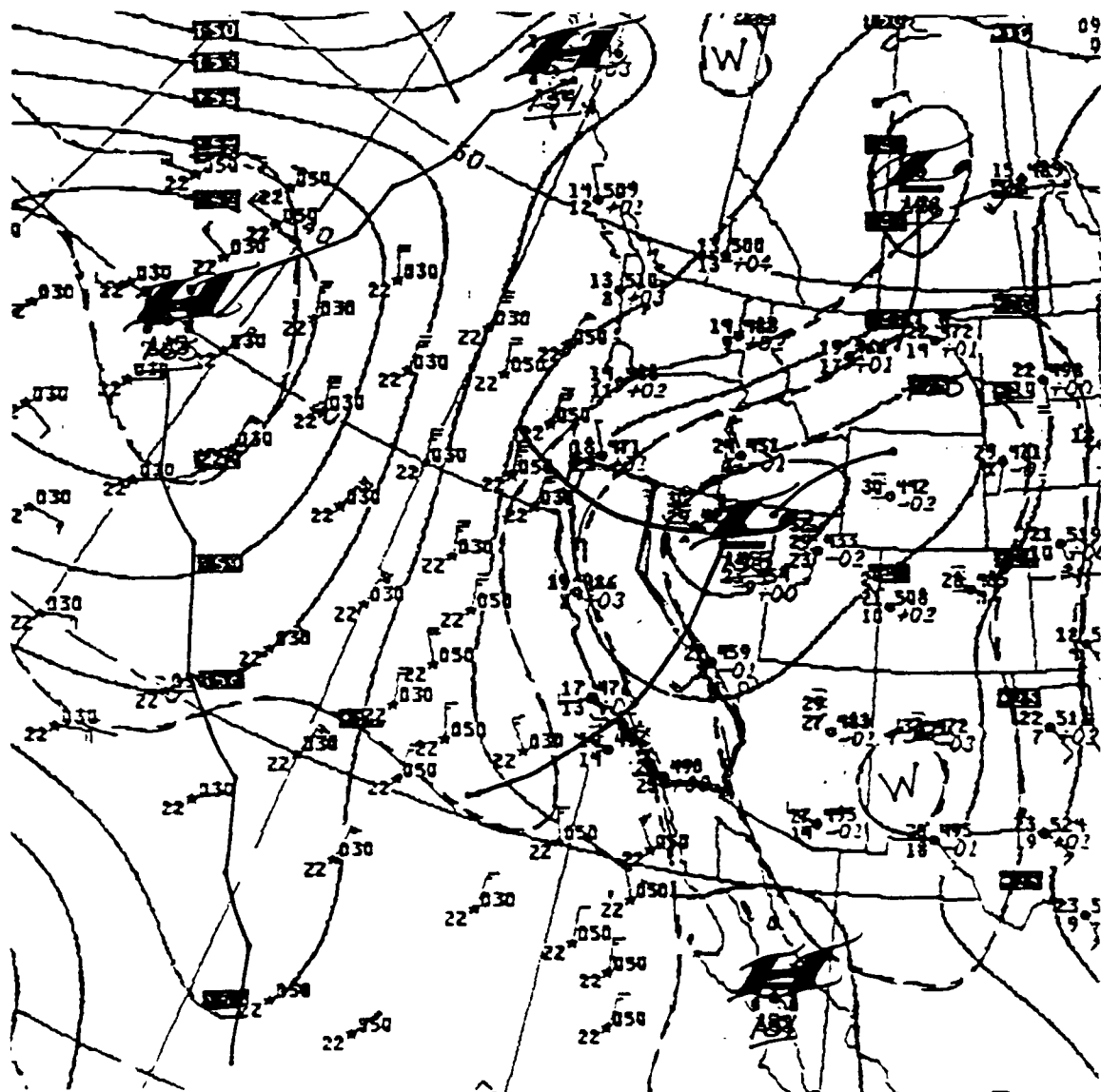
- F12.1 500 mb height field for 7 Aug 0000 UTC.
- F12.2 500 mb height field for 17 Aug 1200 UTC.
- F12.3 850 mb height field for 9 Aug 1200 UTC.
- F12.4 850 mb height field for 15 Aug 0000 UTC.
- F12.5 850 mb height field for 18 Aug 0000 UTC.
- F12.6 Surface pressure field for 10 Aug 0900 UTC.
- F12.7 Surface pressure field for 12 Aug 2100 UTC.
- F12.8 Surface pressure field for 14 Aug 0000 UTC.
- F12.9 Surface pressure field for 16 Aug 0000 UTC.
- F12.10 Surface pressure field for 17 Aug 1800 UTC.
- F12.11 Surface pressure field for 18 Aug 1800 UTC.

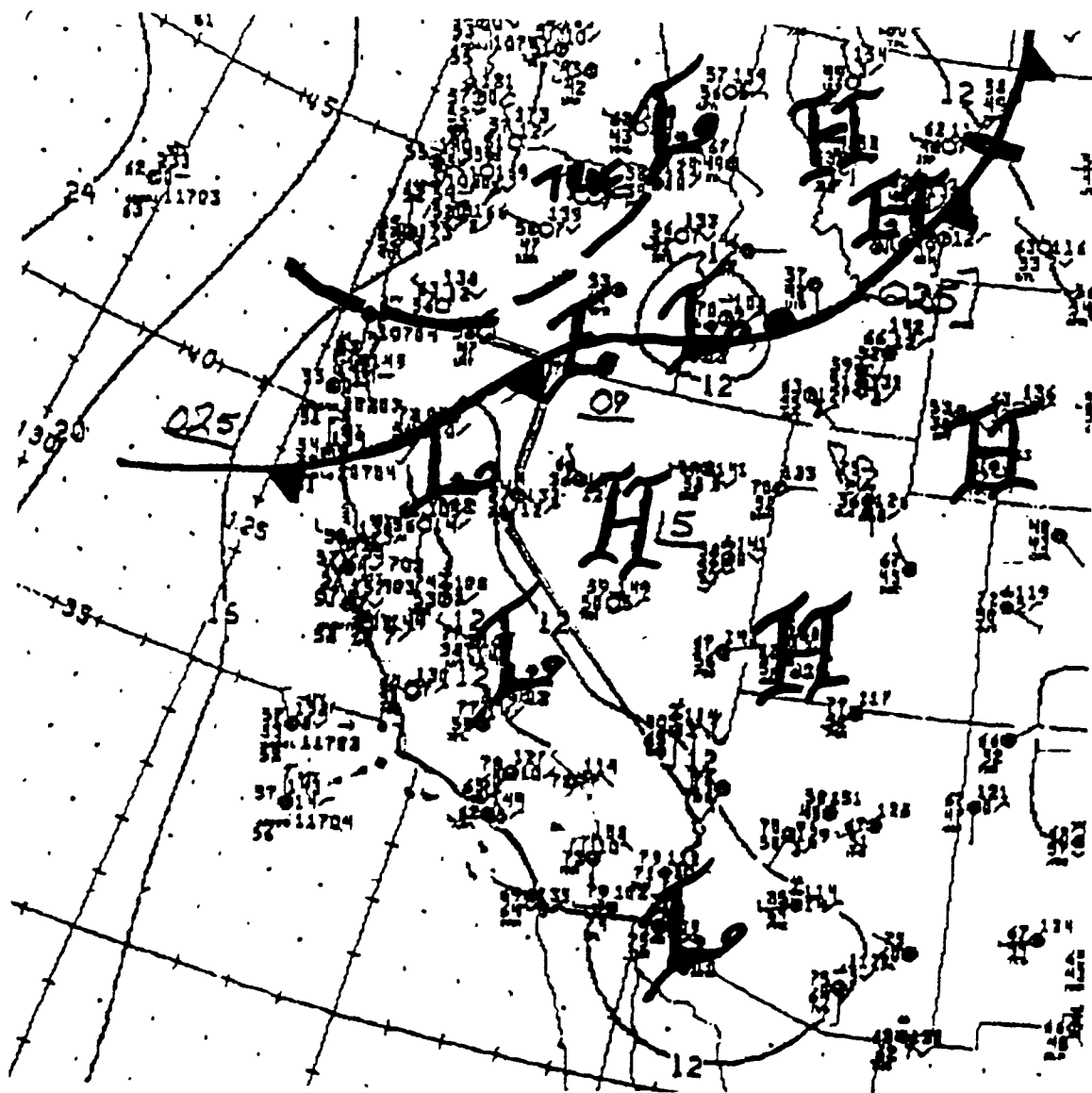




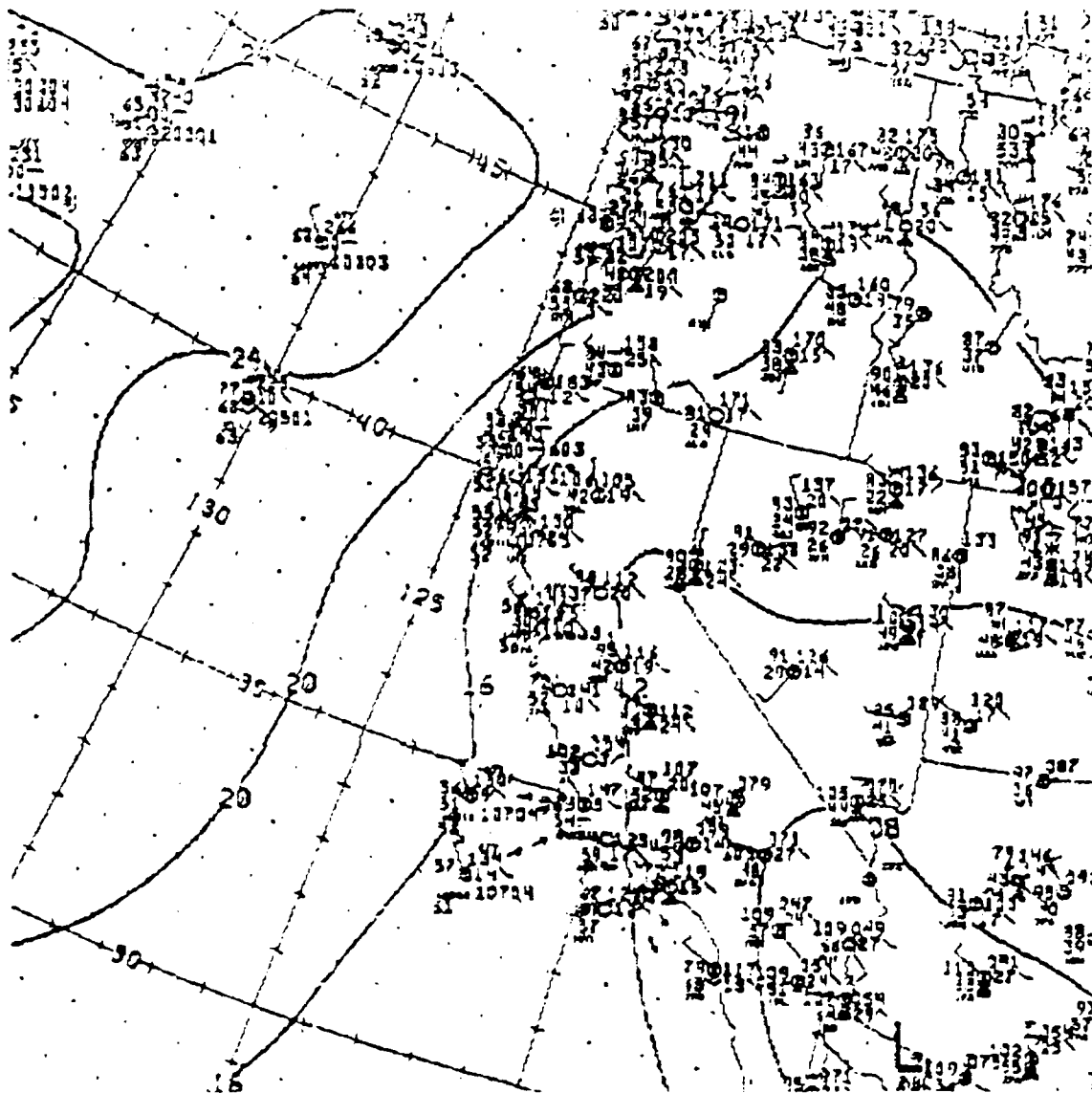


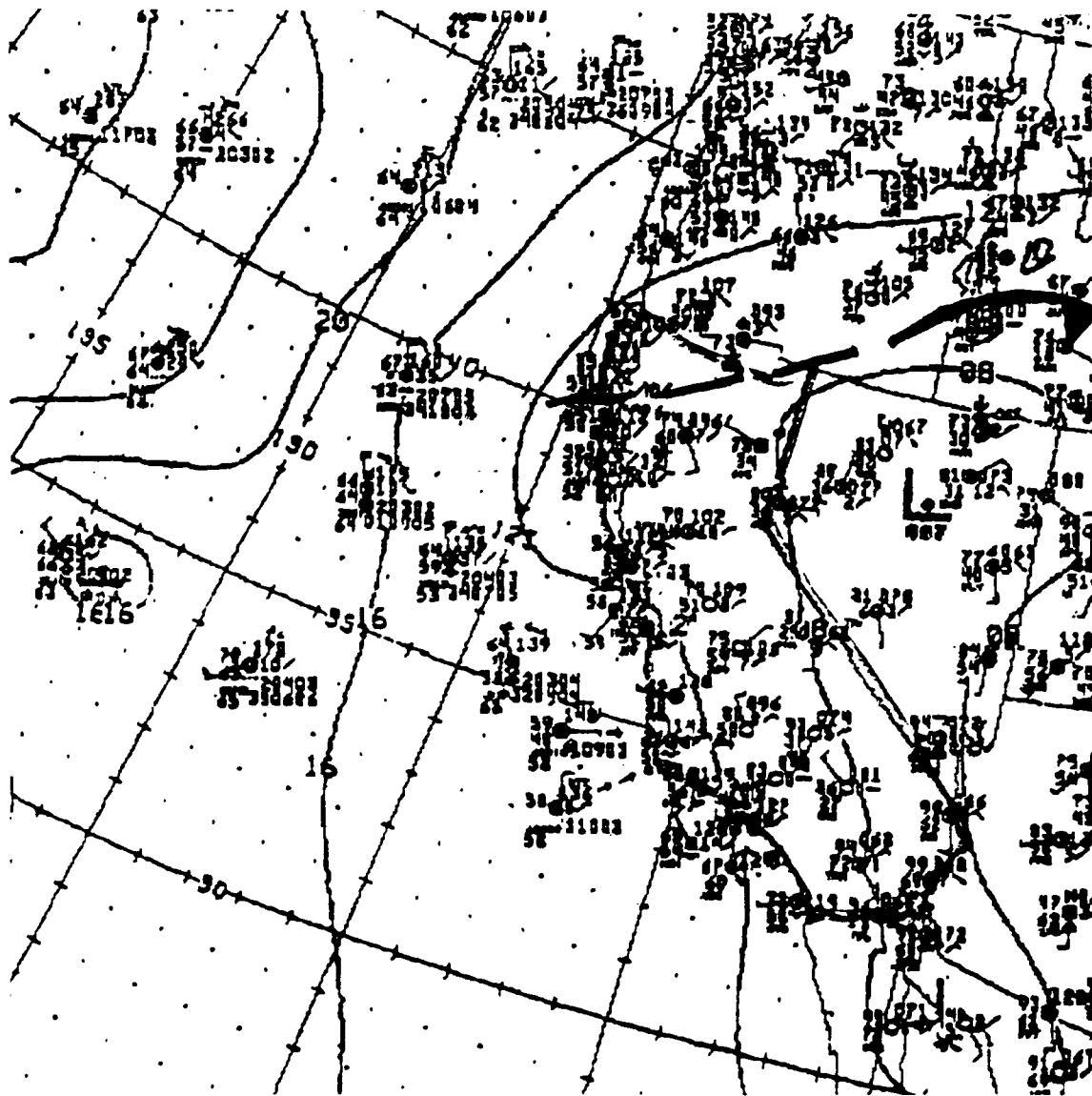


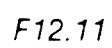












13. ANALYSIS PLAN

In addition to providing a test set for RAMS and other numerical modeling efforts, we anticipate three other major products from the LVDE data: OBDG/Mt. Iron-type diffusion equations, a THC prediction scheme, and a two-zone (cloud/clear sky) diffusion model.

Prior to LVDE, the Mt. Iron Diffusion tests of 1965-66 provided the only direct measurement of atmospheric dispersion at VBG. In order to provide as direct a comparison as possible, we will parameterize the results with the same techniques used in that analysis. I.e., the observed peak concentrations will be correlated with meteorological conditions at the source point. The predictive variables are 12 ft mean wind speed and wind direction variance, 54 ft - 6 ft temperature difference, and the downwind distance of the sample.

Several factors will make this comparison less than direct. First, the experimental design was different. For LVDE, the averaging time of a given crosswind mass distribution can be assumed to be very small due to the rapid transects of the plume with the mobile gas samplers. The measured concentration pattern can therefore be considered an instantaneous cross-section through the tracer cloud. Such dispersion is described by

two-particle dispersion equations, often referred to as 'puff' dispersion. Plume dispersion occurs when the averaging time is long compared to the travel time of the tracer from the release point to the measurement site. The Mt. Iron tests released tracer for roughly 30 min, and collected material continuously at fixed locations following the release. The total amount of material collected by a sampler determined the 'exposure' level at that location. Thus, the time of release essentially defined the averaging time of the sample. Because the travel time of the tracer to the sampler was close to the averaging time for most downwind range/wind speed combinations, the dispersion of the tracer cannot be regarded as either 'puff-like' or 'plume-like'. The concentration patterns observed during the two experiments will be inherently different due to these differences in experimental technique.

One of the main predictors, the wind direction variance, is now calculated differently by the WINDS system than it was during Mt. Iron. If a plume is released continuously, or a series of puffs are released over a long period of time, the cloud center will tend to meander back and forth across the mean wind flow trajectory. The range of the centroid meander added to the average instantaneous plume width should define a THC at VBG. The meander is currently estimated to be proportional to the variance of the wind direction at the meteorological tower situated nearest the source. From there a pie shaped zone

extends out to the maximum range of concern, as determined from the OBDG equations. We will test this technique, using the instantaneous plume transect positions, and suggest modifications to improve THC predictions.

The main anticipated product from LVDE will be a new analytical model for concentration predictions, using current VBG data sources. We anticipate that the data will show dispersion to be strongly influenced by the presence or absence of clouds. During daylight hours, clouds severely restrict the solar insolation which drives atmospheric turbulence and diffusion. Since sources at the coast are often under the clouds, and the potential impact locations are mostly in the clear sky areas to the east, the location of the cloud edge should be a factor in accurately predicting dispersion. We will develop a technique for estimating dispersion in these two zones. The cloud edge can be determined rapidly from satellite, visual, or sensor data. The method will use solar insolation estimates for determining stability to reduce the effects of the near-surface inhomogeneities which handicap tower measurements. DASS data (mean/turbulent wind and boundary layer height) will be used to better describe the flow and turbulence above the surface. This should improve trajectory estimates and give better dispersion estimates for longer ranges, where the plume has essentially filled the boundary layer.

14. ACKNOWLEDGEMENTS

The experiment and analysis work from which this paper was based was financially supported by SSD/CLGR USAF Space Division, Los Angeles. Additional funding was provided by the WSMC/SUO, Vandenberg AFB, California. We greatly appreciate the efforts of many people who aided in the experiment. People working in and around Detachment 30 at Vandenberg AFB were Lt. Col. Jack Hayes, Cpt. Ken Carey, Mr. Jerry Farley, Mr. Ron Cooper, Lt. Riley Jay, Mr. Glen Boire, Sgt. Ron Halverson, Mr. Tom Lettenberger. Maj. Dan Berlinrut and Lt. Steve Judkins (SSD/DEG) provided much needed logistical support.

In addition to the authors, several other LCSP/AC personnel provided technical support during LVDE. E. Gardner assisted the IR imagery crew. J.W. McIntosh, R. Carscallan, and J. Cole operated the mobile sampling trailer. M.A. Rocha assisted in the operation of the mobile sampling truck and designed and constructed the balloon-based sampling system. J.T. Valero and V.T. Hunt manned the balloon-based sampling system.

15. REFERENCES

R. F. Kamada, C. E. Skupniewicz, J. W. Glendening, G. E. Schacher, T. Mikkelsen, S. T. Nielsen, I. Troen, S. Larsen, E. Takle, L. Ly, and J. Griffin (1989): Vandenberg Meteorology and Plume Dispersion Handbook for Boundary Layer Releases. Naval Postgraduate School Technical Report, NPS61-89-004, 450 pp., March 1989.

R.F. Kamada, C. E. Skupniewicz, L. McKay, and S. A. Drake(1990): Comparision of Inversion Height Algorithms for Complex Terrain under Sea Breeze Conditions. Proceedings of the 9th Symposium on Turbulence and Diffusion, Roskilde, Denmark, April 30 - May 3, 1990.

R.F. Kamada, C. E. Skupniewicz, J. W. Glendening, L. McKay, and S. A. Drake(1990): Vandenberg Boundary Layer Survey 1988: A Background for Diffusion Studies in Highly Complex Terrain. Proceedings of the 4th JANAFF Symposium, Livermore, CA, June 18-23 1990.

T. Mikkelsen, S. Thykier-Nielsen, I. Troen, A. F. de Baas, S.E. Larsen, R.F. Kamada, C.E. Skupniewicz, and G.E. Schacher (1988): A Hazard Assessment Model for Complex Terrain. Proceedings of the 8th Symposium on Turbulence and Diffusion, San Diego, CA, Apr 25-29 1988.

Panofsky, H.A., and J.A. Dutton, 1984: Atmospheric Turbulence. New York, NY., John Wiley and Sons, Inc., 209-210.

C. E. Skupniewicz, R. F. Kamada, J. W. Glendening, G. E. Schacher, I. Troen, T. Mikkelsen, S. Thykier-Nielsen, A. F. de Baas, and S. E. Larsen (1988): A Hazard Assessment Technique in Complex Terrain. Proceedings of the 3rd JANAFF Symposium, Monterey, CA, May 26-30 1988.

C. E. Skupniewicz, R. F. Kamada, and G. E. Schacher (1989): Turbulence Measurements over Complex Terrain. Boundary-Layer Meteorology 48: 109-128.

C. E. Skupniewicz R. F. Kamada, and L. McKay (1990): Measurements of the ABL Across a Stratus to Clear Sky Boundary under Sea Breeze Conditions. Proceedings of the 9th Symposium on Turbulence and Diffusion, Roskilde, Denmark, April 30 - May 3, 1990.

C. E. Skupniewicz, R. F. Kamada, and L. McKay (1990): Vandenberg Boundary Layer Survey Final Report - Results. Naval Postgraduate School Technical Report, NPS61-89-004, 341 pp., April 1990.

S. Thykier-Nielsen, T. Mikkelsen, S. E. Larsen, I. Troen, A. F. de Baas, R. Kamada, C. E. Skupniewicz, and G. E. Schacher (1988): A Model for Accidental Release in Complex Terrain. Proceedings of the 17th NATO/CCMS ITM, Cambridge, (UK), Sep 19-22, 1988.

Yamada and Bunker (1990): Atmospheric Dispersion of Rocket Propellant. LA-UR-90-2270, Los Alamos National Laboratory, Los Alamos, New Mexico, 87545.

16. DATA BASE REFERENCE CATALOG

The following list names the data sets described in this report. All data sets are recorded as DOS files. The media is 3.5 inch high density (1.44 Mb) floppy disks.

<u>Section</u>	<u>Disc</u>	<u>File Name</u>	<u>Contents</u>
2	3	RRTABLE.DOC	Copy of Table 2.1
3	3	SAMPLING.RTS	Coordinates of sampling routes shown in fig. 3.1
3	1	\DAYS1-3.TRV\ V###.DSA	FGA traverse statistics and raw data for days 8-10-89 through 8-12-89
3	2	V###.DSA	FGA traverse statistics and raw data for days 8-13-89 through 8-15-89
3	3	V###.DSA	FGA traverse statistics and raw data for days 8-16-89 through 8-17-89
3	3	\AERO\ A###.DSA	GC traverse statistics for all days
3	3	\AERO\ AEROTRUK.RAW	GC raw data collected from truck
3	3	\AERO\ AEROTRAL.RAW	GC raw data collected from trailer
3	1	\STATVERT\ V###.DSA	FGA stationary and vertical statistics and raw data for all days
5	4	DASLV1F.DAT	10 min VBG DASS records 8-4-89 to 8-9-89
5	5	DASLV2F.DAT	10 min VBG DASS records 8-9-89
5	6	DASLV3F.DAT	10 min VBG DASS records 8-9-89 to 8-15-89
5	5	DASLV4F.DAT	10 min VBG DASS records 8-15-89 to 8-17-89
5	5	DASLV5F.DAT	10 min VBG DASS records 8-17-89 to 8-18-89
5	7	DASLVHR#.DAT	1 hour VBG DASS records all days (# correlates with 10 min file)

<u>Section</u>	<u>Disc</u>	<u>File Name</u>	<u>Contents</u>
5	8	DASLW#.DAT	10 min NPS Water Treatment Plant DASS records all days (# = 1 is 8-9-89, # = 2 is 8-10-89, etc.)
5	8	DASLWHR#.DAT	1 hour NPS Water Treatment Plant DASS records all days (# = 1 is 8-9-89, # = 2 is 8-10-89, etc.)
5	8	DASLT#.DAT	10 min NPS Trailer DASS records all days (# = 1 is 8-9-89, # = 2 is 8-10-89, etc.)
6	9	WINDS1.RAW	10 min WINDS system raw data 8-4-89 to 8-10-89
6	10	WINDS2.RAW	10 min WINDS system raw data 8-10-89 to 8-14-89
6	11	WINDS3.RAW	10 min WINDS system raw data 8-14-89 to 8-18-89
6	12	WINDS4.RAW	10 min WINDS system raw data 8-18-89 to 8-20-89
6	12	WINDSLV.HR	1 hour WINDS system base averages
7	13	REGION.HR	1 hour regional tower network data
8	12	SONDESLV.TOT	Rawindsonde data, all days
9	13	PROFILE.DAT	Building 900 profile mast data
10	13	TOWER57.DAT	Release site meteorology

17. DISTRIBUTION LIST

Report

Defense Technical Information Center
Cameron Station
Alexandria, VA 22314

Dudley Knox Library
Naval Postgraduate School
Monterey, CA 93943-5000

Director of Research (81)
Naval Postgraduate School
Monterey, CA 93943-5000

Dept. of Physics (PH)
Naval Postgraduate School
Monterey, CA 93943-5000

Major Sherman Forbes (SSD/CLGR)
Los Angeles AFB
Los Angeles, CA 90009-2960

Capt. Frank Smith (SSD/CLGR)
Los Angeles AFB
Los Angeles, CA 90009-2960

Lt. Col. Richard Riccardi (SSD/SEH)
Los Angeles AFB
Los Angeles, CA 90009-2960

Major Joe Bassi (SSD/WE)
Los Angeles AFB
Los Angeles, CA 90009-2960

Col. Hal Wold (WSMC/SE)
Vandenberg AFB, CA 93437-5000

Lt. Col. John Hayes (WSMC/WE)
Vandenberg AFB, CA 93437-5000

Lt. Col. Winston Crandall (AFSTC/WE)

Lt. Col. Keith Swallom (WSMC/SUO)
Vandenberg AFB, CA 93437-5000

Major John Sigafos (VAFB/6595 ATG)
Vandenberg AFB, CA 93437-5000

Capt. Mike Chulick (VAFB Hosp/SGB)

Vandenberg AFB, CA 93437-5000

Capt. Ken Carey (WSMC/WE)
Vandenberg AFB, CA 93437-5000

Capt. Mike Moss (AFESC/RDVS)
Tyndall AFB, FL 32403-6001

Glen Boire (WSMC/WE)
Vandenberg AFB, CA 93437-5000

Steve Sambol (WSMC/WE)
Vandenberg AFB, CA 93437-5000

Darryl Dargitz (WSMC/SEY)
Vandenberg AFB, CA 93437-5000

Bruce Kunkel (AFGL/LYA)

Bill Boyd (ESMC/WER)
Patrick AFB, FL 32925-5000

Juleah Wojcik (ESMC/SEMP)

Don Cameron (Det 21, 2WS, EAFB)
Edwards AFB, CA 93523-5000

Kevin Wright (1 STRAD/ET)

Jacobs Engineering Group (VAFB)
Vandenberg AFB, CA 93437-5000

Don Nichols (Aerospace/VAFB)
Vandenberg AFB, CA 93437-5000

Larry Mendenhall
Geodynamics Corp.
21171 Western Ave
Suite 100
Torrence, CA 90501

ACTA Inc.
Plaza de Rina
Suite 101
24430 Hawthorne Blvd.
Torrence, CA 90505

Genevieve Denault (Aerospace/El Segundo)
PO Box 92957
Los Angeles, CA 90009

Ken Herr (Aerospace/El Segundo)
PO Box 92957
Los Angeles, CA 90009

Bart Lundblad (Aerospace/El Segundo)
PO Box 92957
Los Angeles, CA 90009

Soft Data

Capt. Frank Smith (SSD/CLGR)

Lt. Col. John Hayes (WSMC/WE)

Capt. Mike Moss (AFESC/RDVS)

Bruce Kunkel (AFGL/LYA)

Ken Herr (Aerospace/El Segundo)

Bart Lundblad (Aerospace/El Segundo)

ADDENDUM TO "LOMPOC VALLEY DIFFUSION EXPERIMENT DATA REPORT"

Date: 4 Dec 1990

Subject: Section 6, Hourly Averages Summary

1. A new data set has been added to disc 12, named "WINDSLV.HR2". This file includes 'sigma theta', the standard deviation of the wind direction, for the 12 ft sensors as calculated from the WINDS system. These data are simple averages of the 10 minute raw values; they do not include variance contributions from changing mean wind direction. The original data, "WINDSLV.HR", also included some erroneous CR/LF's which have now removed. Page 6.8-10 describe the data content of "WINDSLV.HR". The new data set is the same, except for the following changes on 6.8.

Hourly Record Specifics (WINDSLV.HR2)

.
.
.

field 3: TWR12, LATM12, LATS12, LONM12, LONS12, S12(24),
D12(24), SD12(24) {I5,4F5.1,24F6.1,24I5,24F5.1}

.
.
.

Page 6.9, below "D12(24) = ...", should include the definition

SD12(24) = standard deviation of the 12 ft mean
wind directions at the tower

.
.
.

2. Figure 6.1 was left out during printing. It is attached to this addendum.

